NASA/CR-2000-209847

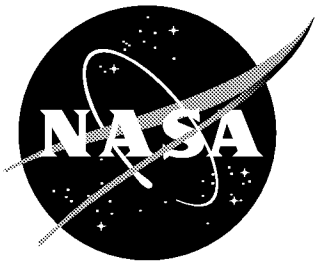

Structural Design Methodology Based on Concepts of Uncertainty

K. Y. Lin, Jiaji Du, and David Rusk
Department of Aeronautics and Astronautics
University of Washington, Seattle, Washington

February 2000

The NASA STI Program Office ... in Profile

Since its founding, NASA has been dedicated to the advancement of aeronautics and space science. The NASA Scientific and Technical Information (STI) Program Office plays a key part in helping NASA maintain this important role.

The NASA STI Program Office is operated by Langley Research Center, the lead center for NASA's scientific and technical information. The NASA STI Program Office provides access to the NASA STI Database, the largest collection of aeronautical and space science STI in the world. The Program Office is also NASA's institutional mechanism for disseminating the results of its research and development activities. These results are published by NASA in the NASA STI Report Series, which includes the following report types:

- TECHNICAL PUBLICATION. Reports of completed research or a major significant phase of research that present the results of NASA programs and include extensive data or theoretical analysis. Includes compilations of significant scientific and technical data and information deemed to be of continuing reference value. NASA counterpart of peer-reviewed formal professional papers, but having less stringent limitations on manuscript length and extent of graphic presentations.

- TECHNICAL MEMORANDUM. Scientific and technical findings that are preliminary or of specialized interest, e.g., quick release reports, working papers, and bibliographies that contain minimal annotation. Does not contain extensive analysis.

- CONTRACTOR REPORT. Scientific and technical findings by NASA-sponsored contractors and grantees.

- CONFERENCE PUBLICATION. Collected papers from scientific and technical conferences, symposia, seminars, or other meetings sponsored or co-sponsored by NASA.

- SPECIAL PUBLICATION. Scientific, technical, or historical information from NASA programs, projects, and missions, often concerned with subjects having substantial public interest.

- TECHNICAL TRANSLATION. English-language translations of foreign scientific and technical material pertinent to NASA's mission.

Specialized services that complement the STI Program Office's diverse offerings include creating custom thesauri, building customized databases, organizing and publishing research results ... even providing videos.

For more information about the NASA STI Program Office, see the following:

- Access the NASA STI Program Home Page at ***http://www.sti.nasa.gov***

- E-mail your question via the Internet to help@sti.nasa.gov

- Fax your question to the NASA STI Help Desk at (301) 621-0134

- Phone the NASA STI Help Desk at (301) 621-0390

- Write to:
  NASA STI Help Desk
  NASA Center for AeroSpace Information
  7121 Standard Drive
  Hanover, MD 21076-1320

NASA/CR-2000-209847

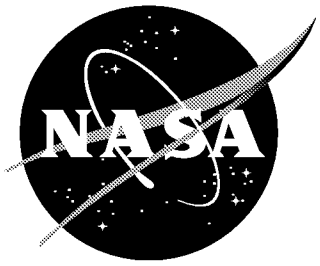

Structural Design Methodology Based on Concepts of Uncertainty

K. Y. Lin, Jiaji Du, and David Rusk
Department of Aeronautics and Astronautics
University of Washington, Seattle, Washington

National Aeronautics and
Space Administration

Langley Research Center
Hampton, Virginia 23681-2199

Prepared for Langley Research Center
under Grant NAG-1-2055

February 2000

Available from:

NASA Center for AeroSpace Information (CASI)
7121 Standard Drive
Hanover, MD 21076-1320
(301) 621-0390

National Technical Information Service (NTIS)
5285 Port Royal Road
Springfield, VA 22161-2171
(703) 605-6000

FOREWORD

This report summarizes the work accomplished during the period of May 16, 1998 – September 30, 1999, under the NASA Langley Research Center Grant No. NAG-1-2055. The principal investigator of this program was Dr. K. Y. Lin. David Rusk was the graduate research assistant. Dr. Jiaji Du, a visiting scientist from West Virginia University, was the researcher for this project. Dr. Bjorn Backman of the Boeing Company also contributed to this project. The NASA project manager is Dr. W. Jefferson Stroud. Invaluable discussions and support of this research from Dr. Jeff Stroud of NASA, Dr. Bjorn Backman of Boeing, Dr. Larry Ilcewicz and Dr. Dave Swartz of the FAA are greatly appreciated.

ABSTRACT

The principal goal of this research program is to develop a design process for damage tolerant aircraft structures using a definition of structural "Level of Safety" that incorporates past service experience. The design process is based on the concept of an equivalent "Level of Safety" for a given structure. The discrete "Level of Safety" for a single inspection event is defined as the compliment of the probability that a single flaw size larger than the critical flaw size for residual strength of the structure exists, and that the flaw will not be detected. The cumulative "Level of Safety" for the entire structure is the product of the discrete "Level of Safety" values for each flaw of each damage type present at each location in the structure.

The design method derived from the above definition consists of the following steps: collecting in-service damage data from existing aircraft, establishing the baseline safety level for an existing structural component, conducting damage tolerance analyses for residual strength of the new structural design, and determining structural configuration for a given load and the required safety level (sizing). The design method was demonstrated on a composite sandwich panel for various damage types, with results showing the sensitivity of the structural sizing parameters to the relative safety of the design. The "Level of Safety" approach has broad potential application to damage-tolerant aircraft structural design with uncertainty.

EXECUTIVE SUMMARY

There are at least two fundamental shortcomings to traditional aircraft design procedures using factors of safety and knockdown factors. First, these procedures may be difficult to apply to aircraft that have unconventional configurations, use new material systems, and contain novel structural concepts. Second, levels of safety and reliability cannot be easily measured for a structural component. As a result, it is not possible to determine the relative importance of various design options on the safety of the aircraft. In addition, with no measure of safety it is unlikely that there is a consistent level of safety and efficiency throughout the aircraft. The principal goal of this research program is to develop a design process for damage tolerant aircraft structures using a definition of structural "Level of Safety" that incorporates past service experience.

In this report, an approach to damage-tolerant aircraft structural design based on the concept of an equivalent "Level of Safety" is studied. The discrete "Level of Safety" for a single inspection event is defined as the compliment of the probability that a single flaw size larger than the critical flaw size for residual strength of the structure exists, and that the flaw will not be detected. The cumulative "Level of Safety" for the entire structure is the product of the discrete "Level of Safety" values for each flaw of each damage type present at each location in the structure.

The design method derived from the above definition consists of the following steps: collecting in-service damage data from existing aircraft, establishing the baseline safety level for an existing structural component, conducting damage tolerance analyses for residual strength of the new structural design, and determining structural configuration for a given load and the required safety level (sizing).

To demonstrate the design methodology on a new structure, a composite sandwich panel was analyzed for residual strength as a function of damage size for disbond, delamination and notch damage. A two-step analysis model was used to determine post-buckling residual strength for each damage type. The residual strength vs. damage size results were used to

demonstrate application of the "Level of Safety" design processes using two example problems. The influence of the structural sizing parameters on the overall "Level of Safety" was also demonstrated in the examples. Bayesian statistical tools are incorporated into the design method to quantify the uncertainty in the probability data, and to allow post-design damage data to be used to update the "Level of Safety" values for the structure. Some methods of obtaining in-service damage data for the current aircraft fleet have been suggested. Concerns regarding the calculation of "Level of Safety" values for existing aircraft components have also been discussed.

The definition of structural "Level of Safety", and the design methodology derived from it, is an extension of reliability theory and statistical analysis tools to the design and maintenance of damage-tolerant aircraft structures. The method presents a unified approach to damage tolerance that allows a direct comparison of relative safety between aircraft components using different materials, construction techniques, loading or operational conditions. It incorporates planning for the service inspection program into the design process. The use of Bayesian statistical tools in the "Level of Safety" method provides a mechanism for validating the damage assumptions made during the design process, and for reducing the level of uncertainty and risk over the life-cycle of the structure.

TABLE OF CONTENTS

TABLE OF FIGURES

1 INTRODUCTION

1.1 Background

Traditional design procedures for aircraft structures are based on a combination of factors of safety for the loads and knockdown factors for the strength. Both the factors of safety and knockdown factors have been obtained from the past five decades of design for metal aircraft.

There are at least two fundamental shortcomings to these traditional design procedures. First, because the procedures were developed for conventional configurations, metallic materials, and familiar structural concepts, these traditional procedures may be difficult to apply to aircraft that have unconventional configurations, use new material systems, and contain novel structural concepts. Consider, for example, the case of composite materials. Adaptations of traditional design procedures to account for larger scatter in composite properties and the sensitivity of composite structures to environmental effects and to damage have led to a very conservative approach for designing composite structures. This approach, in essence, assumes that a "worst case scenario" occurs simultaneously for each design condition – temperature, moisture, damage, loading, etc. This results in substantial and unnecessary weight penalties.

A second shortcoming of traditional design procedures is that measures of safety and reliability are not available. As a result, it is not possible to determine (with any precision) the relative importance of various design options on the safety of the aircraft. In addition, with no measure of safety it is unlikely that there is a consistent level of safety and efficiency throughout the aircraft. That situation can lead to excessive weight with no corresponding improvement in overall safety.

New structural design procedures based on the concept of "design under uncertainty" help to overcome many of these problems. In particular, measures of safety and reliability are available during the design process and for the final design. This information allows the designer to produce a consistent level of safety and efficiency throughout the aircraft – no

unnecessary over-designs in some areas. As a result, designers can save weight while maintaining safety. In addition, in design under uncertainty it is possible to determine the sensitivity of safety to design changes that can be linked to changes in cost. For the same cost, aircraft can be made safer than with traditional design approaches, or, for the same safety and reliability, the aircraft can be made at a lower cost. Design under uncertainty also has application to the flight certification process, as it allows the uncertainty inherent in any new design to be quantified. Thus, flight certification criteria can be established which define the safety margins necessary for compliance based on the level of uncertainty associated with the design.

Based on the above consideration, a research program was established by the University of Washington to study the feasibility of developing a design procedure based on concepts of uncertainty and of applying this procedure to the design of airframe structures for commercial transport. The program is being sponsored by NASA Langley Research Center. The new design procedure is based on the fact that design data such as loading, material properties, damage, etc. are of statistical character. Design procedures based on uncertainty have the potential for reducing the weight and cost of airframe structures while maintaining prescribed level of safety. These procedures could also help reduce the design cycle time, particularly for unconventional aircraft that use new materials and novel structural concepts.

1.2 Review of existing technologies

The non-deterministic design approach is one of the current research emphases in various disciplines of engineering (Ref.1, 2, 3, 4). This design methodology has been applied to civil, mechanical and electronics engineering applications for decades. In recent years, there have been applications to aerospace composite structures as well. Chamis developed a probabilistic design procedure for composite structures (Ref. 5). The research has generated the Integrated Probabilistic Analysis of Composite Structures (IPACS). The procedure combines physics, mechanics, specific structure, system concepts and manufacturing. In IPACS, fiber mechanical and physical properties, resin properties, and the fiber placement techniques are the input data and all of these data are considered random variables. A

probabilistic lamination theory is then established using a micromechanics approach. This is followed by a probabilistic finite element analysis based on structural mechanics. The output of IPACS includes structural sizing, failure prediction and load limiting application. IPACS does not include operational lifetime considerations such as material degradation and random damage processes during service.

Kan, et al., proposed a probabilistic methodology for composite airframe certification. The original work focused on probabilistic models to characterize data scatter in composite static strength and fatigue-life tests (Ref. 6). The goal was to evaluate structural testing requirements to achieve B-basis allowables for flight certification. Their methods were extended to include data scatter in bonded and cocured structures, and to assess impact damage requirements for certification (Ref. 7). The impact threat to aircraft was characterized using a Weibull distribution of impact energy. A damage detection threshold of Barely Visible Impact Damage (BVID) was set for a dent depth $\geq$ 0.05 in. in thin laminates. A method was presented for predicting post-impact residual strength of built-up structures which incorporates a statistical analysis of data scatter from compression test specimens with the impact threat distribution, to give an integrated probabilistic reliability analysis procedure. This model was then modified to reduce the number of empirical coefficients and test data points needed for an analysis (Ref. 8).

Rouchon (Ref. 9) has also contributed to composite structural design, primarily in two major areas: 1) certification and compliance philosophy; 2) probabilistic inspection for fleet reliability. Rouchon's efforts in the area of certification and compliance philosophy address second source material qualification, conditions to simulate environmental effects, and damage tolerance demonstration for accidental impact damage. His work on probabilistic inspection is focused on the need to detect impact damage in composite structures before the critical load level for catastrophic failure is reached (Ref. 10). A simplified probabilistic approach was presented for damage tolerance evaluation, where post-impact residual strength data are combined with probabilistic assessments of impact damage threats and flight load factors to set inspection intervals for maintaining failure probabilities below a threshold

value. This approach is being used to certify the ATR72 and future generations of Airbus aircraft.

Gary and Riskalla investigated the application of Northrop Grumman's Probabilistic Design Model to determine structural reliability values for a modern composite aircraft (Ref. 11). The Northrop Grumman design model is a Monte Carlo simulation in which the probability distributions of operating stress and material strength are subjected to lifetime risk drivers such as material quality, manufacturing quality, thermal stress, gust, operating environment, and operational structural damage. Failure probability is defined as the probability of stress exceeding strength. To validate the design model, site visits were conducted at airline maintenance facilities and Naval aviation depots to gather historical data on operational damage incurred on composite structures. This data was input into the design model to assess the structural reliability of the Lear Fan 2100 wing box.

The works reviewed here are only a small sample of the range of research devoted to probabilistic methods applied to aerospace structures, yet they provide important insight into how far these methods have come, and illustrate areas where further efforts are needed. Chamis's model is an important design tool for assessing the variability in composite manufacture, analysis and testing, but it does not incorporate means for evaluating effects of service damage on reliability. Kan's probabilistic work is geared towards flight certification, and does not directly address design. The methods obtained only apply to a specific damage mechanism in composites (impact), and do not incorporate probabilities associated with detecting impact damage in an aircraft fleet. Rouchon's work also is geared towards flight certification, and acknowledges the role inspection plays in maintaining the safety of damage-tolerant structures. He also addresses some of the limitations inherent in probabilistic methodologies, namely that a large and detailed database is needed to characterize impact damage probabilities, and that the threshold approach to damage detection may be inadequate. At the present time, however, he has not proposed any means of incorporating these concerns into his probabilistic methodologies. Northrop Grumman's design model may be one of the most robust yet to apply probabilistic methodologies in the design process, and has been demonstrated on a modern, flight-certified composite airframe.

However, it does not incorporate the influence of damage detection probabilities in its reliability assessments.

All of the work reviewed thus far focuses on composite impact as the primary damage mechanism driving the use of probabilistic methods in damage tolerance. However, these methods can be applied equally as well to other damage mechanisms, and for other material systems. Most of this work has been focused on specific areas and applications, and does not take a broad overview of the structural design process for reliability. Therefore, there exists a need for a unified probabilistic approach to reliability that is independent of specific material systems and structural configurations, and that can be applied to the entire life-cycle of a structure. It should take into account the influence of detection probabilities in setting inspection intervals and defining critical damage thresholds, and also account for the existence of multiple damages of different types in a structure. This is the thrust of the current research effort outlined in this report.

2 OBJECTIVES

The specific goals of this research program are to establish a workable definition of acceptable structural "Level of Safety" based on probabilistic assessments of in-service accumulated damage to aircraft components, and the ability of non-destructive inspection methods to detect such damage. The resulting definition will be used to develop a design process which evaluates the equivalent "Level of Safety" of an existing aircraft structure, and uses this value in the design of a new structure which matches or exceeds the existing "Level of Safety" value. The new design method is to be an objective, quantifiable, data-driven process that will allow comparisons of relative safety to be made between dissimilar aircraft components and structures using different material systems, load requirements, structural design details, etc. Using the identified design methodology, explicit safety-based resize procedures will be developed incorporating deterministic analyses of residual strength properties for specific structures. The resize procedures will be used to demonstrate structural sizing sensitivities to safety-based design requirements and flight certification criteria. The result will be a uniform design methodology that allows utilization of service data and operational experience to quantify the "Level of Safety" of the existing aircraft fleet, and that can also be used to quantify the uncertainty associated with the use of new materials and structural concepts in future aircraft designs.

3 EQUIVALENT LEVEL OF SAFETY APPROACH

3.1 General Approach

A general approach for determining the equivalent "Level of Safety" of an aircraft structure is defined in this chapter. A mathematical definition of structural "Level of Safety" based on a probabilistic damage tolerance approach is derived in Section 3.2. This method is used to evaluate the "Level of Safety" of existing aircraft structures using damage data collected from in-service experience, combined with detection probabilities for each damage type. The resulting values establish a safety baseline for which future design efforts must meet. A design process is defined for new materials and structural concepts which quantifies the uncertainty in the damage tolerance behavior of these applications, and applies the "Level of Safety" definition to size the structure so that the baseline safety value is maintained or improved upon. Once the structure is built and placed in service, inspection and maintenance data can be used to validate the assumptions used in the design process, and to reduce the level of uncertainty associated with the structure.

A flow-chart of the approach to developing equivalent-safety aircraft structures is given in Figure 1. The detailed explanation of the approach is given in the following context.

3.2 Defining "Level of Safety"

To enable the objective evaluation of the level of safety of an aircraft component, a quantitative method is needed which incorporates design data along with data on the amount and type of damage a part is exposed to during its operational life. Modern damage-tolerance philosophies require that damage accumulated during the service life of a component be detected and repaired before the strength of the component is degraded beyond some design threshold. A convenient way to define the "Level of Safety" based on these criteria is the joint probability density function approach for damage size and NDI detection limit.

This "Level of Safety" concept was initially proposed by Bjorn Backman of the Boeing Commercial Aircraft Group, and is defined in statistical terms as: *"The compliment of the probability that a flaw size that is larger than the critical flaw size for residual strength of the structure is incurred, and that the flaw will not be detected."*

There are two random variables involved: 1. Damage size "a", which is continuous; and 2. Detection state "d", which is discrete. Since they are not independent, the joint probability density function $p_j(d,a)$ is:

$$p_j(d,a) = p_c(d|a)\, p(a) \tag{3.2-1}$$

in which $p_c(d|a)$ is the conditional probability density function and $p(a)$ is the marginal probability density function of actual damage size.

Because random variable "d" has only two possible values, that is:

d_1 ---- damage is detected
d_2 ---- damage is not detected

the marginal probability density function $p(a)$ is the sum of two terms.

$$\begin{aligned} p(a) &= p_j(d_1,a) + p_j(d_2,a) \\ &= p_c(d_1|a)p(a) + p_c(d_2|a)p(a) \\ &= [p_c(d_1|a) + p_c(d_2|a)]p(a) \end{aligned} \tag{3.2-2}$$

Thus,

$$[p_c(d_1|a) + p_c(d_2|a)] = 1 \tag{3.2-3}$$

When the conditional probability density function $p_c(d|a)$ is evaluated at $d = d_1$, it stands for the probability of detection under the condition that the damage size is a. Let $P_D(a)$ denote the probability of detection for damage size a, that is:

$$p_c(d_1|a) = P_D(a) \tag{3.2-4}$$

Using equation (3.2-3), we have

$$p_c(d_2|a) = 1 - P_D(a) \tag{3.2-5}$$

Substituting (3.2-4) and (3.2-5) into (3.2-2) yields:

$$p(a) = p(a)P_D(a) + p(a)[1 - P_D(a)] \tag{3.2-6}$$

The first term of (3.2-6) is proportional to the probability density function of detected damage size $p_0(a)$, or mathematically (Multiplication Rule):

$$p(a)p_c(d_1|a) = f(d_1)g(a|d_1) \tag{3.2-7}$$

in which, $p_c(d_1|a) = P_D(a)$, $g(a|d_1) = p_0(a)$ and $f(d_1)$ is a constant. Therefore,

$$p(a)P_D(a) = Cp_0(a) \qquad \text{or} \qquad p(a) = Cp_0(a)/P_D(a) \tag{3.2-8}$$

where C is a normalizing constant that is determined by the condition of:

$$\int_0^\infty p(a)da = 1 \tag{3.2-9}$$

Substituting (3.2-8) into (3.2-9) yields:

$$\int_0^\infty C\frac{p_0(a)}{P_D(a)}da = 1 \quad \text{or} \quad C = 1/\int_0^\infty \frac{p_0(a)}{P_D(a)}da \tag{3.2-10}$$

Therefore, according to (3.2-8):

$$p(a) = \frac{p_0(a)}{P_D(a)}\Bigg/\int_0^\infty \frac{p_0(a)}{P_D(a)}da \tag{3.2-11}$$

Note that the actual and detected damage size distributions are two distinct functions in this equation.

Finally, "Level of Safety" is defined as 1- *Probability*(damage size ≥ a_c | not detected), where a_c is the critical damage size for failure of the structure:

$$"Level \quad of \quad Safety" = 1 - \int_{a_c}^{\infty} p(a)[1 - P_D(a)]da \tag{3.2-12}$$

Using equation (3.2-11) for *p(a)*:

$$"Level \quad of \quad Safety" = 1 - \int_{a_c}^{\infty} \frac{p_0(a)}{P_D(a)}[1 - P_D(a)]da \Bigg/ \int_0^{\infty} \frac{p_0(a)}{P_D(a)}da \tag{3.2-13}$$

The above definition assumes a single inspection event at a fixed point in time, and that only a single discrete-source flaw is present in the structure. In most real structures, this is generally not true. Sometimes there is no flaw, and other times there are multiple flaws. The number of flaws is another random variable that must be involved to define the Level of Safety.

Assuming that hazard due to an individual flaw is independent of the existence of other flaws and there is no interaction between each of the multiple flaws, then the proper definition of "Level of Safety" for multiple flaws should be:

$$"Level \quad of \quad Safety" = \left\{ 1 - \int_{a_c}^{\infty} \frac{p_0(a)}{P_D(a)}[1 - P_D(a)]da \Bigg/ \int_0^{\infty} \frac{p_0(a)}{P_D(a)}da \right\}^{\mu} \tag{3.2-14}$$

in which the total number of flaws present in the structure at the time of evaluation is a random variable, for which the mean is μ. According to this definition, the "Level of Safety" is reduced as the number of flaws increases. Whether or not there is interaction between multiple flaws is highly dependent on the size and location of the damages relative to each other, and relative to the stress concentration zones in the structure. Damage zone interaction poses a significant analytical and modeling challenge to the structural designer, and will not be addressed any further here in order to simplify the method as much as possible.

In the case that various damage mechanisms exist simultaneously in the structure, each flaw type has its own probability distributions. Thus, the above definition should be modified to:

$$"Level \quad of \quad Safety" = \prod_{i=1}^{N_T} \left\{ 1 - \int_{a_{ci}}^{\infty} \frac{p_{0i}(a)}{P_{Di}(a)} [1 - P_{Di}(a)] da \Big/ \int_{0}^{\infty} \frac{p_{0i}(a)}{P_{Di}(a)} da \right\}^{\mu_i} \tag{3.2-15}$$

where i denotes damage type, μ_i is the mean number of flaws of type i and N_T is the total number of damage types possible in the structure. The lower integration limit a_{ci} is determined by damage tolerance criteria. When N_T, $p_{0i}(a)$, $P_{Di}(a)$, μ_i, (i=1,2,…,N_T) are known, "Level of Safety" can be expressed as a function of a_{ci}, (i=1,2,…,N_T), that is:

$$"Level \quad of \quad Safety" = F\left(a_{c_1}, a_{c_2}, \cdots, a_{c_{N_T}} \right) \tag{3.2-16}$$

For a given structure and load, a_{ci} can be found by deterministic structural analyses as the critical flaw size that can be tolerated by the damaged structure. Hence, a_{ci} is a function of load and structural geometry with specific materials, that is:

$$a_{c_i} = F_i(P, l), \qquad i = 1,2,\cdots N_T \tag{3.2-17}$$

where P is load and l is a structural sizing dimension such as sheet metal gage thickness, or the thickness of a face-sheet laminate in a sandwich panel. Substituting Equations (3.2-17) into Equation (3.2-16) yields:

$$"Level \quad of \quad Safety" = F_o(P, l) \tag{3.2-18}$$

Equation (3.2-18) relates load, structural size and "Level of Safety". When the load applied to a structure and the structure's dimension are given, "Level of Safety" can be evaluated using Equation (3.2-18). Alternatively, when required "Level of Safety" and load are given, the structure can be sized by solving Equation (3.2-18) for l.

In the case of multiple location damage in a structure, the definition of "Level of Safety" is further modified to:

$$"Level \quad of \quad Safety" = \prod_{j=1}^{N_L} \prod_{i=1}^{N_{Tj}} \left\{ 1 - \int_{a_{c_{ij}}}^{\infty} \frac{p_{0ij}(a)}{P_{Dij}(a)} \left[1 - P_{Dij}(a) \right] da \Big/ \int_{0}^{\infty} \frac{p_{0ij}(a)}{P_{Dij}(a)} da \right\}^{\mu_{ij}} \tag{3.2-19}$$

where j denotes damage type, N_L is the total number of damage locations, and N_{Tj} is the total number of damage types at location j.

In turn, the "Probability of Failure" should be:

$$"\Pr obability \quad of \quad Failure" = 1 - "Level \quad of \quad Safety"$$

$$= 1 - \prod_{j=1}^{N_L} \prod_{i=1}^{N_{Tj}} \left\{ 1 - \int_{a_{c_{ij}}}^{\infty} \frac{p_{0ij}(a)}{P_{Dij}(a)} \left[1 - P_{Dij}(a) \right] da \Big/ \int_{0}^{\infty} \frac{p_{0ij}(a)}{P_{Dij}(a)} da \right\}^{\mu_{ij}} \tag{3.2-20}$$

An illustrative example problem is given in Chapter 5.

3.3 Establishing a Baseline Level of Safety

To establish the equivalent "Level of Safety" needed for new designs to maintain the same level of safe operation as the current aircraft they are meant to replace, the "Level of Safety" of the current aircraft fleet must be benchmarked. This process involves collecting service data for the various aircraft types of interest, and using design data from the Original Equipment Manufacturer (OEM) to evaluate the probability that a critical flaw in the aircraft structure will go undetected under the normal inspection regime. Damage-tolerance design philosophy states that a flaw size becomes critical when the residual strength of a structure exposed to the flaw is lower than the strength needed to maintain safe operation of the vehicle. Under current design and certification practices, this residual strength value is at the design Limit Load for the structure.

Detailed analyses must be performed for each aircraft component to ensure that all damage mechanisms and failure modes that the parts are vulnerable to are accounted for. A "Level of Safety" value based on the formula derived in Section 3.2 must be calculated for the various damage types in each component, and these values will be unique to that component in that

particular application. In addition, reliable and repeatable methods of detecting service damage need to be identified and quantified for the existing structures. Much research has been done in the area of defining Probability of Detection (POD) curves for various forms of Non-Destructive Evaluation (NDE), and most of this work has been concentrated in the area of crack detection in stress-skinned metal airframes (Ref. 12, 13, 14). However, not all damage mechanisms inherent in a component have POD curves readily available for the specific application of interest. Many factors, such as part geometry, part location, the skill of the NDE equipment operator, or the environment in which the inspection takes place will significantly affect POD results, and can shift the curve dramatically one way or the other. All of these variables need to be taken into account in the evaluation of equivalent "Level of Safety", as they can have an importance equal to or greater than the deterministic aspects of residual strength calculation. Extensive testing and analysis may be necessary to verify that the assumed values of the POD curves are actually being achieved during service inspections.

Another essential element to the "Level of Safety" calculations is the availability of in-service detected damage data for the specific structures of interest. The data is necessary to define probability density functions of detected damage sizes, and to characterize the amount of damage accumulated in a given time. A more detailed discussion of this topic is presented in Section 3.4.

Establishing the baseline "Level of Safety" for an existing aircraft component may be one of the most difficult and labor-intensive steps in the design under uncertainty process, but it is necessary to establish exactly what the vulnerabilities of existing structures are to service-induced damage. The results of this step are then used to define the minimum allowable "Level of Safety" for future structural designs that share similar functions and operational requirements.

3.4 Collection of Flaw Data on Existing Structures

A critical component in the determination of "Level of Safety" is the characterization of detected damage size distributions $p_o(a)$ based on inspection data for an existing structure.

Inspection data to be obtained for each part must include the type of damage, size of damage, frequency of occurrence over a given time period, damage location and the method of detection. A histogram for the flaw size distribution within a given service period can then be constructed. Although this appears to be a monumental task, much of this data is already collected for the U.S. commercial aircraft fleet on a regular basis. Licensed repair facilities regularly submit maintenance actions on commercial aircraft to the FAA in the form of Service Difficulty Reports (SDR's), which are collected in a database (SDRS) that is accessible to the public. Although the database is not a comprehensive archive of all instances of detection and repair of flaws, it can provide much of the data necessary for aircraft designers and certification authorities to develop consistent damage size distribution curves for structures under real-world operational conditions. Small changes in the format of the system may make it easier to utilize the data for "Level of Safety" calculations. However, further investigation into the details of this specific application is beyond the scope of this research effort.

To demonstrate the possible utility of such a tool, Boeing has succeeded in collecting raw data for discrete-source cracks in the fuselage skins of several of its aircraft using the SDRS database. From this data, a Weibull distribution can be fitted through the data points to give a first-order estimate of the probability density function of detected crack sizes $p_o(a)$ in an aircraft structure. It should be noted that the sizes of these detected cracks are a function of the method of detection, hence the need to define the detection method for each data point utilized.

Other methods have also been used to obtain damage data on in-service aircraft. Gary and Riskalla used on-site visits to airline maintenance facilities and Naval aviation depots to evaluate the damage characteristics of composite airframe structures for their work on probabilistic design methodologies (Ref. 11). Regardless of the data collection methods utilized, it should be apparent that it is virtually impossible to record every instance of detected damage over the lifetime of a component, so we are forced to deal with an incomplete picture of the true distribution of damage in a structure. As the size of the available data set is reduced, more and more uncertainty creeps into the estimation of the

probability density functions. Research is ongoing to characterize the uncertainty of density functions associated with limited data sets, and to explore the sensitivity of "Level of Safety" calculations to these effects.

3.5 Application of Methodology to Advanced Structural Design Concepts

With a baseline value for the "Level of Safety" of an existing structure in place, new materials and structural concepts can be incorporated into the design of replacement structures with higher levels of performance, while maintaining or improving upon current safety levels. The structural integrity of existing aircraft is ensured primarily through deterministic analysis and testing in the design process and extensive in-service experience, most of which has been derived from traditional aluminum alloy, stressed-skin construction techniques. The lack of service experience with new materials and structural concepts makes it difficult for these applications to find their way onto new aircraft designs, owing to the large amount of uncertainty regarding how the advanced structure will perform under an operational environment.

Using a traditional building block approach, damage mechanisms and their effect on residual strength must be identified for any new material or structural system. This process starts at the material level, and gradually works up through the component and sub-structure level to the final system design level. Along the way, assumptions are made about the nature of the damage environment the structure will be exposed to in service, and how the symptoms of damage will manifest themselves to the operator. Reliable means of detecting the various damage mechanisms must be identified and put into place before the concept can be declared ready for service, and there are also uncertainties associated with this process.

The "Level of Safety" methodology defined previously allows the engineer to incorporate these uncertainties into the design process. By carefully choosing the parameters of the statistical functions that define the probability distributions for detected damage size $p_o(a)$ and detection probability $P_D(a)$, the designer can quantify the relative amount of risk in the concept. Use of component test data, experience with similar concepts in different

applications, empirical evidence and engineering judgement are all tools that can be used to define the level of risk inherent in the new design.

With the uncertainties in the damage tolerance characteristics of the new concept accounted for, the "Level of Safety" definition is then used to generate curves of "Level of Safety" values vs. flaw size for each type of damage mechanism present in the structure. Using the baseline "Level of Safety" value as an allowable, critical damage sizes can be identified, either individually or in combination, that will give a safety level equivalent to previous designs. Deterministic analysis methods are then used to generate contour plots of residual strength vs. flaw size for each damage mechanism, as a function of the structural sizing parameters chosen beforehand. With these relationships defined, the structure can now be sized for a given load level to yield a relative damage-tolerance safety equal to, or greater than the existing structure.

3.6 Damage Size Updating Schemes

Once a new structure has been built and put into service, data on how it is actually performing under operational conditions becomes available through scheduled inspection and maintenance actions. The data can be utilized to validate the initial assumptions about damage tolerance behavior made in the design process, and to reduce the level of uncertainty inherent in those assumptions. This can be accomplished by the use of Bayesian statistical methods (Ref. 15) to modify the distribution curves for detected damage sizes. Based on the revised curves, "Level of Safety" values can be recalculated for the structure. If it is found that the value has decreased due to the accumulation of larger or more frequent damage than initially assumed during design, the inspection and maintenance program can be revised to provide earlier or more frequent detection opportunities in a given time period, and the "Level of Safety" can be returned to its design value.

The Weibull relation is a very well known model used to predict systems reliability in manufactured products. Failure mechanisms in many different mechanical systems can often be found to approximate Weibull distributions, so this model will be chosen to represent the probability density function of detected damage size $p_o(a)$ in the "Level of Safety" method.

Other statistical models, such as Normal, Gamma or Log-Normal distributions may be appropriate, depending on the behavior of the damage mechanism of interest. For simplicity, we will only be concerned with the Weibull distribution here, however the concepts discussed are equally applicable to any statistical model of a continuous random variable distribution. The probability density function of the Weibull model is:

$$p_o(a) = \frac{\alpha}{\beta^{\alpha}} a^{\alpha-1} \exp\left[-\left(\frac{a}{\beta}\right)^{\alpha}\right] \tag{3.6-1}$$

Assume that the initial detected damage size distribution has Weibull parameters $\alpha = 2$ and $\beta = 4$. In Bayesian analyses, the parameters in the density function are considered random variables. However, for simplicity, the scale parameter β is assumed to be a constant 4 for initial detected damage size distribution:

$$p_o(a \mid \alpha) = \frac{\alpha}{4^{\alpha}} a^{\alpha-1} \exp\left[-\left(\frac{a}{4}\right)^{\alpha}\right] \tag{3.6-2}$$

The shape parameter α is assumed to follow a Gamma distribution with its mean of 2, and a standard deviation of 0.4, that is:

$$f_o(\alpha) = \frac{1}{0.08^{25}\,\Gamma(25)} \alpha^{24} \exp\left(-\frac{\alpha}{0.08}\right) \tag{3.6-3}$$

for $\alpha > 0$, otherwise $f_o(\alpha) = 0$. When new detected damge size data are obtained as $a_1, a_2, \ldots, a_n$, the detected damage size distribution can be updated using the new information. The actual detected damage sizes, $a_1, a_2, \ldots, a_n$, are random variables.

Let $f_j(a_1,a_2,\ldots,a_n,\alpha)$ denote joint probability density function of $a_1,a_2,\ldots,a_n$ and α. The probability density function of α under condition of given detected damage size data, $a_1,a_2,\ldots,a_n$, is:

$$f_u(\alpha \mid a_1, a_2, \cdots, a_n) = \frac{f_j(a_1, a_2, \cdots, a_n, \alpha)}{\int_{-\infty}^{\infty} f_j(a_1, a_2, \cdots, a_n, \alpha) d\alpha} \tag{3.6-4}$$

Let $g(a_1,a_2,\ldots,a_n|\alpha)$ denote conditional joint probability density function of $a_1,a_2,\ldots,a_n$ under condition of given α. Then:

$$f_j(a_1, a_2, \cdots, a_n, \alpha) = g(a_1, a_2, \cdots, a_n \mid \alpha) f_o(\alpha) \tag{3.6-5}$$

Substituting (3.6-5) into (3.6-4) yields:

$$f_u(\alpha \mid a_1, a_2, \cdots, a_n) = \frac{g(a_1, a_2, \cdots, a_n \mid \alpha) f_o(\alpha)}{\int_{-\infty}^{\infty} g(a_1, a_2, \cdots, a_n, \mid \alpha) f_o(\alpha) d\alpha} \tag{3.6-6}$$

Since random variables $a_1,a_2,\ldots,a_n$ are mutually independent, we have:

$$g(a_1, a_2, \cdots, a_n \mid \alpha) = \prod_{i=1}^{n} p_o(a_i \mid \alpha) \tag{3.6-7}$$

Substituting (3.6-7) into (3.6-6) yields:

$$f_u(\alpha \mid a_1, a_2, \cdots, a_n) = \frac{\prod_{i=1}^{n} p_o(a_i \mid \alpha) f_o(\alpha)}{\int_{-\infty}^{\infty} \prod_{i=1}^{n} p_o(a_i \mid \alpha) f_o(\alpha) d\alpha} \tag{3.6-8}$$

That is, the probability density function of α under condition of given $a_1,a_2,\ldots,a_n$. The prior and the posterior distributions of α are plotted in Figure 2. The Bayesian estimate of α is the mean of the updated random variable α, that is:

$$\hat{\alpha} = \int_{-\infty}^{\infty} \alpha f_u(\alpha \mid a_1, a_2, \cdots, a_n) d\alpha \tag{3.6-9}$$

The updated distribution of detected damage size is obtained using the Bayesian estimate of alpha for the Weibull distribution of detected flaw size:

$$p_o(a \mid \hat{\alpha}) = \frac{\hat{\alpha}}{4^{\hat{\alpha}}} a^{\hat{\alpha}-1} \exp\left[-\left(\frac{a}{4} \right)^{\hat{\alpha}} \right] \tag{3.6-10}$$

The initial and updated flaw size distributions are given in Figure 3. An alternative approach to reach an updated detected flaw size distribution is to use the marginal probability density function of $p_o(a|\alpha)$ of Equation (3.6-2), that is:

$$p_o(a) = \int_{-\infty}^{\infty} p_o(a \mid \alpha) f_u(\alpha) d\alpha = \int_{-\infty}^{\infty} \frac{\alpha}{4^{\alpha}} a^{\alpha-1} \exp\left[-\left(\frac{\alpha}{4} \right)^{\alpha} \right] f_u(\alpha) d\alpha \tag{3.6-11}$$

where $f_u(\alpha)$ is the updated probability density function of α, which is given in Equation (3.6-8). As an example, when newly detected damage sizes are a_1 = 3 inch, a_2 = 4 inch, a_3 = 5 inch, n = 3, the Bayesian estimate of α is calculated as 2.1831 using equations (3.6-2), (3.6-3), (3.6-8), (3.6-9). The updated probability density function of the detected damage size is equation (3.6-10).

When both Weibull parameters α and β are treated as random variables, these parameters can be updated simultaneously. Let us assume that initial α and β are independent. Then, the joint probability density function of α and β is:

$$f_o(\alpha, \beta) = f_o(\alpha) f_o(\beta) \tag{3.6-12}$$

Similar to the derivation of (3.6-8), the updated joint probability density function of α and β, under the condition of measured flaw sizes $a_1, a_2, \ldots, a_n$, is obtained from:

$$f_u(\alpha, \beta \mid a_1, a_2, \cdots, a_n) = \frac{\prod_{i=1}^{n} p_o(a_i \mid \alpha, \beta) f_o(\alpha, \beta)}{\int_{-\infty}^{\infty} \int_{-\infty}^{\infty} \prod_{i=1}^{n} p_o(a_i \mid \alpha, \beta) f_o(\alpha, \beta) d\alpha d\beta} \tag{3.6-13}$$

The marginal probability density functions of α or β are then derived through integration as:

$$f_{\alpha u}(\alpha \mid a_1, a_2, \cdots, a_n) = \int_{-\infty}^{\infty} f_u(\alpha, \beta \mid a_1, a_2, \cdots, a_n) d\beta \tag{3.6-14}$$

$$f_{\beta u}(\beta \mid a_1, a_2, \cdots, a_n) = \int_{-\infty}^{\infty} f_u(\alpha, \beta \mid a_1, a_2, \cdots, a_n) d\alpha \tag{3.6-15}$$

The Bayesian estimate of α or β is the mean of the updated random variable α or β, respectively.

$$\hat{\alpha} = \int_{-\infty}^{\infty} \alpha f_{\alpha u}(\alpha \mid a_1, a_2, \cdots, a_n) d\alpha \tag{3.6-16}$$

$$\hat{\beta} = \int_{-\infty}^{\infty} \beta f_{\beta u}(\beta \mid a_1, a_2, \cdots, a_n) d\beta \tag{3.6-17}$$

The updated distribution of detected damage size is obtained using Bayesian estimates of α and β for the Weibull distribution:

$$p_o(a \mid \hat{\alpha}, \hat{\beta}) = \frac{\hat{\alpha}}{\hat{\beta}^{\hat{\alpha}}} a^{\hat{\alpha}-1} \exp\left[-\left(\frac{a}{\hat{\beta}} \right)^{\hat{\alpha}} \right] \tag{3.6-18}$$

Alternatively, the updated distribution of detected damage size can also be obtained using the marginal density function through integration as follows:

$$\begin{aligned} p_o(a) &= \int_{-\infty}^{\infty} \int_{-\infty}^{\infty} p_o(a \mid \alpha, \beta) f_u(\alpha, \beta \mid a_1, a_2, \cdots, a_n) d\alpha d\beta \\ &= \int_{-\infty}^{\infty} \int_{-\infty}^{\infty} \frac{\alpha}{\beta^{\alpha}} a^{\alpha-1} \exp\left[-\left(\frac{a}{\beta} \right)^{\alpha} \right] f_u(\alpha, \beta \mid a_1, a_2, \cdots, a_n) d\alpha d\beta \end{aligned} \tag{3.6-19}$$

It should be pointed out that the above Bayesian approach is to update detected damage size distribution using later obtained damage size measurements that must have the same probability of detection. When different probabilities of detection are employed, the detected damage size must be modified before being used in Bayesian updating. Such a modification can be performed accordingly as:

$$a_2 = a_1 \frac{P_{D2}(a_2)}{P_{D1}(a_1)} \tag{3.6-20}$$

where a_1 and a_2 are damage sizes obtained by inspection type 1 and 2, respectively and $P_{D1}(a)$ and $P_{D2}(a)$ are corresponding probabilities of detection. When functions $P_{D1}(a)$ and $P_{D2}(a)$ are available and a_1 is detected, then a_2 can be determined by solving Equation (3.6-20), and vice versa.

An alternative way of combining new and old information is to update "actual" damage size distribution instead of detected damage size distribution. The "actual" damage size distribution $p(a)$ can be estimated from detected damage size distribution and probability of detection using Equation (3.6-11).

If $p(a)$ is selected to be the basic variable, the definitive equation for "Level of Safety" (3.2-14) becomes:

$$"Level \quad of \quad Safety" = \prod_{j=1}^{N_L} \prod_{i=1}^{N_{Tj}} \left\{ 1 - \int_{a_{c_{ij}}}^{\infty} p_{ij}(a)[1 - P_{Dij}(a)]da \right\}^{\mu_{ij}} \tag{3.6-21}$$

and the "Probability of Failure" should be:

$$"Probability \quad of \quad Failure" = 1 - \prod_{j=1}^{N_L} \prod_{i=1}^{N_{Tj}} \left\{ 1 - \int_{a_{c_{ij}}}^{\infty} p_{ij}(a)[1 - P_{Dij}(a)]da \right\}^{\mu_{ij}} \tag{3.6-22}$$

The same Bayesian method as that developed for $p_0(a)$ can be applied to update "actual" damage size distribution, $p(a)$.

3.7 Discussion

The definition of structural "Level of Safety", and the design methodology derived from it, is an extension of reliability theory and statistical analysis tools to the design and maintenance

of damage-tolerant aircraft structures. This methodology is one of the first attempts to develop a unified probabilistic approach to damage tolerance that encompasses all of the parameters specific to the design of aircraft structures, but that is flexible and general enough to be applicable to any type of material or structural configuration. Several characteristics of this approach are unique from other reliability-based damage tolerance methods that precede it.

The first is the differentiation in the method between probability distributions of detected damage size $p_0(a)$ and actual damage size $p(a)$. This is a very important distinction often overlooked in previous methods. Any attempt to collect data on damage size distributions in a structure is subject to the probability of detection of the inspection method used. Thus, damage size data should generally be represented by probability density functions for detected damage size whose distributions go to zero as the damage size goes to zero. This is necessary because an inspection method does not exist that can detect a flaw of zero size. The implications of this are that the actual distribution of damage size in a structure can never be exactly characterized, because there will always be uncertainty associated with the distributions of $p_0(a)$ and detection probability $P_D(a)$. Many probabilistic analysis methods in use today assume that the detected and actual damage size distributions are the same, which may lead to erroneous or unconservative reliability results.

A second aspect unique to this methodology is the use of Bayesian statistical tools to provide a means to characterize the uncertainty associated with the probability distributions in the "Level of Safety" method, and to enable the use of post-design inspection data to validate the probabilistic assumptions. The tools allow the designer to investigate the effects unknown risk factors may have on the safety of the structure, without having specific data available a priori. These effects can then be incorporated into the design without resorting to arbitrary knock-down factors.

Another unique aspect is the incorporation of inspection intervals to the reliability estimates for a structure. Although the addition of this variable to the derivations of the "Level of Safety" formulas has not been accomplished to date, it will be included in future iterations of

the "Level of Safety" methodology. This ultimately will allow the important parameters of an inspection and maintenance program to be included as essential variables in the preliminary design process, where maximum benefit can be realized in the sizing of the structure to obtain the best performance for the lowest life-cycle cost.

3.8 Mathematical Considerations in the Level of Safety Formulation

As mentioned in Section 3.7, the "Level of Safety" methodology differentiates between probabilities of detected damage size $p_0(a)$ and actual damage size $p(a)$. The resulting derivations have important statistical and numerical implications on the shapes that these distributions can assume. By examining the first form of Equation (3.2-8), it can be seen that the detected damage size distribution $p_0(a)$ is highly dependent on the distributions of actual damage size $p(a)$ and detection probability $P_D(a)$.

$$Cp_0(a) = p(a)P_D(a) \tag{3.2-8}$$

The form of the PDF for detection probability should be such that as the damage size approaches either zero or some minimum detection threshold, the probability of detection will go to zero. One assumption implicit in the statement of Equation (3.2-8) is that we can assign a probability to the actual distribution of damage sizes in a structure. This implies that $p(a)$ must be finite over any interval of damage size greater than zero, and zero elsewhere. Therefore, the product of the actual damage size and detection probability distributions, detected damage size distribution $p_0(a)$, must also go to zero as the damage size approaches zero. These characteristics are inconsequential for the formulation of Equation (3.2-8), but pose significant problems in the calculation of the normalizing constant C if it is in the form of Equation (3.2-10).

$$C = 1/\int_0^\infty \frac{p_0(a)}{P_D(a)}da \tag{3.2-10}$$

In this form, C is an improper integral with the value 0/0 at the lower integration limit of zero. Plotting the integrand as a function of a would show that it approaches infinity as a

goes to zero. Since the integrand is proportional to $p(a)$, the actual damage size distribution will also go to infinity as a goes to zero. Improper integrals of this type can be integrated depending on the shape of the distribution. Assume that the integrand function is proportional to the function $1/a^{\beta}$ for values of a close to zero. In order for the integral to be finite on the interval [0, ∞], the order of singularity β must be less than 1. For the types of distributions assumed for $p_0(a)$ and $P_D(a)$, a closed-form expression for the integrand is not generally available, so the order of singularity of the function cannot be determined analytically. Numerical integration can be used to check the relative convergence of the integral, provided that convergence is rapid enough to be evaluated satisfactorily before the roundoff limits of the integration routine are encountered. Equation (3.2-10) can be redefined as:

$$\lim_{\varepsilon \to 0} C = 1/\int_{\varepsilon}^{\infty} \frac{p_0(a)}{P_D(a)} da \tag{3.8-1}$$

where the limit is approximated by some small value of ε away from zero. Note that relative numerical convergence is a necessary, but insufficient condition to guarantee absolute convergence of the integral. There may be cases where the integral appears to converge, but actually diverges in the limit, particularly if the order of singularity is near one.

The parameters that define the distributions of $p_0(a)$ and $P_D(a)$, and in fact the distributions themselves, must be carefully chosen so that the integral converges to a finite value. If the integral diverges, the initial assumption that we can assign a probability to the actual damage size distribution is violated, and the values used for the parameters of the distributions are not admissible for the function. The results of these discussions emphasize the need to carefully quantify the probability of detection for any damage size data accumulated on a given structure. Failure to do so can result in distributions of actual damage size that are not valid probability density functions.

4 RESIDUAL STRENGTH DETERMINATION OF EXAMPLE STRUCTURE

4.1 Introduction

To demonstrate the equivalent "Level of Safety" approach as applied to an advanced structural concept, a graphite-epoxy honeycomb sandwich composite was selected to be used as an example material system for the redesign of a metal structure. The damage mechanisms inherent in composite sandwich structures have been well-characterized through many years of research and testing. Also, there are many composite sandwich structures (flaps, ailerons, elevators, rudders, etc.) currently in use throughout the civil and military aircraft fleets. Service-induced damage data is therefore available for a variety of these applications.

As part of the process of applying the equivalent safety methodology to a new structure, a deterministic structural analysis is developed for the characterization of the residual strengths of the sandwich panels under different types of damage. The established damage tolerance results were then used as inputs into the probabilistic design methodology.

4.2 Material Systems and Properties

The selected material system is a honeycomb sandwich panel, in which the face-sheet is a graphite-epoxy laminate and the core is made of Nomex. Variations in the strength and stiffness of the laminate were created by changing the number of plies and their stacking sequence. Three different lamination systems are used in this research. The stiffness of the core varies with honeycomb density, and Nomex honeycomb cores of three different densities were used in the study.

The ply properties of graphite/epoxy and the honeycomb core are:

Tension: $E_1 = 22.9$ mpsi, $E_2 = 1.34$ mpsi, $\nu_{12} = 0.34$,
$G_{12} = G_{13} = G_{23} = 0.29$ mpsi,
Strength in fiber direction, X = 350 ksi.
Maximum longitudinal strain, $\varepsilon_L = 15300\ \mu\varepsilon$
Maximum transverse strain, $\varepsilon_T = 5680\ \mu\varepsilon$
Maximum engineering shear strain, $\gamma_{LT} = 21000\ \mu\varepsilon$

Compression: $E_1 = 22.0$ mpsi, $E_2 = 1.34$ mpsi, $\nu_{12} = 0.34$,
$G_{12} = G_{13} = G_{23} = 0.29$ mpsi,
Strength in fiber direction, X' = 295 ksi.
Maximum longitudinal strain, $\varepsilon_L' = 13500\ \mu\varepsilon$
Maximum transverse strain, $\varepsilon_T' = 5680\ \mu\varepsilon$
Maximum engineering shear strain, $\gamma_{LT}' = 21000\ \mu\varepsilon$

Core (1): $E_1 = E_2 = 200$ psi, $E_3 = 20$ ksi, $\nu_{12} = 0.5$, $\nu_{13} = \nu_{23} = .01$,
$G_{12} = 20$ psi, $G_{13} = 7$ ksi, $G_{23} = 3.5$ ksi.

Core (2): $E_1 = E_2 = 600$ psi, $E_3 = 60$ ksi, $\nu_{12} = 0.5$, $\nu_{13} = \nu_{23} = .01$,
$G_{12} = 60$ psi, $G_{13} = 13$ ksi, $G_{23} = 6$ ksi.

Core (3): $E_1 = E_2 = 900$ psi, $E_3 = 90$ ksi, $\nu_{12} = 0.5$, $\nu_{13} = \nu_{23} = .01$,
$G_{12} = 90$ psi, $G_{13} = 17$ ksi, $G_{23} = 9$ ksi.

The thickness of the lamina is 0.005 inch and the thickness of the core is 1.0 inch.

The three laminate lay-up sequences are:

Laminate (1): $[-45/0/45/0/90]_s$ laminate thickness = 0.05 inch;

Laminate (2): $[-45/0/45/90]_{2s}$ laminate thickness = 0.08 inch;

Laminate (3): $[-45/0/45/0/90]_{2s}$ laminate thickness = 0.10 inch.

4.3 Tensile Strength of the Laminates

The tensile strength of the laminates is determined by first-ply failure theory. Using lamina property data for Laminate (1), $[-45/0/45/0/90]_s$,we have:

$$[A^{(1)}] = \begin{bmatrix} 0.6198 & 0.1220 & 0 \\ 0.1220 & 0.4027 & 0 \\ 0 & 0 & 0.1451 \end{bmatrix} \quad mpsi$$

When the longitudinal strain reaches the maximum transverse strain of the lamina, $\varepsilon_{22} = 5680$ με, the 90° ply fails. The resultant stress versus strain relation is obtained as:

$$\begin{Bmatrix} N_x^{(1)} \\ 0 \\ 0 \end{Bmatrix} = \begin{bmatrix} 0.6198 & 0.1220 & 0 \\ 0.1220 & 0.4027 & 0 \\ 0 & 0 & 0.1451 \end{bmatrix} \begin{Bmatrix} -5680 \\ \varepsilon_y \\ \gamma_{xy} \end{Bmatrix}$$

The solution of the above equation is:

$N_x = -3311$ lb/in

$\varepsilon_y = 1721$ με

$\gamma_{xy} = 0$ με

As the load increases further, the stiffness properties of the 90° ply lamina change to $E_1 = 22.9$ mpsi, $E_2 = \nu_{12} = G_{12} = 0$. Then, the stiffness matrix of the laminate becomes:

$$[A^{(2)}] = \begin{bmatrix} 0.6063 & 0.1174 & 0 \\ 0.1174 & 0.4010 & 0 \\ 0 & 0 & 0.1359 \end{bmatrix} \quad mpsi$$

According to stress resultant versus strain relation:

$$\begin{Bmatrix} N_x^{(2)} \\ 0 \\ 0 \end{Bmatrix} = \begin{bmatrix} 0.6063 & 0.1174 & 0 \\ 0.1174 & 0.4010 & 0 \\ 0 & 0 & 0.1359 \end{bmatrix} \begin{Bmatrix} \varepsilon_x \\ \varepsilon_y \\ \gamma_{xy} \end{Bmatrix}$$

The strain components in terms of load intensity are expressed as:

$\varepsilon_x = 1.5609\ N_x^{(2)}\ \mu\varepsilon$

$\varepsilon_y = -0.4570\ N_x^{(2)}\ \mu\varepsilon$

$\gamma_{xy} = 0\ \mu\varepsilon$

Using Mohr's circle, strain components in ±45 degree directions are determined as:

$\varepsilon_{45} = 0.5520\ N_x^{(2)}\ \mu\varepsilon$

$\varepsilon_{-45} = 0.5520\ N_x^{(2)}\ \mu\varepsilon$

$\gamma_{45} = 2.0179\ N_x^{(2)}\ \mu\varepsilon$

Using the maximum strain failure criteria, the failure load intensity can be determined as:

For the 0° ply lamina:

$$N_x^{(2)} = \begin{cases} \dfrac{15300}{1.5609} = 9802 & lb/in \quad longitudinal \quad direction \\ \dfrac{5680}{0.4570} = 12429 & lb/in \quad transverse \quad direction \end{cases}$$

For the 45° ply lamina:

$$N_x^{(2)} = \begin{cases} \dfrac{15300}{0.5520} = 27717 \quad lb/in \quad longitudinal \quad direction \\ \dfrac{5680}{0.5520} = 10289 \quad lb/in \quad transverse \quad direction \\ \dfrac{21000}{2.0179} = 10406 \quad lb/in \quad shear \quad failure \end{cases}.$$

Comparing these results, the 0° ply fails first in its longitudinal direction with increasing load. The failure load intensity is 9802 lb/in. After that, the strength of the laminate tremendously drops, which means the laminate fails. Therefore, the tensile strength of Laminate (1) is 9802 lb/in.

Following the same procedure, the tensile strength of Laminate (2), $[-45/0/45//90]_{2s}$, and Laminate (3), $[-45/0/45/0/90]_{2s}$, are determined as 10490 lb/in and 19604 lb/in, respectively.

4.4 Compressive strength of the laminates

The same approach used to determine the tensile strength of the laminates was also used for compressive strength. The results are:

Laminate (1), $[-45/0/45/0/90]_s$, Compressive strength = 7435 lb/in

Laminate (2), $[-45/0/45//90]_{2s}$, Compressive strength = 8930 lb/in

Laminate (3), $[-45/0/45/0/90]_{2s}$, Compressive strength = 14870 lb/in

4.5 Residual Strength of Damaged Honeycomb Sandwich Panels

Three types of possible damage commonly found in honeycomb sandwich panels, as shown in Figure 4, were analyzed. For each damage type, circular and elliptical flaw areas were considered. In order to model the skin between two stringers, the length and the width of the panel are 18 inches and 24 inches, respectively. Analysis is categorized into three cases according to the damage configuration as follows:

Case 1. A honeycomb panel with variable sizes of circular or elliptical disbonds between face sheet and core. The maximum size of the circular disbond is 8 inches in diameter. The maximum size of the elliptical disbond is 12 inches in major axis. The aspect ratio of the ellipse is 3.

Case 2. A honeycomb panel with variable sizes of circular or elliptical delaminations in one face sheet. The maximum size of the circular delamination is 8 inches in diameter. The maximum size of the elliptical delamination is 12 inches in major axis. The aspect ratio of the ellipse is 3.

Case 3. A honeycomb panel with variable sizes of circular or elliptical notches through one face sheet or through the thickness of the panel. The maximum size of the circular notch is 8 inches in diameter. The maximum size of the elliptical notch is 12 inches in major axis. The aspect ratio of the ellipse is 3.

Loading conditions in the analysis include in-plane tension or compression applied at the edges of the face-sheets of the sandwich panel. The distribution of the load along the edge is assumed to be uniform.

4.5.1 Case 1: Panels with a Disbond.

It is observed that the weakest portion of a honeycomb panel is the bonding between the face sheets and the core. The causes of the damage may be either impact from outside or manufacturing defects. When the panel is loaded in in-plane tension, the local disbond has little strength degradation since the load is carried mostly by the face-sheets. This results from the core having a much smaller in-plane stiffness than the face-sheet.

However, the disbond significantly reduces the in-plane compressive strength of the sandwich panel because of local buckling of the face sheet in the disbond area. Therefore, the tensile residual strength of the sandwich panel is assumed to be the same as the total

tensile strength of the two face-sheets, and only sandwich panels that are loaded in in-plane compression are analyzed to determine their residual strength due to disbond.

4.5.1.1 Tensile Residual Strength of a Sandwich Panel with a Disbond.

Based on the above discussion, the residual strengths of honeycomb sandwich panels with a disbond loaded in in-plane tension are independent of disbond size and core properties and thickness. Since the tensile strength of the laminates are already obtained and the sandwich panel has two face sheets, the residual strengths of the sandwiches should be:

Residual tensile strength of the sandwich with laminate (1) = 19604 lb/in,

Residual tensile strength of the sandwich with laminate (2) = 20980 lb/in,

Residual tensile strength of the Sandwich with laminate (3) = 39208 lb/in.

4.5.1.2 Compressive Residual Strength of a Sandwich Panel with a Disbond.

The residual strength of the disbond-damaged sandwich panel loaded in in-plane compression is actually its post-buckling strength. The post-buckling strength here means the maximum load the sandwich panel can take when post-buckling occurs in the disbond area. The value of the post-buckling strength depends on the size and shape of the disbond area, the stiffness of the face-sheet and the stiffness of the core.

A novel two-step analysis approach has been utilized to determine post-buckling strength of damaged sandwich panels due to local buckling. The two steps are: i) determination of critical buckling load, and ii) using the critical buckling load and maximum strain criterion of the lamina to determine post-buckling residual strength.

Step 1. Determination of critical buckling load

Finite element model

Due to the complexity of the geometry of the sandwich panel with a disbond, a finite element method must be used to obtain the solution. The general-purpose commercial finite element code ABAQUS is adopted as the tool for this task (Ref. 16). In this analysis, the face sheet laminate is modeled by shell elements with six degrees of nodal freedom and layered orthotropic elasticity as the material property. The honeycomb core is modeled by elastic springs connecting two face sheets with equivalent compressive stiffness of the core material. The local disbond is modeled by disconnecting the springs within the corresponding area.

Due to the symmetry of the panel, the geometry of the disbond damage and the loading condition, only a quarter of the panel needs to be analyzed. The finite element mesh used in the analysis is shown in Figure 5 for a circular disbond and in Figure 6 for an elliptical disbond. Symmetric boundary conditions are prescribed along the left and lower edges of the finite element model. Pressure load is applied along the top edges of the face sheet of the finite element model.

Determination of Equivalent Spring Stiffness

Due to the stress concentration at the edge of the damage area, the finite element mesh is not uniform. When one spring is connected to each node of the face sheet, the equivalent stiffness of the spring depends on the local density of the mesh. In order to determine the equivalent stiffness of each spring, the following method is used:

(1) Prescribe out-of-plane constraint on all the nodes of the finite element model of a face sheet, which is comprised of shell elements.

(2) Apply a uniform pressure on the top surface of the face-sheet finite element model. The amount of the pressure is equal to the out-of-plane stiffness of the honeycomb core.

(3) Perform ABAQUS static stress analysis to obtain reaction forces at all the nodes. The reaction force at each node is the equivalent stiffness of the spring that will be connected to the same node.

(4) Convert the ABAQUS output data format into its input data format for these spring stiffness' through a Fortran program.

(5) Alterations of the core stiffness, as required in the parametric study, only need to multiply the ratio of the core stiffness to the known equivalent spring stiffness through another Fortran program.

Since the disbond sizes are variable, the above procedures were used once for the finite element model associated with each disbond size.

Verification of Finite Element Models for Buckling Load Determination

In order to obtain reliable results, the finite element model was verified with available solutions of buckling analyses. Since closed-form solutions of the critical load of a sandwich panel due to local buckling are generally not available, only a face–sheet with out-of-plane constraint is considered in the verification. The out-of-plane constraint to the face sheet is on all the nodes except the nodes within the disbond area. The buckling loads of an isotropic rectangular plate with a circular disbond of varying sizes were computed and compared with Timoshenko's solution (Ref. 17) as shown in Figure 7. The case of an isotropic rectangular plate with an elliptical disbond of varying size is also checked with existing solutions in Yin and Jane (Ref. 18, 19) as shown in Figure 8. The material properties used in the verification computation are Young's modulus E = 10 Msi., Poisson's ratio $\nu = 0.3$, and a plate thickness of 0.005 inch. Reasonable agreement is reached between the present results and the well-known solution.

Results of Critical Buckling Load Versus Disbond Size.

The critical buckling load of a face-sheet laminate with a circular disbond or an elliptical disbond loaded in compression was computed using the finite element model described above. The results of the critical buckling load versus damage size relationship are shown in Figure 9 and Figure 11 for the case of a circular disbond, and shown in Figure 10 and Figure 12 for the case of an elliptical disbond.

Parametric studies were also conducted in terms of lamina stacking sequence or laminate thickness. In Figure 11 and Figure 12, the varying parameter is stacking sequence. Even though the laminates have the same percentage of plies in each orientation, the critical buckling loads are different, especially in the case of elliptical disbond damage. In Figure 9 and Figure 10, laminate thickness is varied. To provide enough data points, an intermediate thickness is plotted using a different stacking sequence than for the other two laminates. A nonlinear relationship between the critical buckling load and the laminate thickness is observed. When the disbond damage size is small, a small increase in laminate thickness results in a large increase in critical buckling load. This is consistent with the bending stiffness versus thickness relation.

Step 2. Determination of Post-Buckling Residual Strength due to Local Buckling.

Background

In general, post-buckling residual strength of a laminate face-sheet with local damage can be determined through a geometrically nonlinear finite element analysis and a material failure criterion (Ref. 18, 19, 20, 21). This type of analysis is extensive and is presently beyond the thrust of this research effort. Thus, an efficient engineering approach needed to be developed.

In the earlier work of Dost, et al. (Ref. 22), a simple model was proposed. This model assumes that the effect of the buckled area on the laminate is a soft inclusion. A reduced elastic modulus for the inclusion is used in determining the residual strength of the damaged

laminate. Obviously, this model can only be used for isotropic plates and Quasi-isotropic laminates, and is not suitable for the present study.

Model for post-buckling residual strength determination

According to linear-elastic stability theory, when buckling occurs, a constant load can still be carried by the buckled portion of the structure, but an uncertain level of deflection may exist. According to this concept, the following three assumptions are made.

1. As an increasing load is applied to the edge of the laminate, the buckled area of the laminate carries a constant load, that is, the critical buckling load. This load causes a normal strain in the loading direction throughout the laminate, but no stress or strain concentration occurs even at the critical location of the edge of the buckled area.

2. Other portion of the laminate can carry additional load. However, the total strain at the critical location of the edge of the buckled area is the sum of the strain caused by the additional load and the critical buckling load. The laminate fails when the total strain reaches the maximum strain limit of the zero degree ply lamina.

3. The additional load is carried by the laminate excluding the material of the buckled portion. This loaded structure is modeled as the original laminate with a through notch located at the buckled area. The size and the shape of the notch are the same as buckled portion of the laminate. The critical location is the notch-tip.

Based on these assumptions, the post-buckling residual strength, P_{post} should be:

$$P_{post} = P_{cr} + P_{add} \tag{4.5.1-1}$$

where P_{cr} and P_{add} denote the critical buckling load and the additional load, respectively. The additional load is determined by maximum normal strain criterion, that is:

$$(P_{cr} + P_{add}\, K)\varepsilon_o = \varepsilon_{max} \tag{4.5.1-2}$$

in which K is the notch-tip strain concentration factor, ε_o and ε_{max} represent the uniform strain of the undamaged laminate in the loading direction due to unit load and maximum

strain the material can endure, respectively. As listed in the lamina property section, the maximum compressive strain of the present lamina is ε_{max} =13500 με. ε_o is derived in the laminate property determination procedures and the results are that ε_o = 1.8158 με for Laminate (1), ε_o = 1.5117 με for Laminate (2), and ε_o = 0.9079 με for laminate (3), respectively. Since K can be determined by finite element analysis, there are only two unknowns, P_{post} and P_{add} in Equation (4.5.1-1) and Equation (4.5.1-2). Solving for P_{post} yields:

$$P_{post} = P_{cr} + \left(\frac{\varepsilon_{max}}{\varepsilon_o} - P_{cr} \right) \frac{1}{K} \qquad (4.5.1\text{-}3)$$

Equation (4.5.1-3) is then used to calculate post-buckling residual strength of the sandwich panels with either a circular disbond or an elliptical disbond. The strain concentration factor K is calculated by a finite element analysis using ABAQUS. In order to obtain reliable results, the appropriateness of the finite element model as well as the subsequent data reduction method must be examined in advance.

Verification of Finite Element Models for Notch-Tip Strength Analysis

The same finite element models were constructed as that for the buckling analysis except that the elements in the disbond area are removed. In order to make comparisons with the classical solution, material property of isotropic elasticity is used. The stress computed by the finite element analysis is extrapolated to the notch-tip. The computed stress values from three closest to the notch-tip elements along the line of symmetry are used. A second order polynomial is selected to fit the data.

Figure 13 and Figure 14 show the comparisons of the computed normal stress distribution in loading direction and the analytical solution (Ref. 23). Acceptable accuracy of the simple finite element model is obtained. The same extrapolation procedures are used in the evaluation of notch-tip strain to determine the strain concentration factors for both circular disbond and elliptical disbond situations.

Results of Post-Buckling Residual Strength Versus Disbond Size

The post-buckling residual strength of the sandwich panel with a circular disbond or an elliptical disbond on a face-sheet laminate loaded in compression was computed using the method described above. The results of post-buckling residual strength versus damage size relationship are shown in Figure 15 and Figure 17 for the case of circular disbond, and shown in Figure 16 and Figure 18 for the case of elliptical disbond.

Parametric studies were also conducted in terms of lamina stacking sequence or laminate thickness. In Figure 17 and Figure 18, the varying parameter is stacking sequence. There is no significant difference in the post-buckling residual strength as a result of variation in stacking sequence. In Figure 15 and Figure 16, the varying parameter is laminate thickness. An almost linear relationship between the critical buckling load and the laminate thickness is observed. When the damage size is small, the residual strength is limited by the compressive strength of the sandwich panel, which is the total compressive strength of the two face-sheets. This result means that the sandwich panel can tolerate small areas of disbond without reduction of compressive strength.

4.5.2 Case 2: Panels with a Delamination

Another commonly observed damage mechanism in sandwich panels is the delamination of the face-sheet laminate. Delaminations may be caused by either impact damage from outside or manufacturing defects. When the panel is loaded in in-plane tension, there should be, in general, a variable level of strength degradation since the materials on the opposite sides of the delamination do not have the same in-plane strain. Consequently, fracture mechanics analysis must be conducted and extensive computations are required. For the purposes of this research effort, such an analysis and computation is not intended and only a simple case is selected to show the feasibility of the approach and the relative data trends.

The simple case is that the delamination occurs in the plane of symmetry of the symmetric laminate analyzed in the study. Since the load is primarily carried by the face-sheet, the load can be assumed as acting in the plane of symmetry of the laminate. In this situation, the

material on two sides of the delamination will still have the same in-plane strain and the load carrying capacity of the laminate is not affected.

However, the delamination significantly reduces the in-plane compressive strength of the sandwich panel because of local buckling of the face sheet in the delaminated area. Therefore, the tensile residual strength of the sandwich panel is assumed to be the same as the total tensile strength of the two face-sheets, and only sandwich panels that are loaded in in-plane compression were analyzed to determine their residual strength due to delamination.

4.5.2.1 Tensile Residual Strength of a Sandwich Panel with a Delamination

Based on the above discussion, the residual strengths of honeycomb sandwich panels with delaminations loaded in in-plane tension are independent of delamination size and core properties and thickness. Since the tensile strength of the laminates are already obtained and the sandwich panel has two face sheets, the residual strengths of the sandwich should be:

Residual tensile strength of the sandwich with laminate (1) = 19604 lb/in,

Residual tensile strength of the sandwich with laminate (2) = 20980 lb/in,

Residual tensile strength of the Sandwich with laminate (3) = 39208 lb/in.

4.5.2.2 Compressive Residual Strength of a Sandwich Panel with a Delamination

The residual strength of the delamination damaged sandwich panel loaded in in-plane compression is actually its post-buckling strength. The post-buckling strength here means the maximum load the sandwich panel can take when post-buckling of the sub-laminate occurs in the delamination area. The value of the post-buckling strength depends on the size and shape of the delamination area, the stiffness of the sub-laminate of the face-sheet and the stiffness of the core.

The two-step analysis approach to the residual strength of sandwich panels due to disbond was also used to determine post-buckling residual strength of damaged sandwich panels due to delamination.

Step 1. Determination of Critical Buckling Load

Finite element model

In order to model the delamination, the locally delaminated face sheet is represented by two bonded layers of shell elements. The same type of element was used as for the panel with a disbond. The two layers of the shell elements are connected by rigid beam elements at each in-plane nodal point. The honeycomb core is modeled by elastic springs connecting the two face sheets with equivalent compressive stiffness of the core material. The local delamination is modeled by disconnecting the two layers of shell elements within the corresponding area.

Only a quarter of the sandwich panel needs to be analyzed, owing to the symmetry of the panel, the geometry of the delamination damage and the loading condition. The same in-plane finite element meshes as in the analysis of a panel with a disbond were used, which are shown in Figure 5 for a circular delamination and in Figure 6 for an elliptical delamination, respectively. Symmetric boundary conditions are also prescribed along the left and lower edges of the finite element model, and pressure load is also applied along the top edges of the face sheet of the finite element model as in the disbond model.

Determination of Equivalent Spring Stiffness

The same procedures used for Case 1 were used for this case. The only difference is that in this case the stiffness of the springs are independent of damage size. The reason is that one layer of the face-sheet laminate is always bonded to the core. Every node of this layer of the finite element model is connected to a spring regardless of the size of the delamination.

Verification of Finite Element Models for Buckling Load Determination

The verification of the finite element analysis for critical buckling load determination provided in the section of disbond damage is still meaningful for the case of delamination damage. Hence, it is not repeated here.

Results of Critical Buckling Load Versus Delamination Size

The critical buckling load of a face-sheet laminate with a circular delamination or an elliptical delamination loaded in compression was computed using the finite element model described above. The results of the critical buckling load versus damage size relationship are shown in Figure 19 and Figure 21 for the case of circular delamination, and shown in Figure 20 and Figure 22 for the case of elliptical delamination.

Parametric studies were also conducted in terms of lamina stacking sequence or laminate thickness. In Figure 21 and Figure 22, the varying parameter is stacking sequence. Even though the laminates have the same percentage of plies in each orientation, the critical buckling loads are different. In Figure 19 and Figure 20, the varying parameter is laminate thickness. To provide enough data points, an intermediate thickness is plotted using a different stacking sequence than for the other two laminates. A nonlinear relationship between the critical buckling load and the laminate thickness is observed. When the damage size is small, a small increase in laminate thickness results in a large increase in critical buckling load. This is consistent with the bending stiffness versus thickness relation.

Step 2. Determination of Post-Buckling Residual Strength due to Local Buckling

Background

The method for determination of post-buckling residual strength due to local buckling, as described in the section of disbond damage, is still valid for the case of delamination. The exception is that the assumed notch in the model described in the last section is only on the buckled layer of the sub-laminate of the face-sheet laminate instead of being through-the-thickness. The same extrapolation procedures as those used for the case of disbond damages

are used in the evaluation of notch-tip strain to determine the strain concentration factors for the case of delamination damages.

Results of Post-Buckling Residual Strength Versus Delamination Size

The post-buckling residual strength of the sandwich panel with a circular delamination or an elliptical delamination on a face-sheet laminate loaded in compression was computed using the method described above. The results of post-buckling residual strength versus damage size relationship are shown in Figure 23 and Figure 25 for the case of a circular delamination, and shown in Figure 24 and Figure 26 for the case of an elliptical delamination.

Parametric studies were also conducted in terms of lamina stacking sequence or laminate thickness. In Figure 25 and Figure 26, the varying parameter is stacking sequence. There is no significant difference in the post-buckling residual strength as a result of the variation in stacking sequence. In Figure 23 and Figure 24, the varying parameter is laminate thickness. An almost linear relationship between the critical buckling load and the laminate thickness is observed. When the damage size is small, the residual strength is limited by the compressive strength of the sandwich panel, which is the total compressive strength of the two face-sheets. This result means that the sandwich panel can tolerate small areas of delamination.

4.5.3 Case 3: Panels with Notches

Severe impact damage occurring in a face sheet laminate is often treated as an open hole for convenience. The open hole can then be modeled as a through-the-thickness notch in the damaged area. Notch data can also be used to model cracks, and so notch analyses results for this study were assumed to be applicable to both open hole and through-thickness crack behavior of the sandwich. The notched strength of the laminate cannot be directly calculated from the stress concentration factor and the unnotched strength of the laminate. In fact, the strength of the laminate material in the stress concentration area is usually higher than the global strength of the laminate. Extensive research has been conducted in past two decades and many theories have been developed to describe this phenomenon (Ref. 23, 24, 25, 26, 27,

28). However, due to the complicated nature of the composite structure subject to damage, up to now there is still no means to determine notched strength without testing a notched laminate specimen.

The residual strength of a sandwich panel with a notch on its one or two face-sheet laminates or through its thickness is primarily determined by the residual strength of the constitutive laminates. Therefore, test data on the residual strength of a laminate were used. The data are characterized by the well-accepted Mar-Lin model (Ref. 25). However, the Mar-Lin parameters are for laminates that are infinitely large and have different lamina tensile and compressive strengths from the material used here. In order to use the test data to determine residual strength of the sandwich panels, three-dimensional finite element analyses were performed to make the correction.

Mar-Lin Model Parameters

The fracture model proposed by Mar and Lin is expressed in the following form:

$$\varepsilon_N^{\infty} = \frac{H_c}{(2c)^m Y} \qquad (4.5.3\text{-}1)$$

in which:

ε_N^{∞} = remote strain

m = order of singularity

H_c = composite fracture toughness

c = half crack length

Y = geometry factor

The basic material properties and the Mar-Lin model parameters used in this study are:

In tension:

Ply strength in fiber direction, X = 250 ksi,

Laminate (1) $[-45/0/45/0/90]_s$ $H_c = 0.00667$ in^m, $m = 0.225$,

Laminate (2) $[-45/0/45/90]_{2s}$ $H_c = 0.00667$ in^m, $m = 0.203$,

Laminate (3) $[-45/0/45/0/90]_{2s}$ $H_c = 0.00667$ in^m, $m = 0.225$,

In compression:

Ply strength in fiber direction, X' = 220 ksi,

Laminate (1) $[-45/0/45/0/90]_s$ $H_c = 0.0034$ in^m, $m = 0.35$,

Laminate (2) $[-45/0/45/90]_{2s}$ $H_c = 0.0043$ in^m, $m = 0.26$,

Laminate (3) $[-45/0/45/0/90]_{2s}$ $H_c = 0.0034$ in^m, $m = 0.35$,

The remote load intensity is then calculated by:

$$P_N^\infty = \varepsilon_N^\infty E_N T_L \qquad (4.5.3\text{-}2)$$

in which E_N is the in-plane elastic modulus of the laminate in loading direction and T_L is the thickness of the laminate. For the laminate used here, these parameters are:

In tension:

Laminate (1) $[-45/0/45/0/90]_s$ $E_N = 11.653$ mpsi, $T_L = 0.05$ inch,

Laminate (2) $[-45/0/45/90]_{2s}$ $E_N = 8.841$ mpsi, $T_L = 0.08$ inch,

Laminate (3) $[-45/0/45/0/90]_{2s}$ $E_N = 11.653$ mpsi, $T_L = 0.10$ inch,

In compression:

Laminate (1) $[-45/0/45/0/90]_s$ $E_N = 11.233$ mpsi, $T_L = 0.05$ inch,

Laminate (2) $[-45/0/45/90]_{2s}$ $E_N = 8.541$ mpsi, $T_L = 0.08$ inch,

Laminate (3) $[-45/0/45/0/90]_{2s}$ $E_N = 11.233$ mpsi, $T_L = 0.10$ inch,

The elastic modulus values are calculated from lamina properties given in Section 4.2 using lamination theory.

Finite Element Model

Two finite element models were constructed for the analysis of the sandwich panels with notches. One of them is for the case that a notch is in one face-sheet and the other is for the case of a through-the-thickness notch. The finite element model of the two face sheets is the same as that used in the analysis of a panel with a disbond. The honeycomb core is modeled by eight-node solid elements with linear elastic properties. The connection between each face sheet and the core is built with rigid beam elements positioned at every in-plane nodal point of the 3-D finite element model of the sandwich panel.

In the case of only one face-sheet having a notch, the geometry of the notched panel and its associated loading condition allow only a quarter of the panel to be analyzed. Due to the same reason and the symmetry about the mid-plane of the sandwich panel, only one eighth of the panel needs to be analyzed for the case of both the face-sheet and the core having a through-the-thickness notch. The in-plane finite element meshes used in this analysis are also the same as those in the previous cases. The boundary conditions and the loading conditions are also prescribed in the same manner as in the previous cases.

Geometry Factors

The geometry factors for the case of one face-sheet having a notch and the case of the sandwich panel having a through-the-thickness notch of variable size were obtained by finite element analysis. The baseline case is that the laminate size is 90 in $\times$ 90 in, which is at least 60 times the notch size.

Results of Residual Strength Versus Notch Size

Assuming that the Mar-Lin model parameter H_c is proportional to the corresponding lamina strength in both tension and compression, the residual strength of the sandwich panel with a face-sheet laminate having a circular notch or an elliptical notch loaded in tension or in compression was calculated according to the formula:

$$P_R = \frac{2H_c E_N T_L}{(2c)^m Y} \frac{S}{S_o} \qquad (4.5.3\text{-}3)$$

in which S denotes the current ply strength in the fiber direction and S_o the ply strength in the fiber direction of the test specimen used in the test. Equation (4.5.3-3) is derived using Equation (4.5.3-1), Equation (4.5.3-2), the assumption on H_c and consideration of two laminates carrying load.

The results of the tensile residual strength versus damage size relationship are shown in Figure 27 and Figure 29 for the case of a circular notch, and shown in Figure 28 and Figure 30 for the case of an elliptical notch, respectively. The results of the compressive residual strength versus damage size relationship are shown in Figure 31 and Figure 33 for the case of a circular notch, and shown in Figure 32 and Figure 34 for the case of an elliptical notch, respectively. Parametric studies were also conducted in terms of laminate thickness and the results are given in the figures.

4.6 Discussion

It was found that the core stiffness cannot be an independent variable. The thicker the laminate, the stiffer the core must be to avoid global buckling of the face sheet. Another factor for selecting core stiffness is the weight of the sandwich panel. For the same core material, the stiffer core will generally be heavier. Therefore, the best core density or stiffness must be determined for each face–sheet laminate.

4.7 Summary

- Methods for residual strength analyses of sandwich panels with a disbond, delamination or notch have been developed.

- Appropriate finite element models for the residual strength analyses of the three cases (disbond, delamination and notch) have been constructed.

- Results on critical buckling loads and post-buckling strength for sandwich panels with disbond or delamination have been obtained.

- Results on residual strength for sandwich panels with a single notch on one face sheet or a through the thickness notch have been obtained.

- Parametric studies have been conducted to determine the critical buckling load of face sheets and post-buckling residual strength of sandwich panels with a disbond, delamination or a notch.

- Both tension and compression loading conditions are included in the damage tolerance analysis for all the cases studied.

5 DEMONSTRATION OF DESIGN METHOD

5.1 Introduction

The general method and equations for the equivalent "Level of Safety" design approach have been defined in Section 3.2. To demonstrate the process as applied to an advanced structural concept, a composite honeycomb material system was chosen for analysis. The damage tolerance behavior of the composite has been investigated using the deterministic analysis methods outlined in Section 4. Design charts of the residual strength of a sandwich panel versus flaw size for various types of damage are shown in the figures of the Appendix. Using this data, the "Level of Safety" methodology is applied to the sandwich panel to determine the size of panel necessary to meet the design safety criteria for a given load level. The details of this example are described in the following section.

5.2 Outline of Design Procedures

Detailed derivations and assumptions inherent in the "Level of Safety" method have been defined previously in Section 3.2. The overall method of application is restated and condensed into a step-by-step process here to illustrate how the design procedure progresses using the given examples.

"Level of Safety" Evaluation on Existing Structure

The "Level of Safety" of an existing structure can be determined through the following steps:

1. Collect damage data on the distributions of flaw sizes, flaw types, number of flaws and detection methods for an existing structure, as described in Section 3.4.

2. Estimate the probability of detection curves for each type of damage detected on the existing structure, using the assumptions described in Section 3.3.

3. Using the data from Steps 1 and 2, coupled with design data on the residual strength of the structure as a function of damage size, determine the "Level of Safety" of the existing structure using the formulas derived in Section 3.2. This result becomes the allowable value of "Level of Safety" for new designs.

"Level of Safety" Approach for Design

Use of the equivalent "Level of Safety" approach for the design of new structures can be accomplished through the following steps:

4. Perform analysis to determine the residual strength of the new structure as a function of damage size and the various structural sizing parameters of interest.

5. Assume distributions of detected damage size $p_0(a)$ and probability of detection curves $P_D(a)$ based on available data and engineering judgement.

6. Using the "Level of Safety" formulas derived in Section 3.2, combined with the data from Steps 4 and 5, determine the relation between structural geometry and "Level of Safety" for given load levels.

7. Using the allowable value of "Level of Safety" from Step 3, size the structure to give a "Level of Safety" equal to or greater than the allowable.

8. After the structure has been built and put into service, collect data on the damage accumulated during operation.

9. Bayesian statistical methods defined in Section 3.6, combined with the data from Step 8, can be used to update the assumed probability distributions of Step 5, and to recalculate the "Level of Safety" of the structure.

10. If the "Level of Safety" falls below the allowable value, the inspection and maintenance program can be updated to provide earlier or more frequent detection opportunities to return the "Level of Safety" to its design value.

5.3 Examples of Equivalent Safety Based Design

Some illustrative examples are used here to demonstrate the application of the equivalent safety design approach. The task is to design a composite sandwich compression panel that will at a minimum maintain the same Level of Safety as an existing aluminum one. The allowable Level of Safety, taken from the metal structure, is 99.9%. This translates into a Probability of Failure of 0.1%.

For the sake of simplicity, consider a case of only one damage type (disbonding), one damage location and one flaw in the sandwich structure. Two different types of inspection methods are to be used to detect the damage. The probability of detection of disbond damage for the two inspection types are assumed to be $P_{D_I}(a) = 1 - e^{-a^{1.4}/1.2}$ for Inspection Type I and $P_{D_{II}}(a) = 1 - e^{-a^{1.4}/2}$ for Inspection Type II. The detection probabilities as a function of damage size are plotted in Figure 35. Each inspection type has a different detected damage size distribution $p_0(a)$ associated with it. The detected damage is assumed to follow a Gamma distribution with the parameters k = 2.1, θ = 1.3 for Inspection Type I, and parameters $k = 2.2$, $\theta = 1.5$ for Inspection Type II:

$$p_o(a) = \frac{1}{\theta^k \Gamma(k)} a^{k-1} Exp\left[-\left(\frac{a}{\theta}\right)\right] \tag{5.3-1}$$

Detected damage probabilities are plotted in Figure 36. The damage size variable a is taken to be the disbond diameter in inches for each function.

Using equation (3.2-10) from Section 3.2, along with the probability distributions assumed above, the normalizing constant for the "Level of Safety" calculation is integrated numerically using the SLATEC DQAGI Gaussian quadrature subroutine in double-precision FORTRAN. For each iteration, relative and absolute error for convergence of the subroutine

was set at 10^{-12}. To illustrate the convergence properties of the assumed distributions, the integral solutions are listed in Table 1 as the lower limit of integration ε approaches zero.

Table 1. Convergence Table of Normalizing Constant 1/*C*

ε	Inspection Type I	Inspection Type II
10^{-3}	1.80084780	2.22544611
10^{-4}	1.80730322	2.22955533
10^{-5}	1.80859168	2.23020679
10^{-6}	1.80884877	2.23031005
10^{-7}	1.80890007	2.23032641
10^{-8}	1.80891030	2.23032900

Roundoff error was detected by the integration subroutine at ε values of 10^{-9}, so the most reliable estimates for the normalizing constants are listed at 10^{-8}. Based on the behavior shown, the integral is assumed to converge to a finite value for both inspection types, and the distribution of $p(a)$ is assumed to be a valid probability function.

Using Equation (3.2-13) and the normalizing constants calculated previously, the "Level of Safety" of the sandwich panel is calculated as a function of disbond size and inspection type. The equations are integrated numerically using a trapezoidal scheme in an Excel spreadsheet, with the results plotted in Figure 37. Elimination of disbond size from the Level of Safety plots can be performed by substituting the residual strength versus critical damage size relations obtained in Section 4. Relations between design load and "Level of Safety", as a function of the sizing parameters of laminate thickness and stacking sequence, are then established and shown in Figures 38 through 41. Data points with a "Level of Safety" lower than 80% are not shown in the figures, as these are generally outside the design range of interest. Alternatively, plots of design load versus "Probability of Failure" relationships can also be obtained, and are shown in Figures 42 through 45. It is more practical to use these

curves rather than the "Level of Safety" plots since "Level of Safety" is so close to unity for the typical design range of interest.

For a given limit load P_{lim} of 8000 lbs./in., the minimum laminate thickness and stacking sequence necessary to provide a "Level of Safety" above the metal structure is found from the charts of Figures 42 through 45. At an allowable "Probability of Failure" PF_{allow} of 0.1%, the results are:

Inspection Type I

Circular Disbond - min. laminate $(-45/0/45/90)_{2s}$

Elliptical Disbond - min. laminate $(-45/0/45/90)_{2s}$

Inspection Type II

Circular Disbond - min. laminate $(-45/0/45/0/90)_{2s}$

Elliptical Disbond - min. laminate $(-45/0/45/90)_{2s}$

From these results, it can be seen that the parameters of the inspection type have a strong influence on the resulting size of the structure. Inspection Type 2 has a somewhat lower detection probability than Inspection Type 1, as is shown in Figure 35. This means that if only Inspection Type 2 were used in the inspection and maintenance program for the structure, the largest laminate thickness of $(-45/0/45/0/90)_{2s}$ must be used to maintain the "Level of Safety" above that of the existing metal structure. If only Inspection Type 1 is used, or some combination of Types 1 and 2, a smaller laminate thickness $(-45/0/45/90)_{2s}$ may be utilized, thus realizing substantial weight and cost savings for the design.

This type of design trade is also subject to the costs and operational considerations of the different inspection types. In general, as detection probabilities increase for a specific detection method, the cost and difficulties in applying the method to the inspection of actual aircraft components also increase. Therefore, from a life-cycle standpoint, it may be better to accept the lower detection probability associated with Inspection Type 2 and use a larger

laminate thickness in the final design. The "Level of Safety" methodology, and the data that results from it, allows the designer to make these types of cost-benefit trades on a quantitative basis early in the design process.

Once the structure is in service, the data collected on the damage sizes detected during operational inspections is used with the Bayesian statistical method to update the assumed damage size distributions. Since an example of this process is described in Section 3.6, it will not be repeated here. The revised damage size distribution can be used to recalculate the "Level of Safety" of the structure, thus validating the assumptions made in the design process.

A more detailed example is also shown to illustrate the equivalent safety method using multiple damage types in different locations. The composite sandwich panel discussed previously will be redesigned for a load concentration at a particular location. The far-field loading area on the panel is referred to as Location 1, and the load concentration area is referred to as Location 2. Location 1 uses a laminate stacking sequence of $(-45/0/45/90)_{2s}$, and Location 2 uses a $(-45/0/45/0/90)_{2s}$ stacking sequence. Location 1 is subject to two flaws: a circular disbond and an elliptical delamination. Location 2 is subject to an elliptical disbond and a circular delamination. Each flaw type at each location has a unique detected damage size distribution $p_0(a)$ and detection probability $P_D(a)$ associated with it. The nomenclature of each curve is listed below, where μ is an array of the mean number of flaws at each damage location:

Location 1

Circular Disbond (a = diameter)	$p_{o11}(a),\ P_{D11}(a),\ \mu_{11} = 1$
Elliptical Delamination (a = major axis)	$p_{o21}(a),\ P_{D21}(a),\ \mu_{21} = 1$

Location 2

Elliptical Disbond (a = major axis)	$p_{o12}(a),\ P_{D12}(a),\ \mu_{12} = 1$

Circular Delamination (a = diameter) $p_{o22}(a)$, $P_{D22}(a)$, $\mu_{22} = 1$

For simplicity, it is assumed that all of the detected damage size distributions follow the curves of Equation (5.3-1). Inspection Type II is to be used at Location 1, and Inspection Type I is to be used at Location 2. The detection probabilities for each inspection type are the same as those in the previous example:

$$p_{o12}(a) = p_{o22}(a) = p_{oI}(a)$$

$$p_{o11}(a) = p_{o21}(a) = p_{oII}(a)$$

$$P_{D12}(a) = P_{D22}(a) = P_{DI}(a)$$

$$P_{D11}(a) = P_{D21}(a) = P_{DII}(a)$$

A design limit load of $P_{lim\text{-}1}$ = 6000 lbs./in. is applied to Location 1, and a limit load of $P_{lim\text{-}2}$ = 17,500 lbs./in. is applied to Location 2. The allowable "Level of Safety" for the entire structure is 99.9%. For the circular disbond damage at Location 1, Figure 44 can be used to determine the "Probability of Failure" for the sandwich at a 6000 lb./in. load. The result is $PF_{11} = 1\text{x}10^{-4}$, which translates into a "Level of Safety" of $LS_{11} = 0.9999$. For the elliptical delamination damage at Location 1, Figure 53 is used to find a "Probability of Failure" of $PF_{21} = 0.0$. This is because the damage tolerance analysis shows that a panel with a circular delamination will not fail at the given limit load for any of the damage sizes investigated. For the elliptical disbond at Location 2, Figure 43 is used to find a "Probability of Failure" of $PF_{12} = 6\text{x}10^{-5}$. For the circular delamination at Location 2, Figure 50 is used to find a "Probability of Failure" of $PF_{12} = 5\text{x}10^{-7}$. These results are listed in tabular form as:

Location 1

Circular Disbond	$PF_{11} = 1\text{x}10^{-4}$, $LS_{11} = 0.9999$
Elliptical Delamination	$PF_{21} = 0.0$, $LS_{21} = 1.0$

Location 2

Elliptical Disbond	$PF_{12} = 6\text{x}10^{-5}$, $LS_{12} = 0.99994$

Circular Delamination $PF_{22} = 5\text{x}10^{-7},\ LS_{22} = 0.9999995$

Using Equation (3.2-19), the overall "Level of Safety" of the structure can be determined as:

$$LS = LS_{11} \cdot LS_{12} \cdot LS_{21} \cdot LS_{22} = (0.9999)\ (1.0)(0.99994)(0.9999995) = 99.98\%$$

For the allowable "Level of Safety" of $LS_{allow} = 99.9\%$, the calculated "Level of Safety" value exceeds the allowable by 0.02%. Thus, for the damage profile analyzed, the new design has a higher safety than the existing structure it will replace.

The "Level of Safety" method provides an estimate of the actual damage size distribution in a structure. These estimates will vary depending on the inspection method utilized and the accuracy of the probability distributions in the formula. The actual damage size distribution based on the detected damage sizes and detection probabilities can be calculated by the equation:

$$p(a) = \frac{p_0(a)}{P_D(a)} \Bigg/ \int_0^\infty \frac{p_0(a)}{P_D(a)} da \qquad (5.3\text{-}2)$$

The results of this calculation using the distributions assumed in the example problems are plotted in Figure 54 for the two inspection types. The curves are very close to each other, indicating that the distributions assumed in the example problem closely approximate the actual damage distributions for both inspection types. Results using actual data may vary significantly, however, for various inspection types. Figure 54 also illustrates the behavior of the distribution of *p(a)* as discussed in Section 3.8, in that it asymptotically approaches infinity as the damage size *a* goes to zero.

6 RESULTS AND CONCLUSIONS

6.1 Benefits of an Equivalent Level of Safety Approach

The benefits of an equivalent "Level of Safety" approach to aircraft design are many and varied. By taking a probabilistic approach to structural failure, the need for arbitrary factors of safety based on traditional design practices is substantially reduced. This frees the designer to pursue maximum structural efficiencies in the design, while still maintaining safety equivalent to, or better than existing structures. The "Level of Safety" methodology is a data-driven process that also allows for the inclusion of empirical, or "soft" data, along with engineering judgement, to quantify the uncertainty associated with the damage tolerance characteristics of a structure. It incorporates planning for the service inspection program into the design process. The method is applicable to any type of structure or material system where damage mechanisms have been characterized, and allows an objective comparison of relative safety to be made between dissimilar structures, or similar structures in different operating environments. The incorporation of Bayesian statistical tools into the "Level of Safety" method provides a mechanism for validating the damage assumptions made during the design process, and for reducing the level of uncertainty and risk over the life-cycle of the structure. Also important, the method provides a valuable tool for airlines and flight certification authorities to manage risk in a fleet of aircraft, and over a range of aircraft types.

6.2 Limitations of the Current Formulation

As presented here, the equivalent safety methodology does not currently encompass the range of damage tolerance issues needed to fully characterize the operational "Level of Safety" of a particular structure. The existing derivation only describes a structure's "Level of Safety" for a single inspection event at a fixed point in time, and is essentially a state variable. However, the state of damage in the structure is continually changing with time, meaning that the "Level of Safety" value just calculated is invalid at any other point in time other than the instant of calculation. Past experience with mechanical systems holds that

structures in an operational environment accumulate damage over a period of time, and previously accumulated damage may grow due to cyclical loading. However, the current formulation does not account for this. As damage is accumulated, the "Level of Safety" of the structure will decrease over time, until the damage is detected and repaired at the next scheduled inspection event. Undetected damage will continue to grow until reaching a size that can be detected at some future time. Therefore, it is also necessary to incorporate the scheduling of multiple inspection and repair events into the method to periodically return the "Level of Safety" to a point above its critical design value.

Interactions between different damage types, and multiple damage events are also neglected in the current formulation. The location of the damage plays a strong role in these effects, and can be modeled partially by assuming the worst-case location for damage accumulation in the analysis of the residual strength vs. damage size for the structure. However, this may lead to overly-conservative residual strength results. To alleviate this, detailed data must be collected on the locations of damage relative to the zones of stress concentration, which could prove difficult to obtain.

The behavior of the detection probability and detected damage size distributions needs to be investigated using experimental data for a range of structural configurations. It is unknown how difficult it will be for probability distributions based on actual data to meet the conditions discussed in Section 3.8. The criteria that the probability density function estimate of actual damage must be integrable over the entire domain of damage sizes my prove to be so difficult to satisfy for the current "Level of Safety" formulation that the method may need to be reformulated to be of any practical use.

Another unquantified variable in the method is the effect that finite data sets have on the confidence level of the equivalent safety estimates. Generally, the more data points that are used, the higher the confidence level will be. With a finite number of data and a required confidence level, the valid "Level of Safety" can only be the lower limit of the one-side confidence interval of the quantity. This may unnecessarily penalize the structure in the design phase, when detailed damage data is most difficult to come by.

6.3 Topics for Further Research

The following topics are recommended for further research to investigate the sensitivity of the method to some of the issues mentioned previously, and to extend the method to cover a broader range of damage tolerance issues:

- Behavior of probability distributions derived from actual damage data for a variety of structures.

- Extension of present method to incorporate rates of damage accumulation, and multiple inspection intervals.

- Demonstration of method on built-up and monolithic structures, including wings, fuselages, empennage, etc.

- Investigation of finite data set effects and confidence level determination.

- Incorporation of damage interaction and growth effects.

- Extension of method to incorporate probabilistic assessments of other variables such as loading, material properties, manufacturing variation, etc.

- Characterization of probability of detection curves for service inspection methods of composite structures.

7 APPENDIX

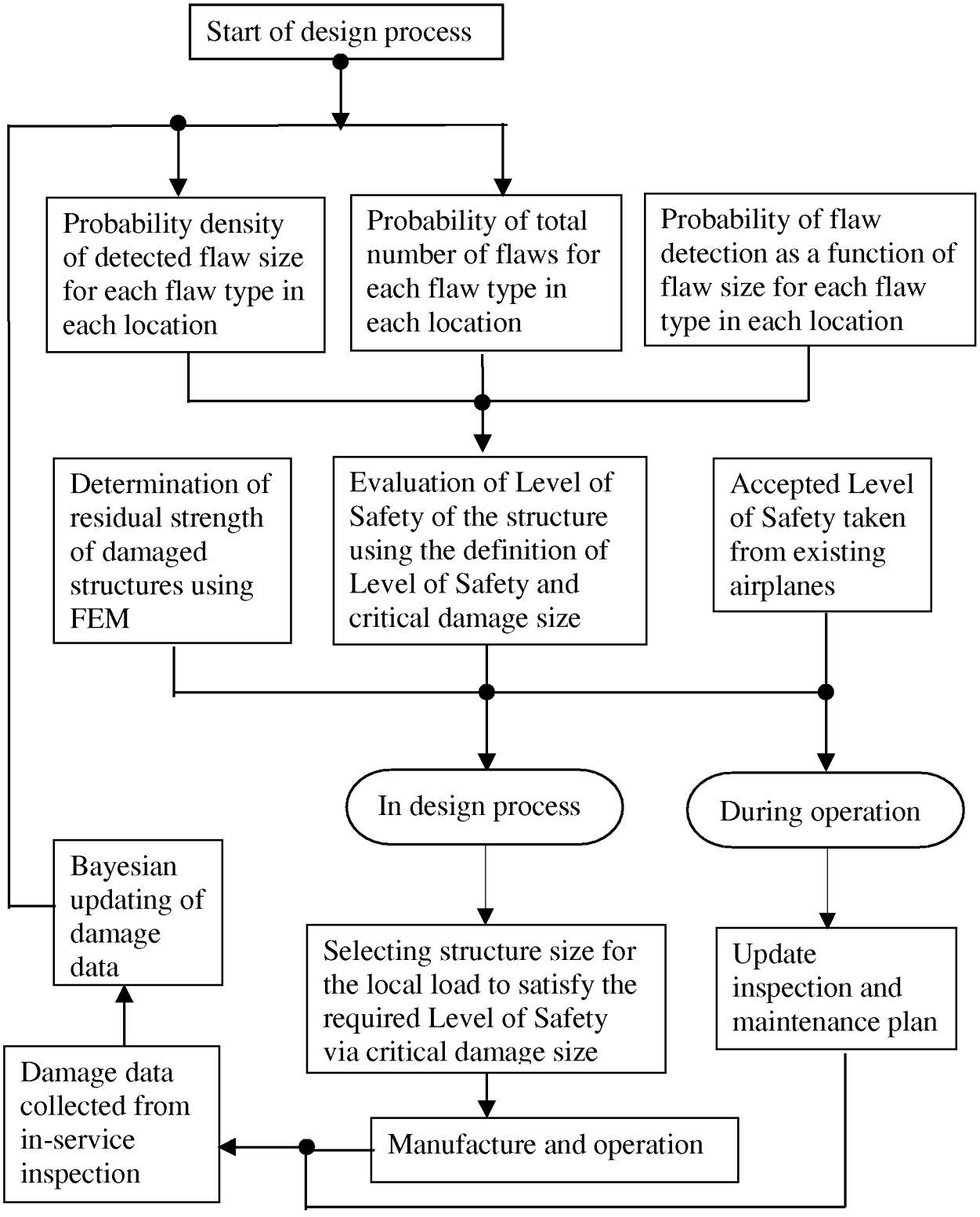

Figure 1. Flow-Chart of Developing Equivalent Safety Aircraft

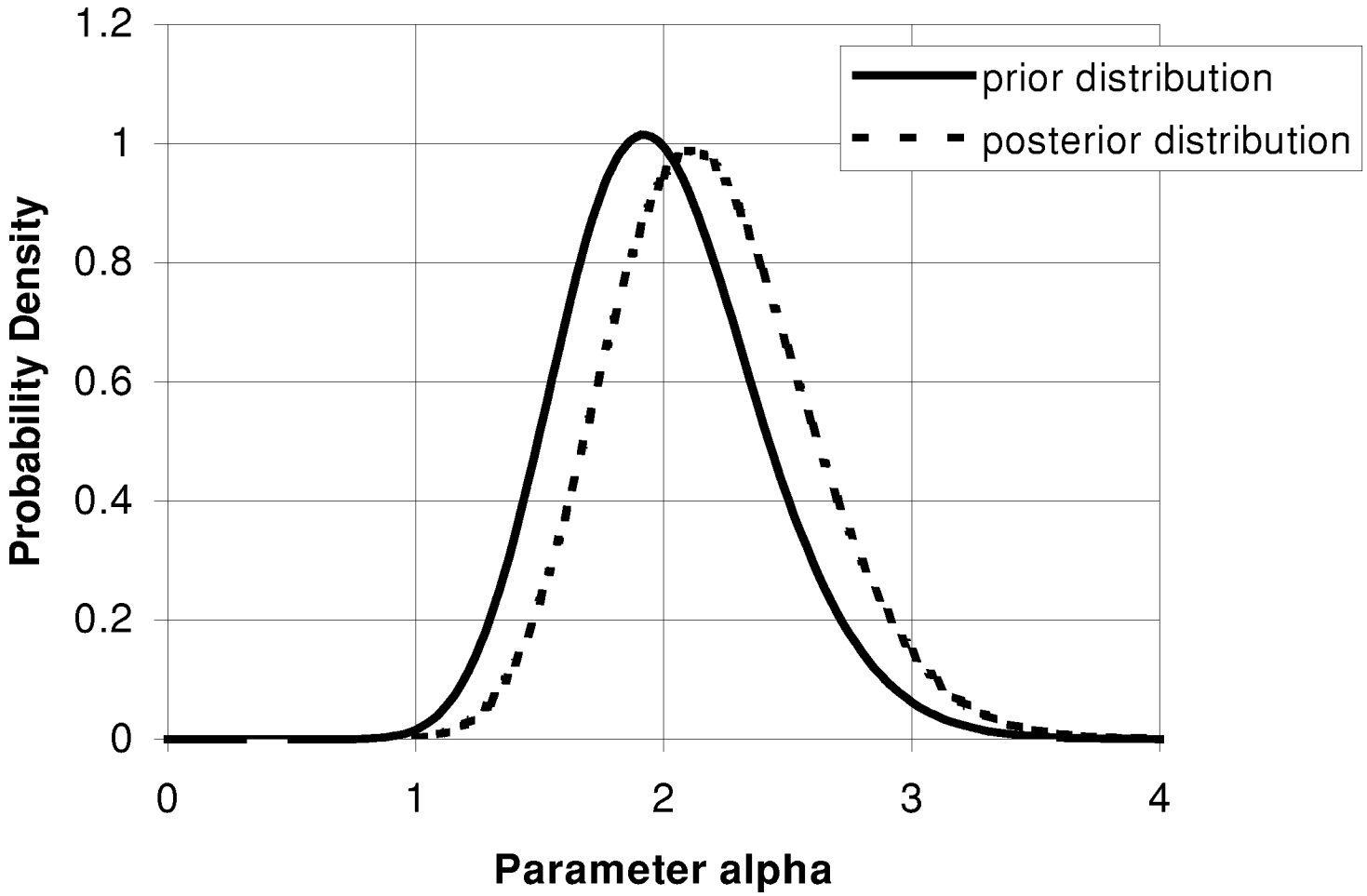

Figure 2. Prior and Posterior Distributions of Parameter Alpha Updated with Measured Damage Sizes of 3,4,5 Inches

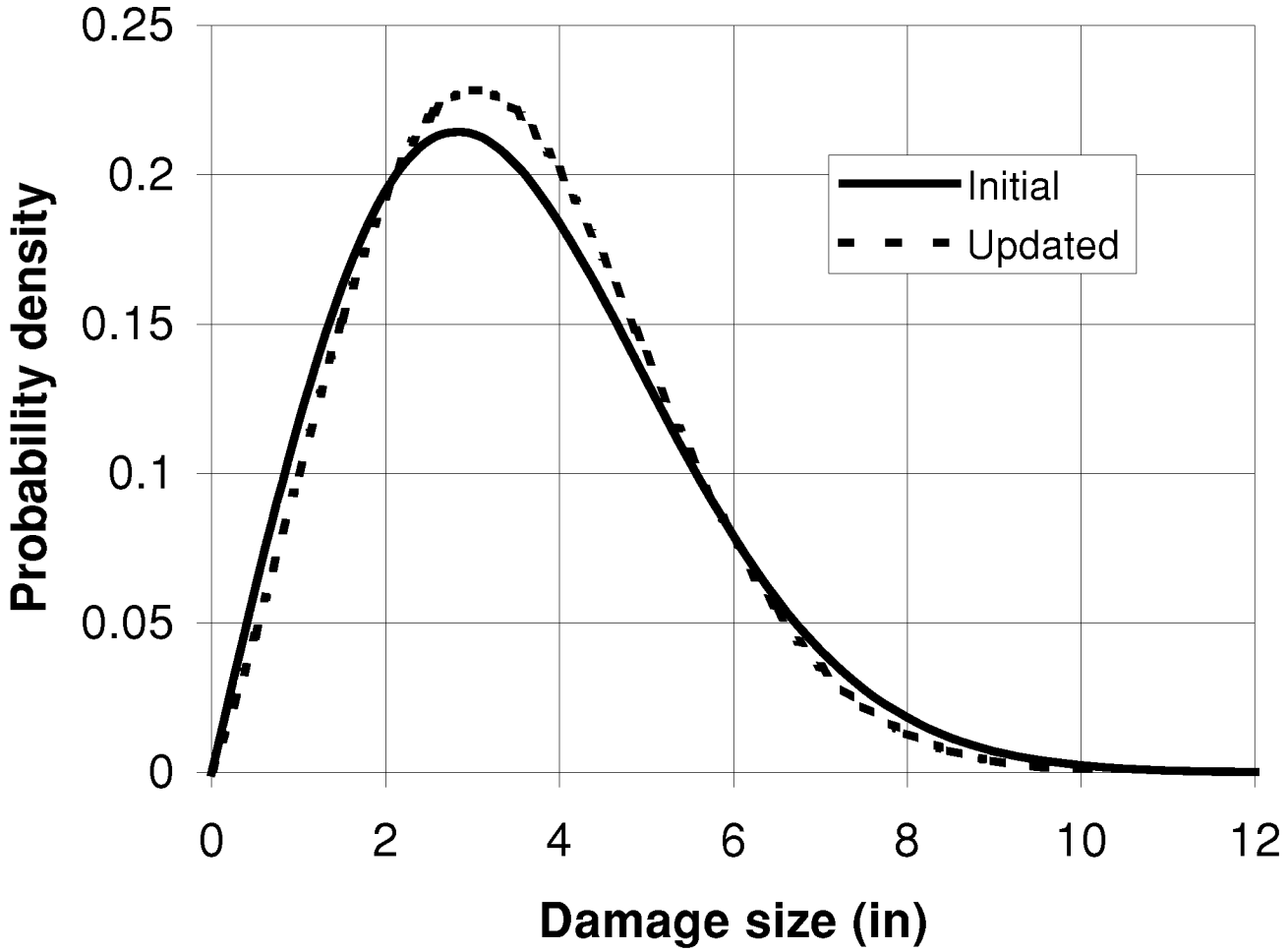

Figure 3. Bayesian Updating of Detected Damage Size Distribution with Measured Damage Size of 3,4,5 Inches

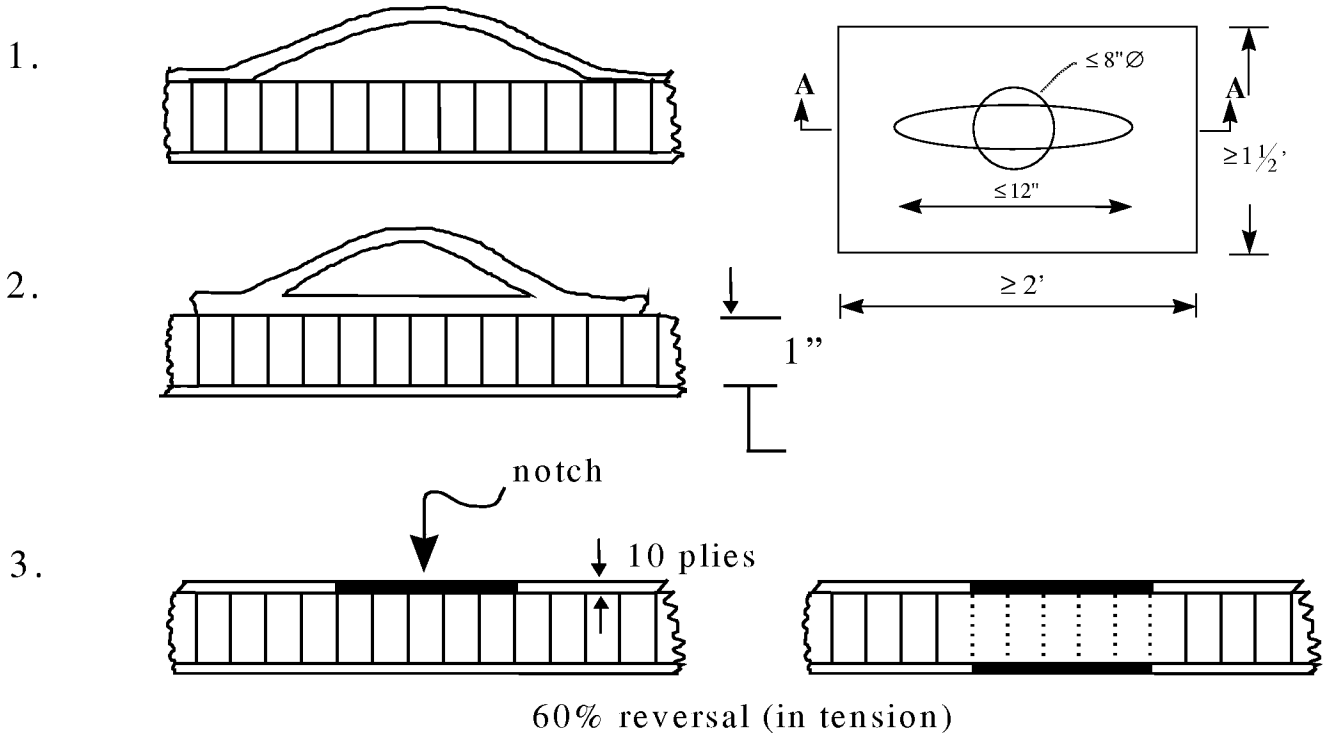

Figure 4. Three Cases of Damage: Case 1. Disbond; Case 2. Delamination; Case 3. Notches

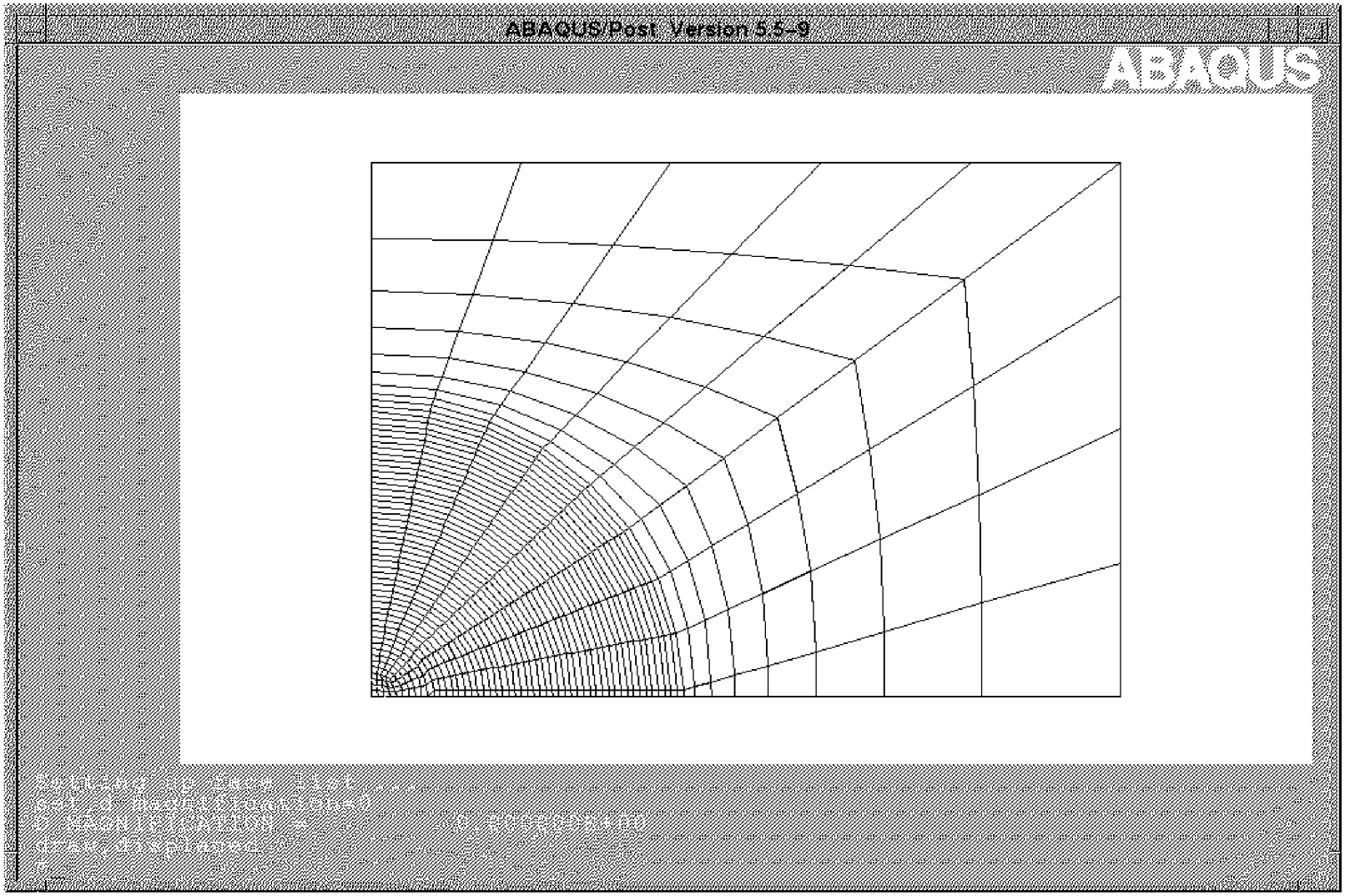

Figure 5. Finite Element Mesh for a Sandwich Panel with a Circular Damage

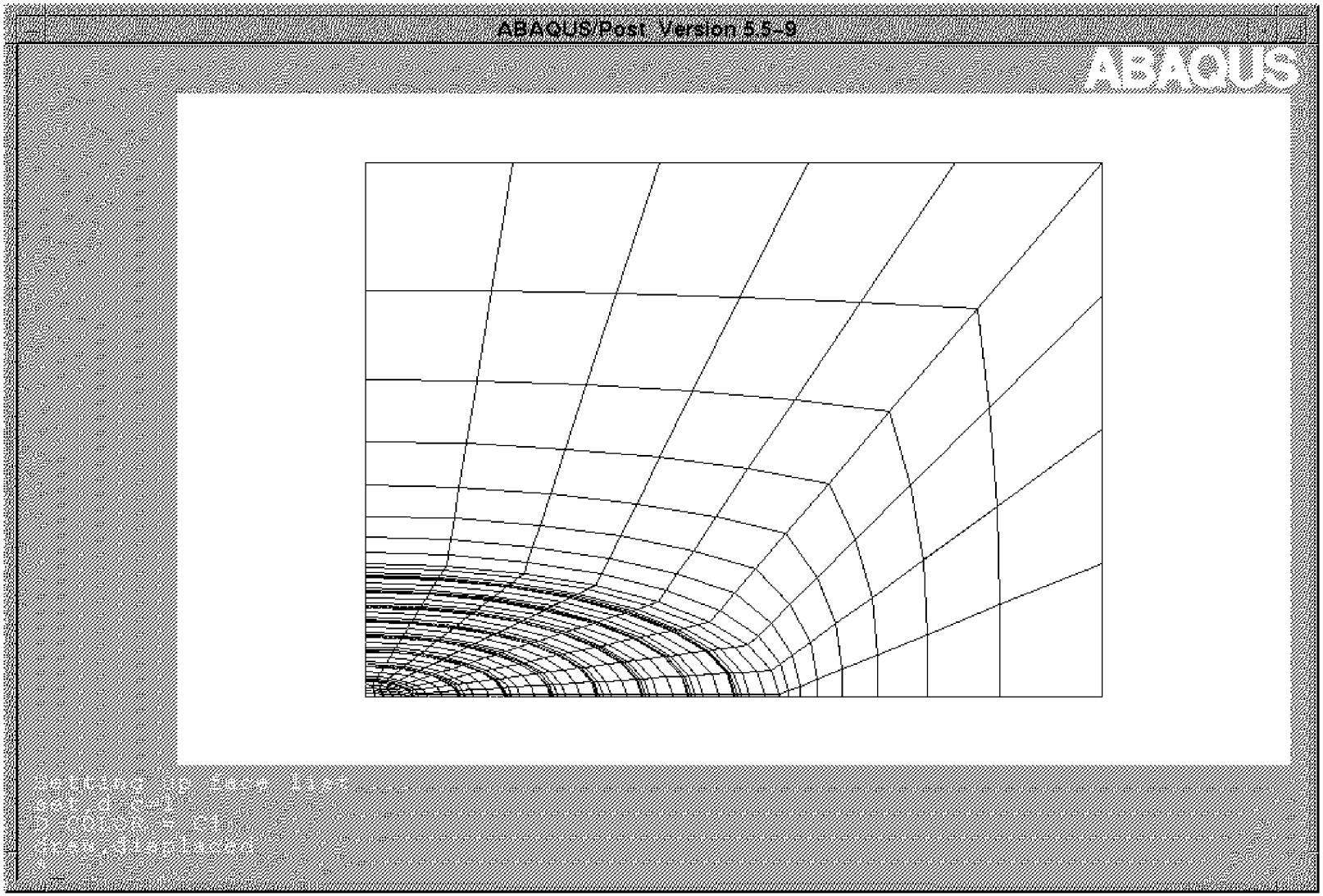

Figure 6. Finite Element Mesh for a Sandwich Panel with an Elliptical Damage

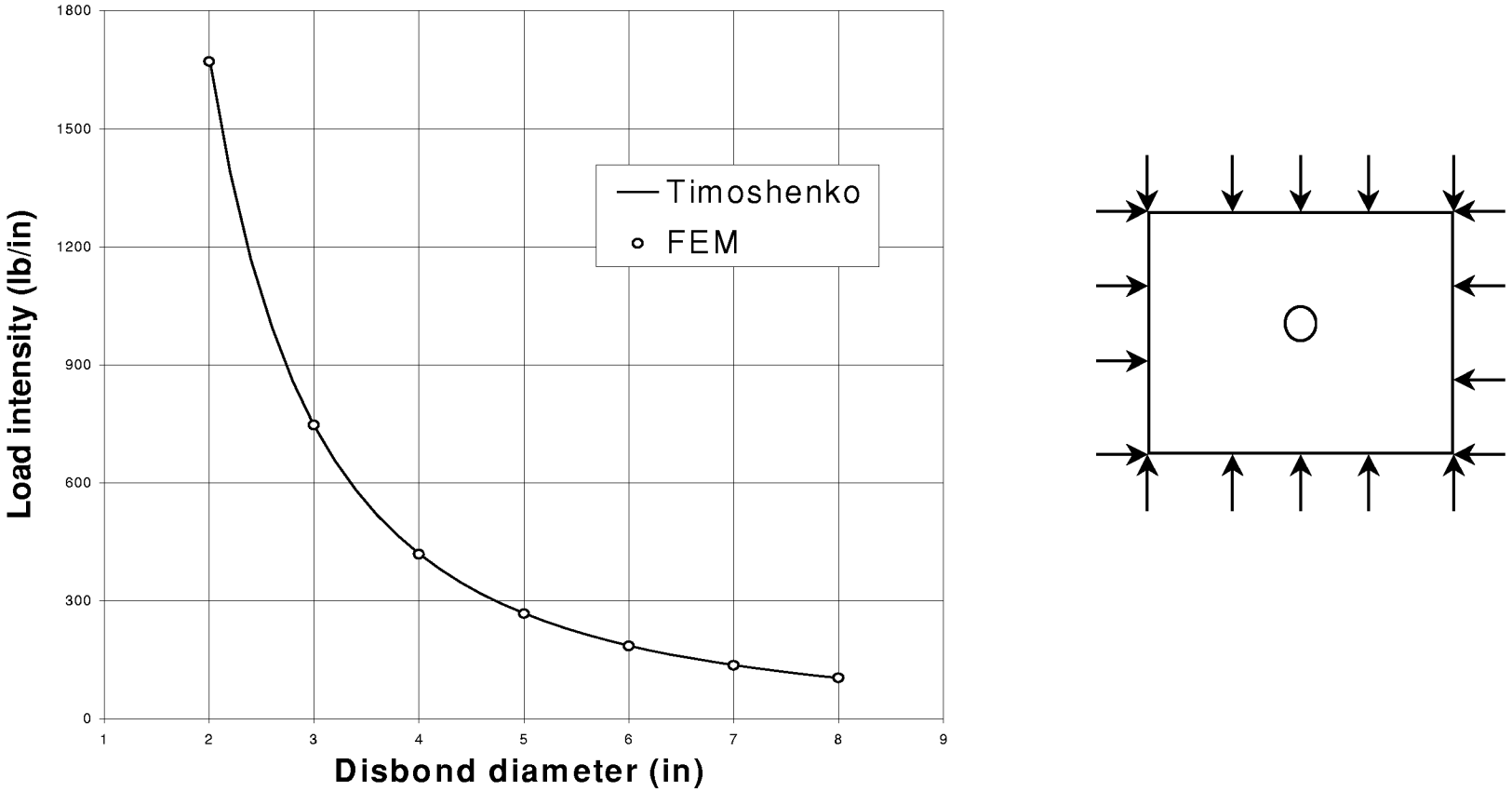

Figure 7. Verification of Finite Element Model for Buckling Load Determination

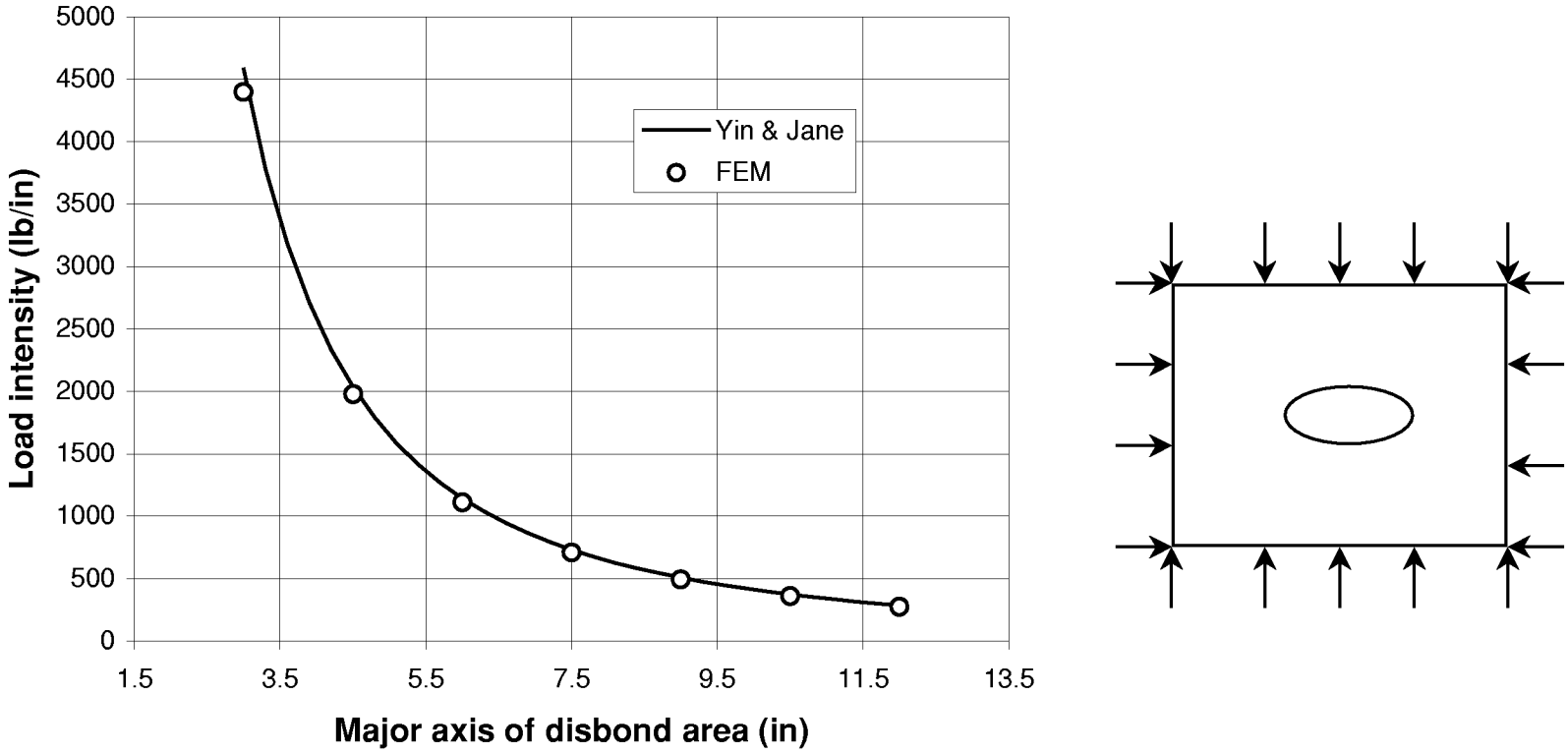

Figure 8. Buckling Load of an Elliptical Disbond under Uniform Pressure

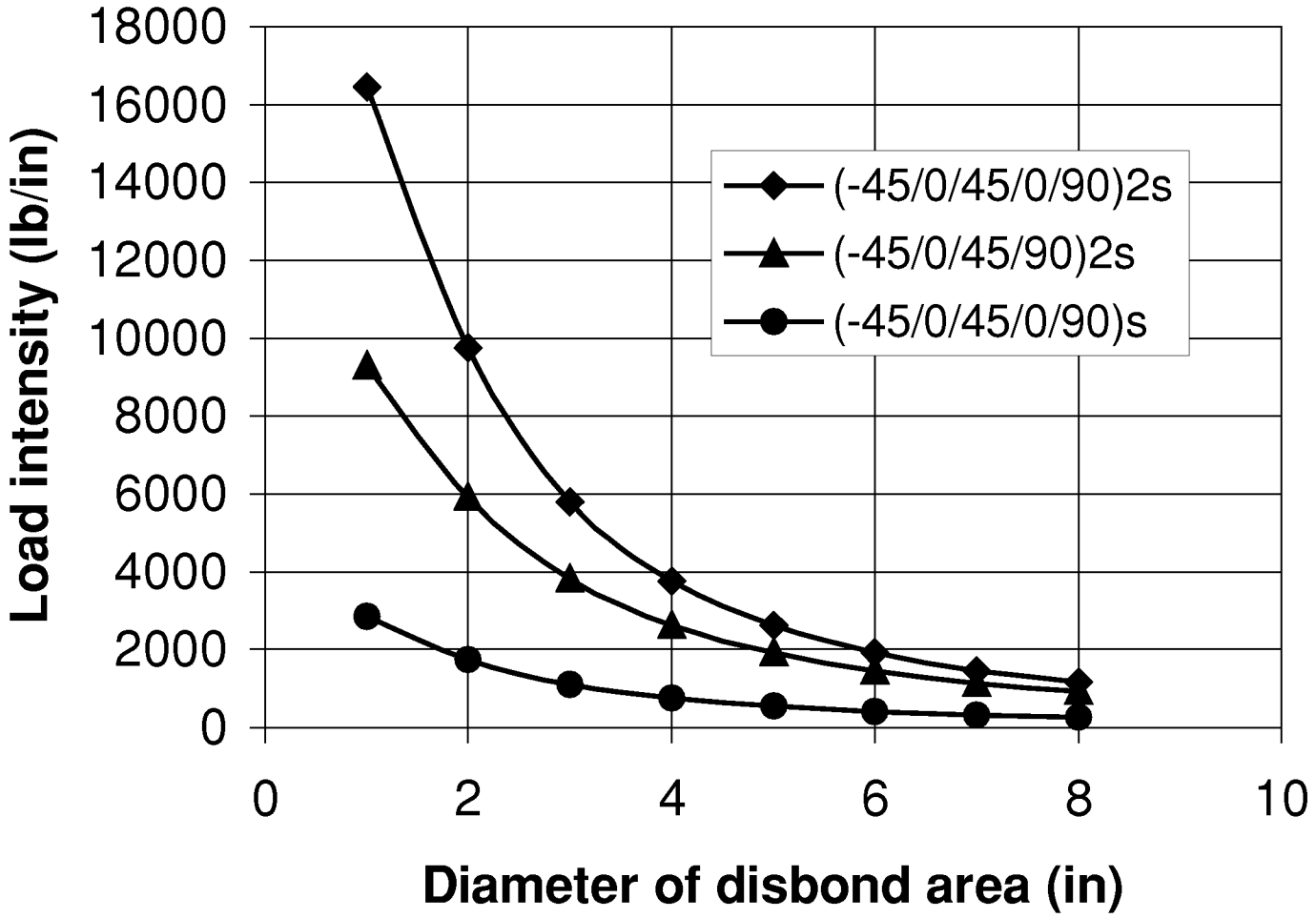

Figure 9. Case 1: Buckling Load of a Face Sheet with a Circular Disbond (Variation in Thickness)

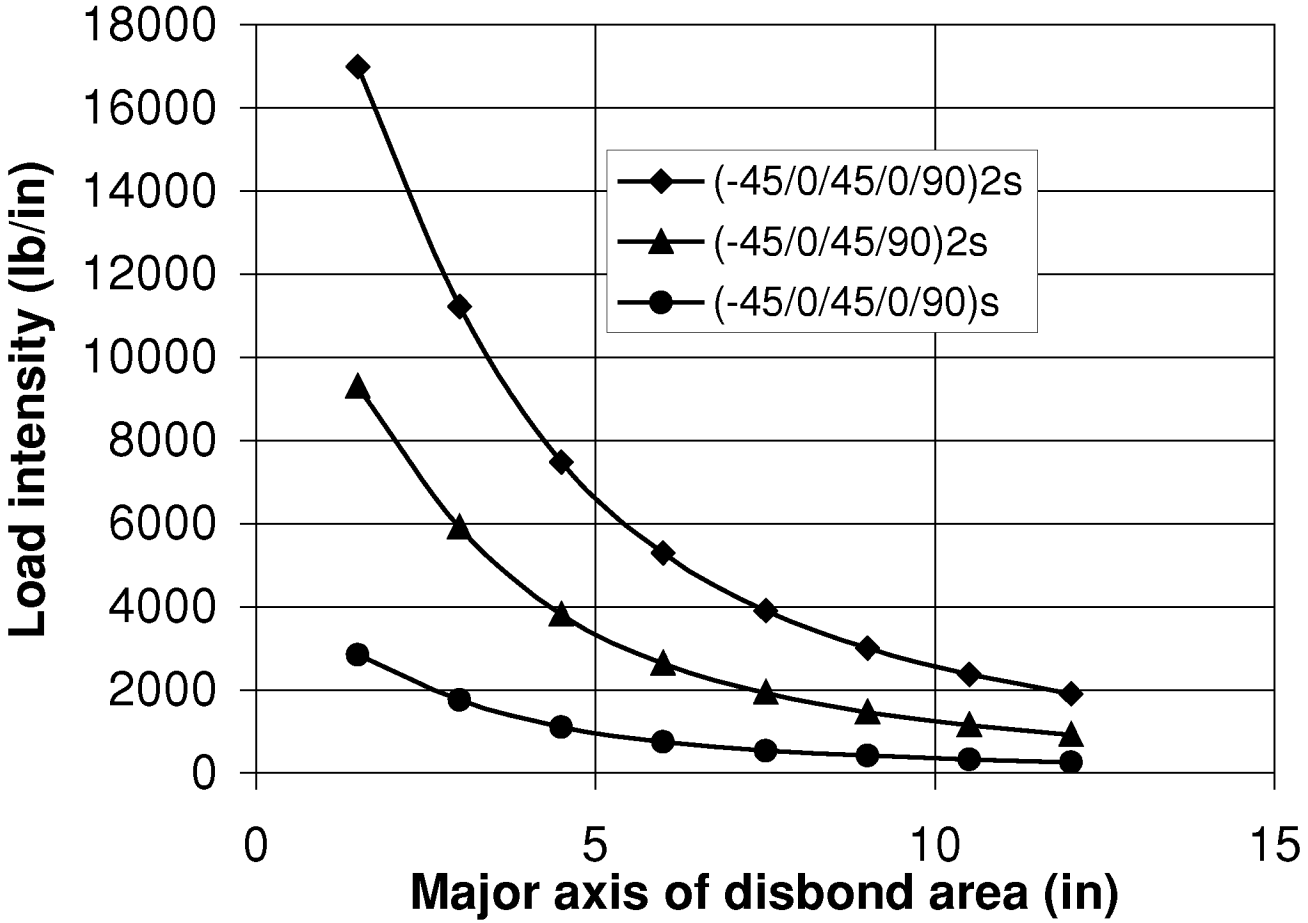

Figure 10. Buckling Load of a Face Sheet with an Elliptical Disbond (Variation in Thickness)

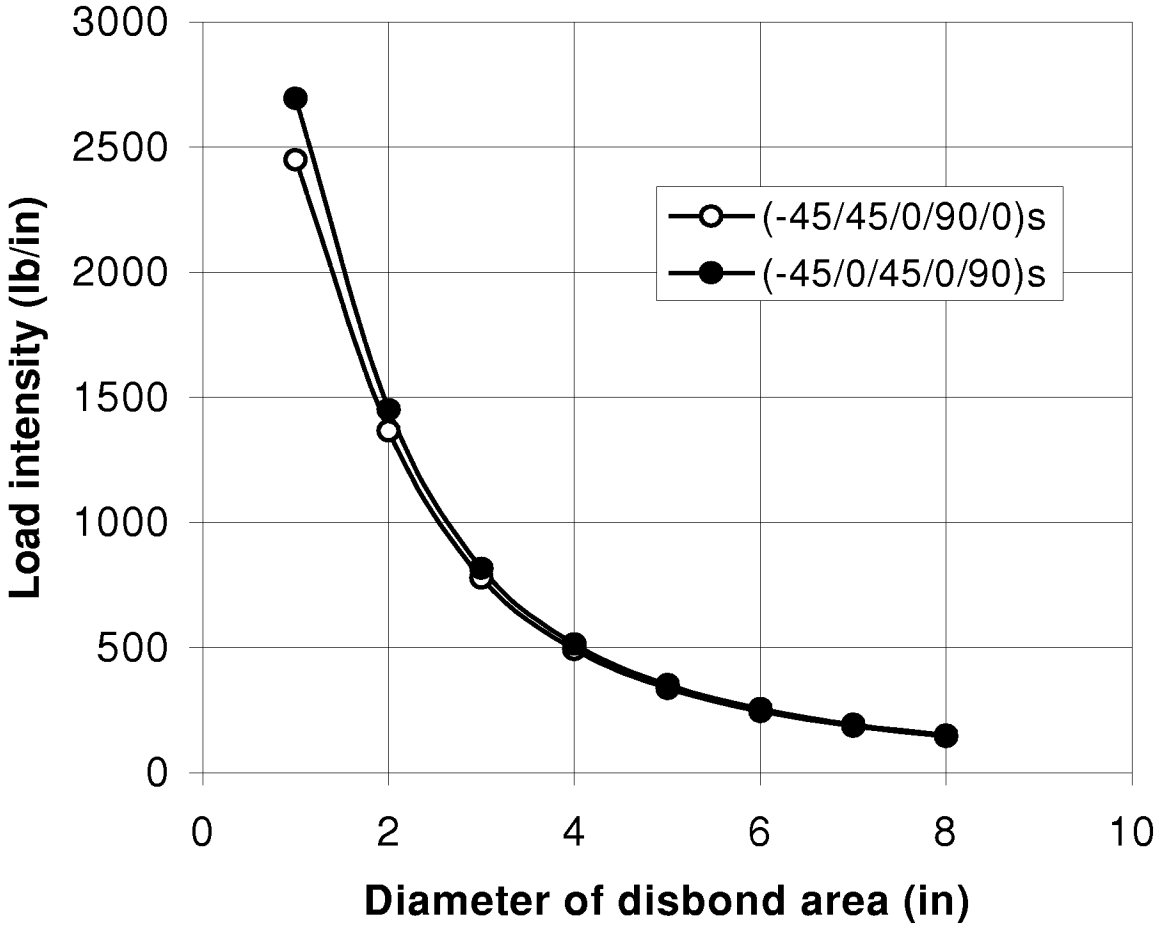

Figure 11. Case 1. Buckling Load of a Face Sheet with a Circular Disbond (Variation in Stacking Sequence)

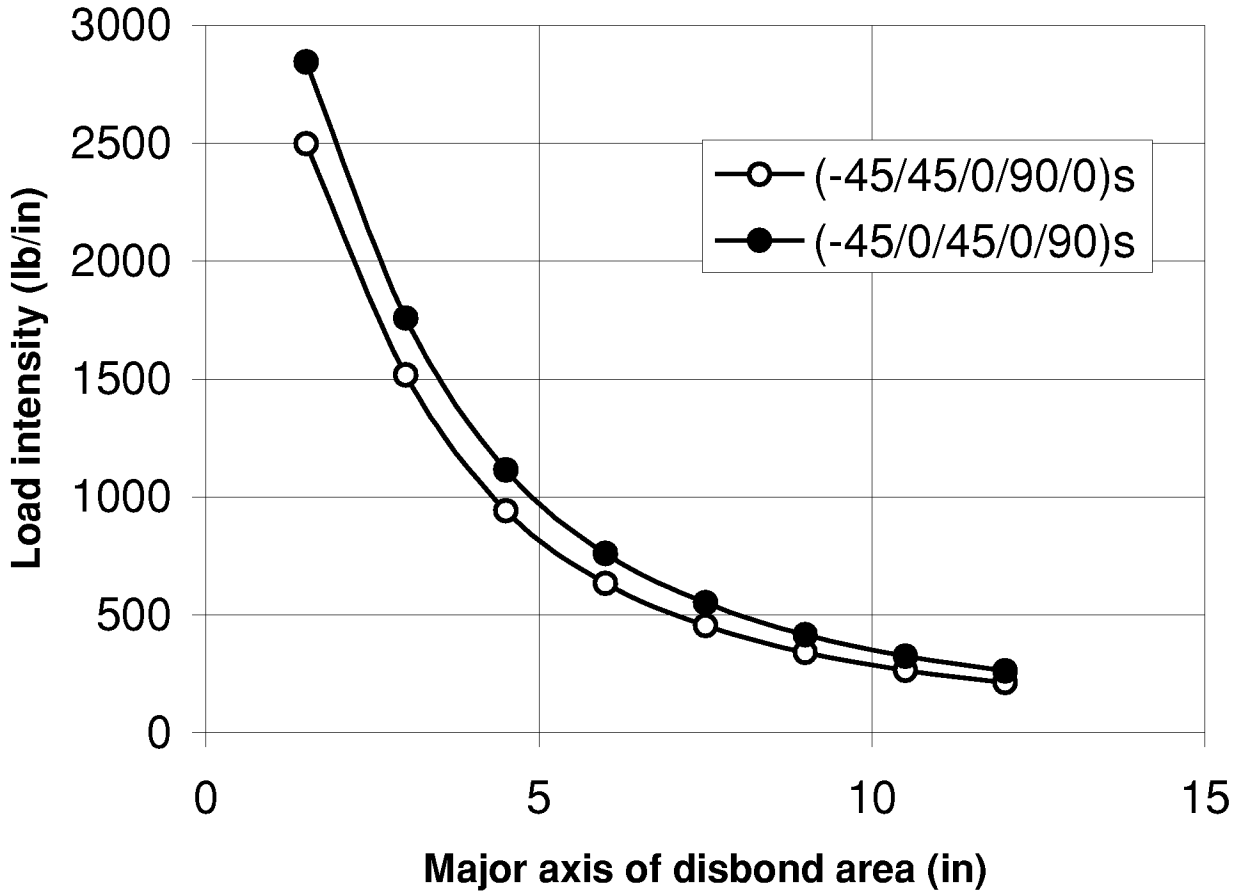

Figure 12. Case 1: Buckling Load of a Face Sheet with an Elliptical Disbond (Variation in Stacking Sequence)

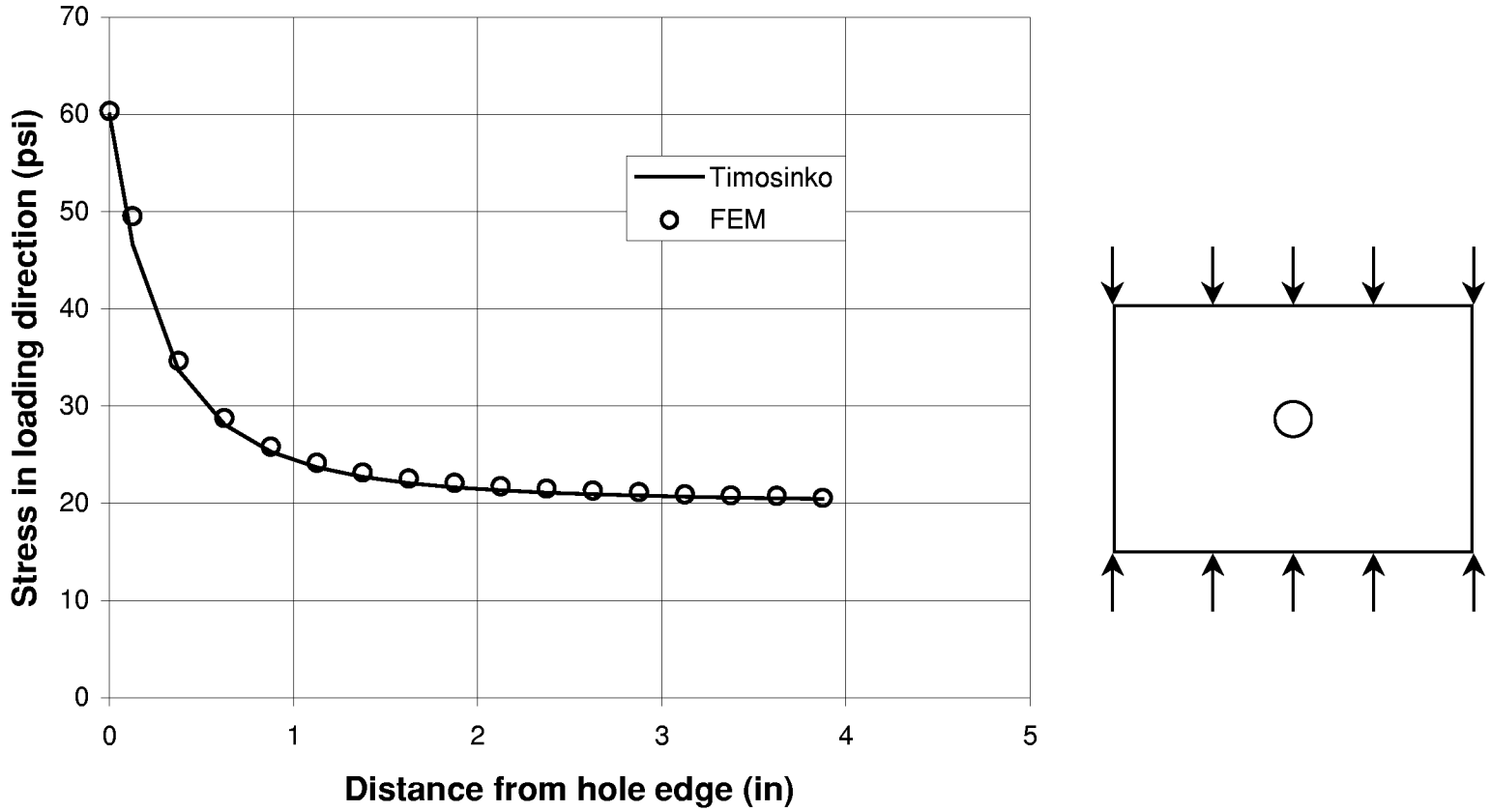

Figure 13. Comparison of Finite Element Analysis Result with Analytical Solution for an Isotropic Plate with a Circular Open Hole

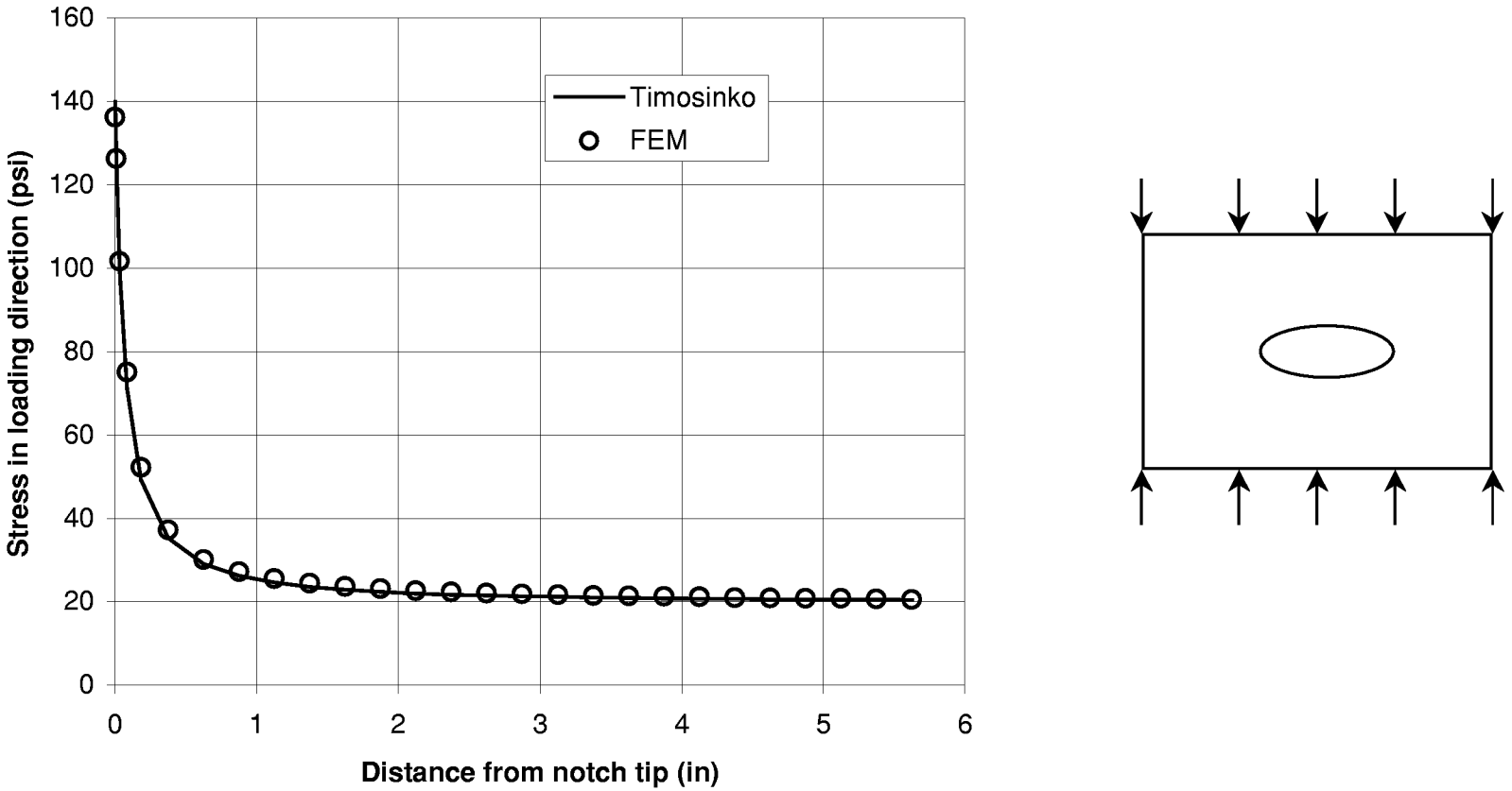

Figure 14. Comparison of Finite Element Analysis Results with Analytical Solution for an Isotropic Plate with an Elliptical Through Notch

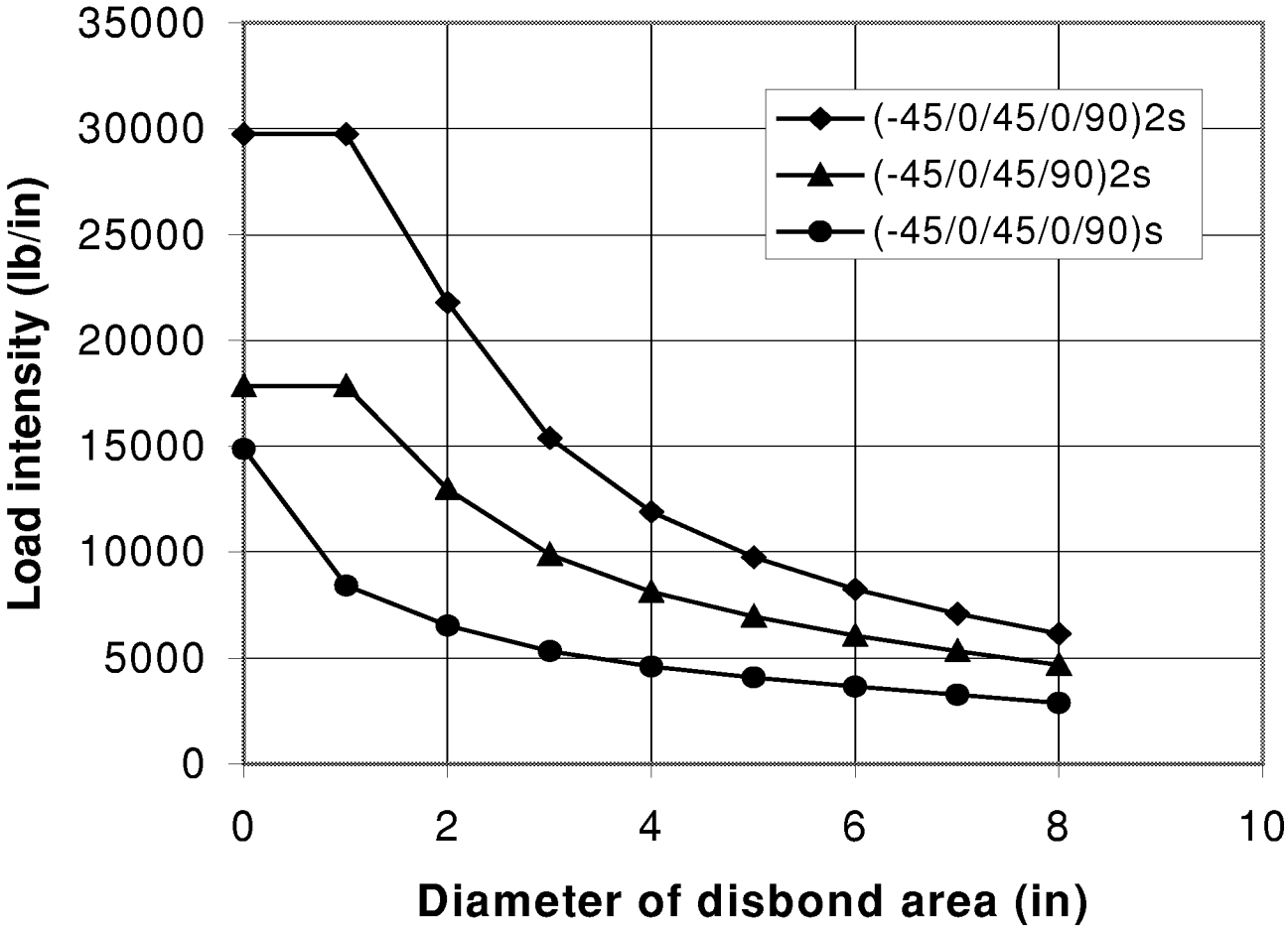

Figure 15. Residual Strength of a Sandwich Panel with a Circular Disbond Loaded in Compression (Variation in Thickness)

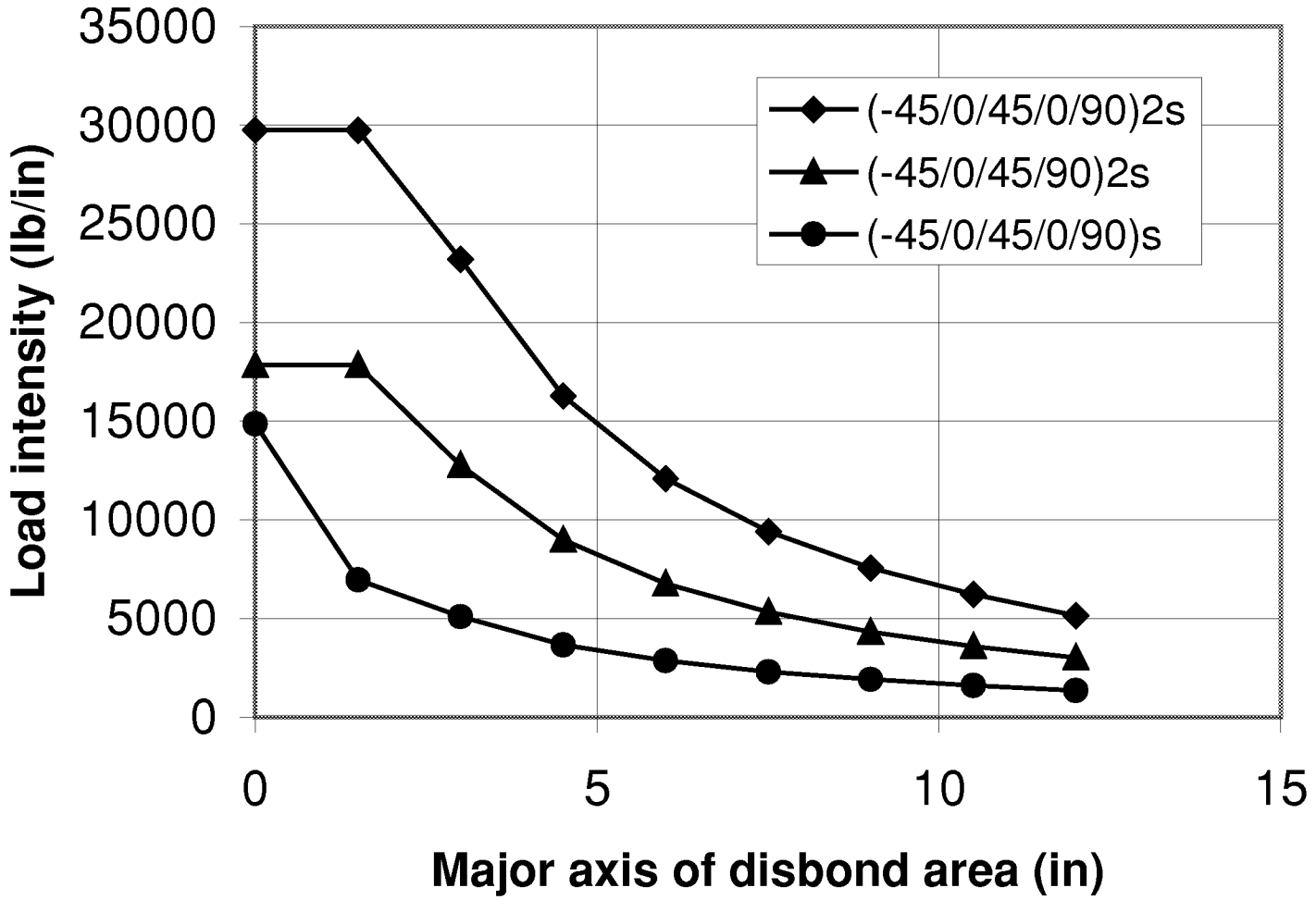

Figure 16. Case 1: Residual Strength of a Sandwich Panel with an Elliptical Disbond Loaded in Compression (Variation in Thickness)

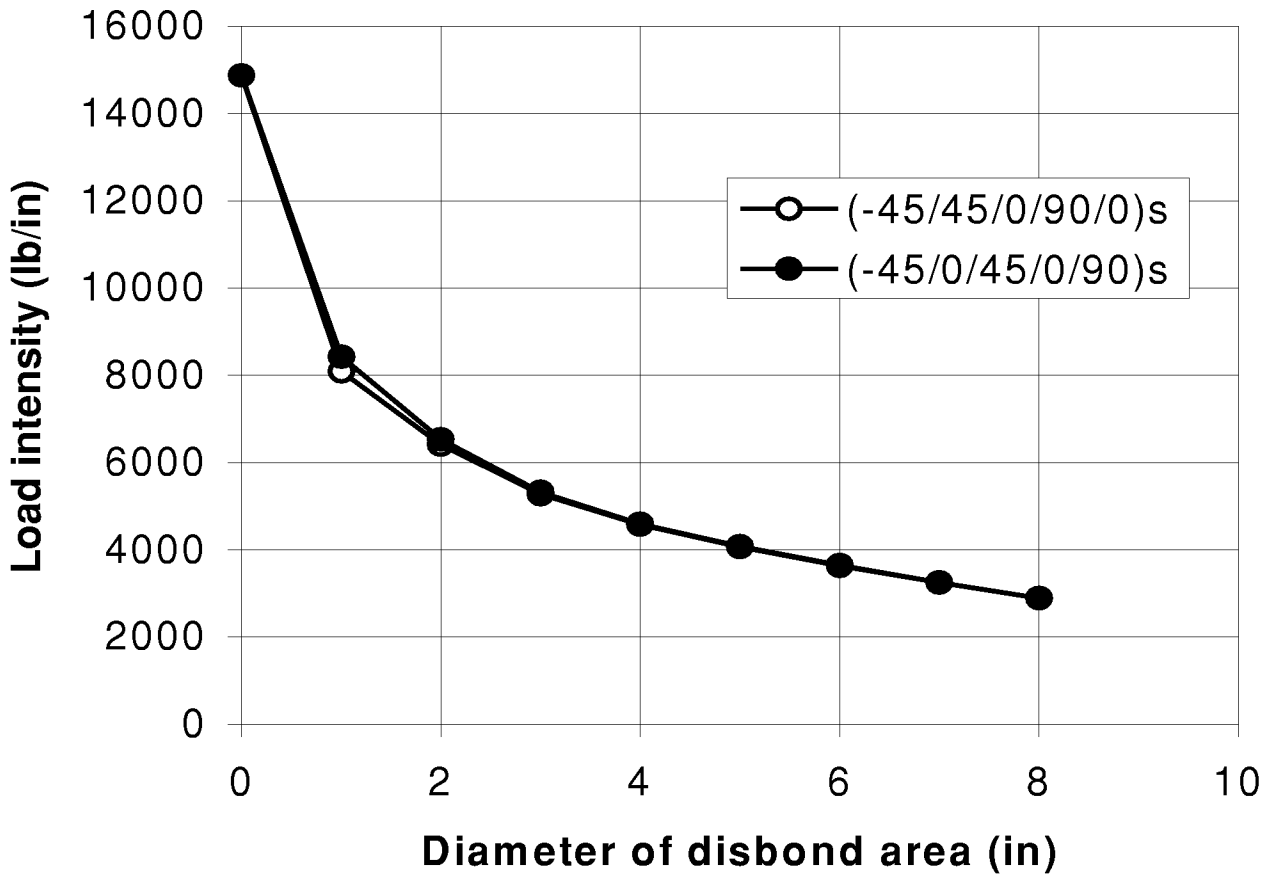

Figure 17. Residual Strength of a Sandwich Panel with a Circular Disbond Loaded in Compression (Variation in Stacking Sequence)

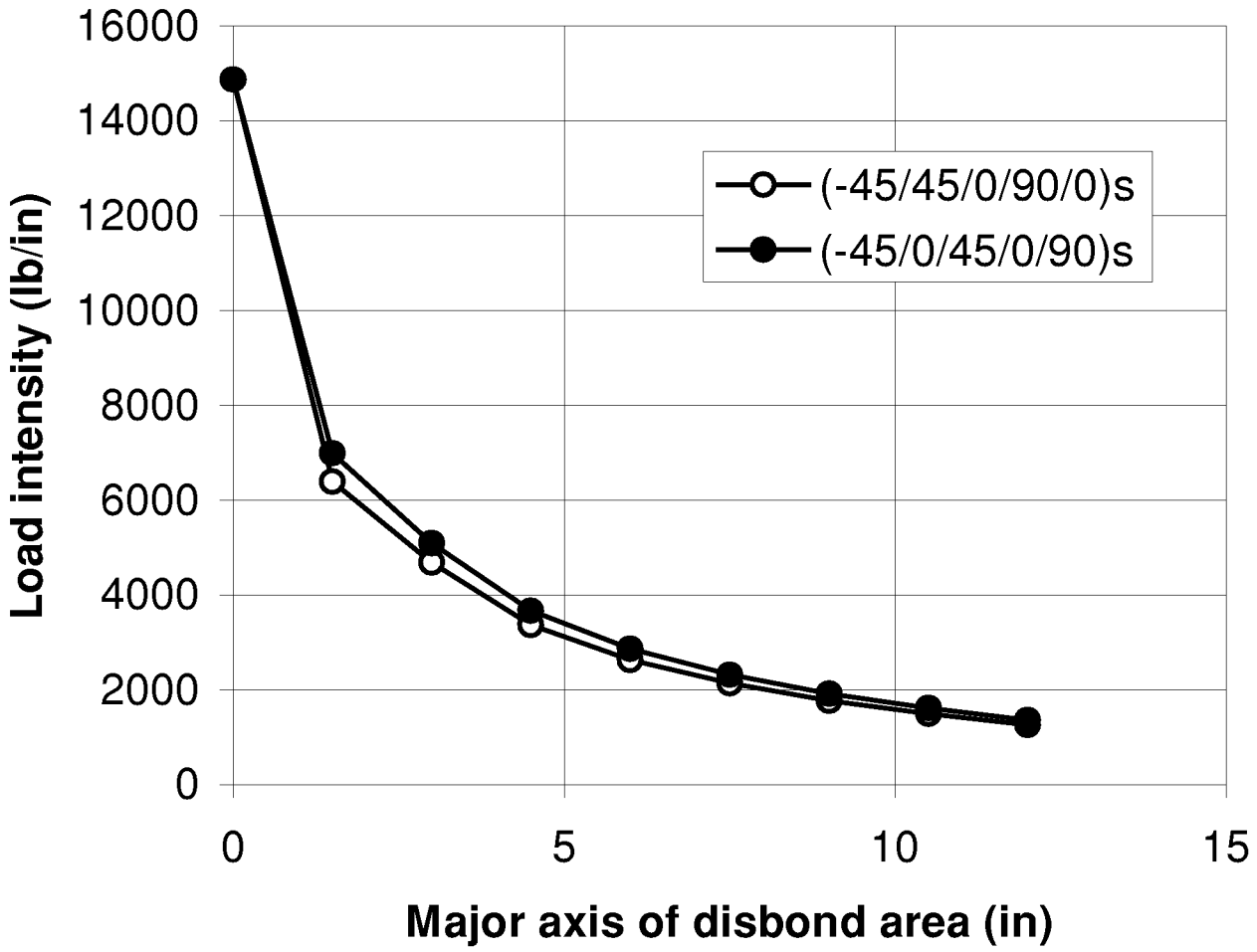

Figure 18. Residual Strength of a Sandwich Panel with an Elliptical Disbond Loaded in Compression (Variation in Stacking Sequence)

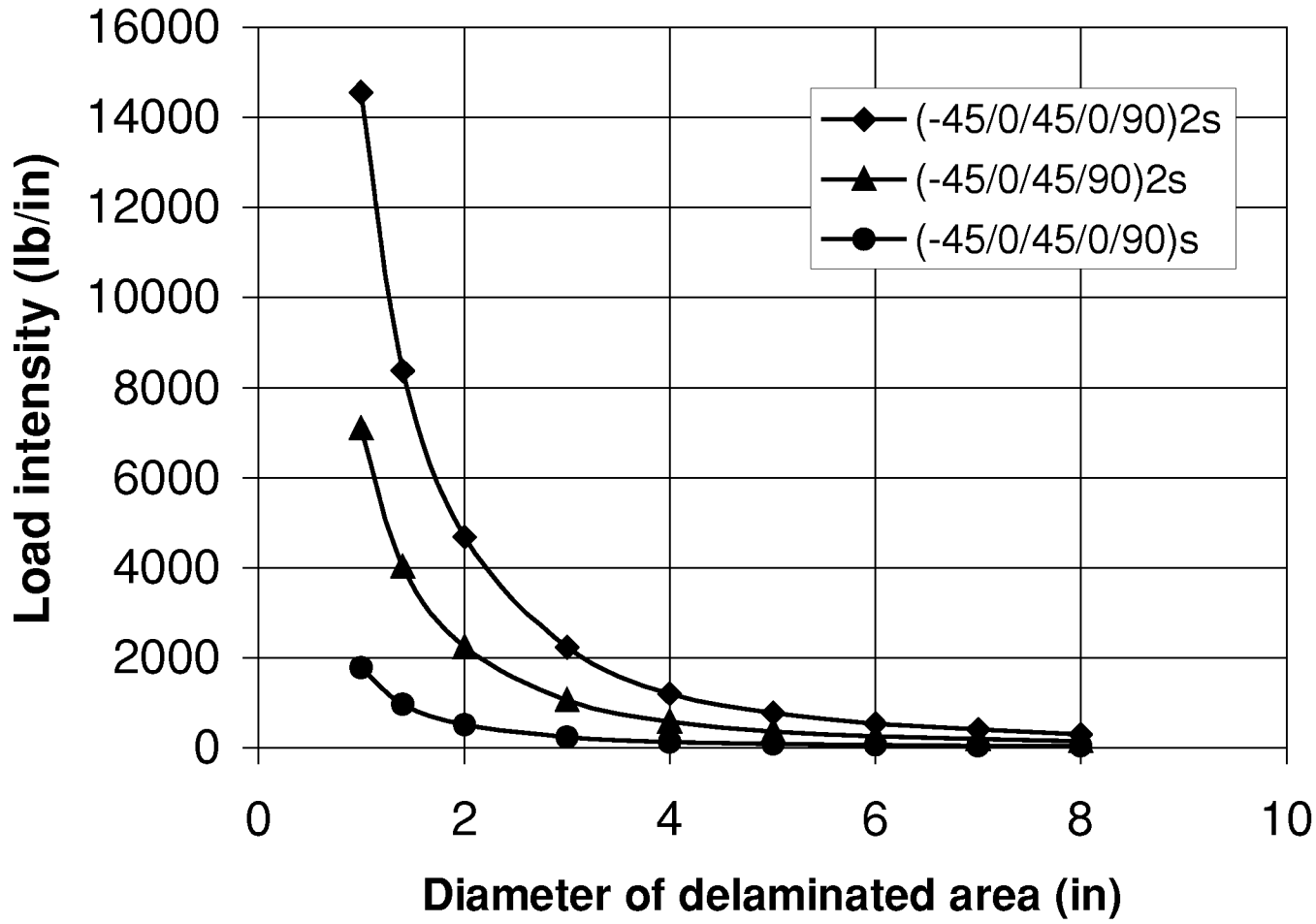

Figure 19. Case 2: Buckling Load of a Face Sheet with a Circular Delamination (Variation in Thickness)

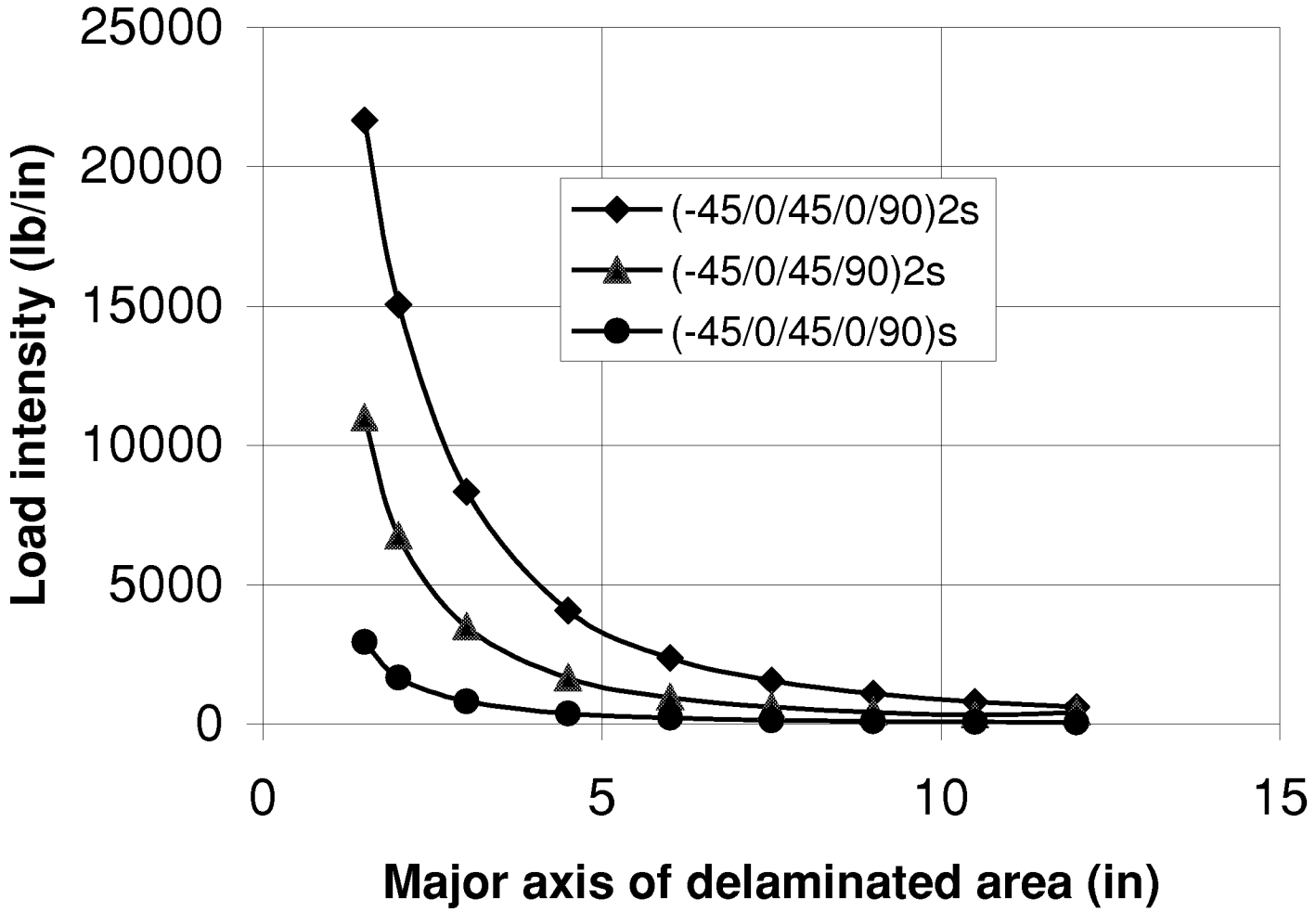

Figure 20. Case 2: Buckling Load of a Face Sheet with an Elliptical Delamination (Variation in Thickness)

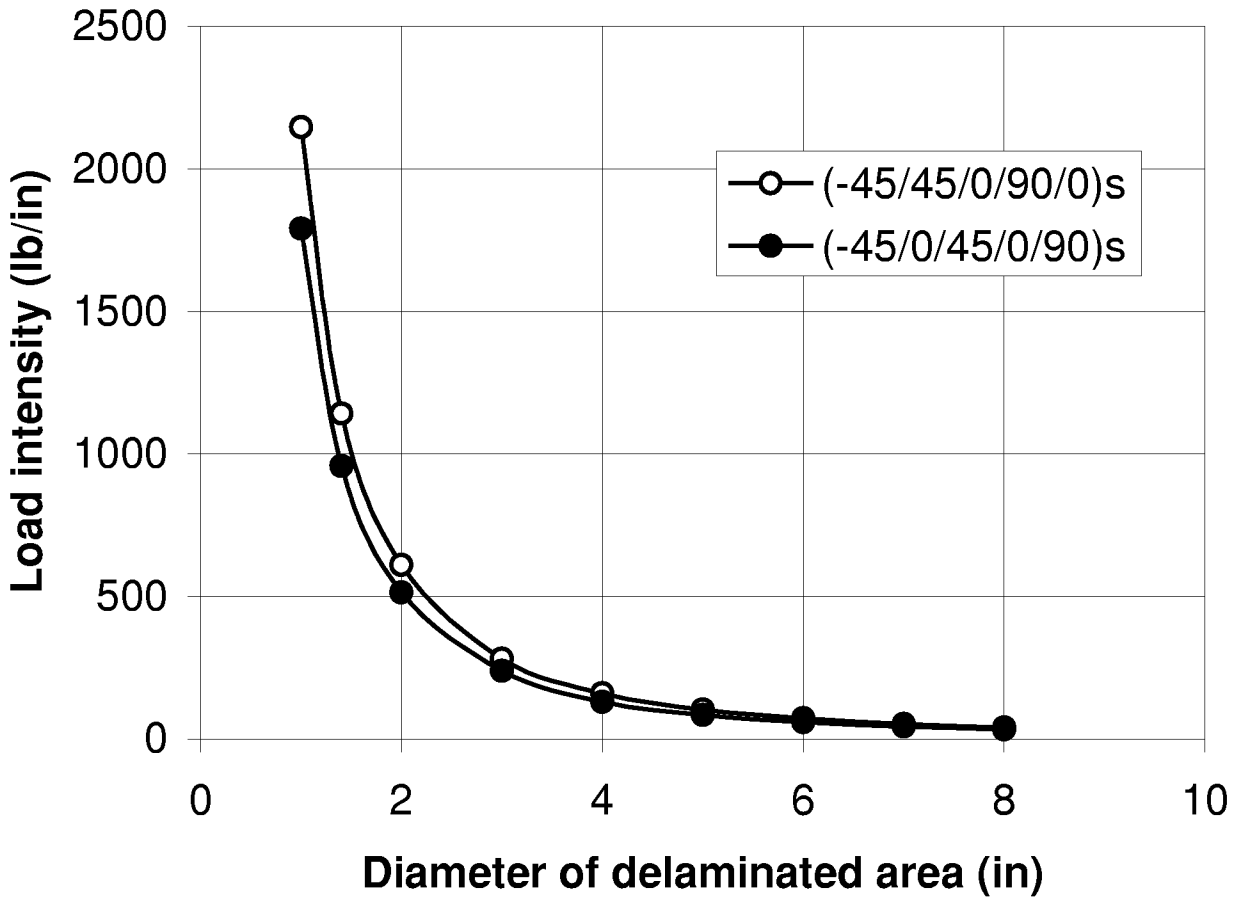

Figure 21. Case 2: Buckling Load of a Face Sheet with a Circular Delamination (Variation in Stacking Sequence)

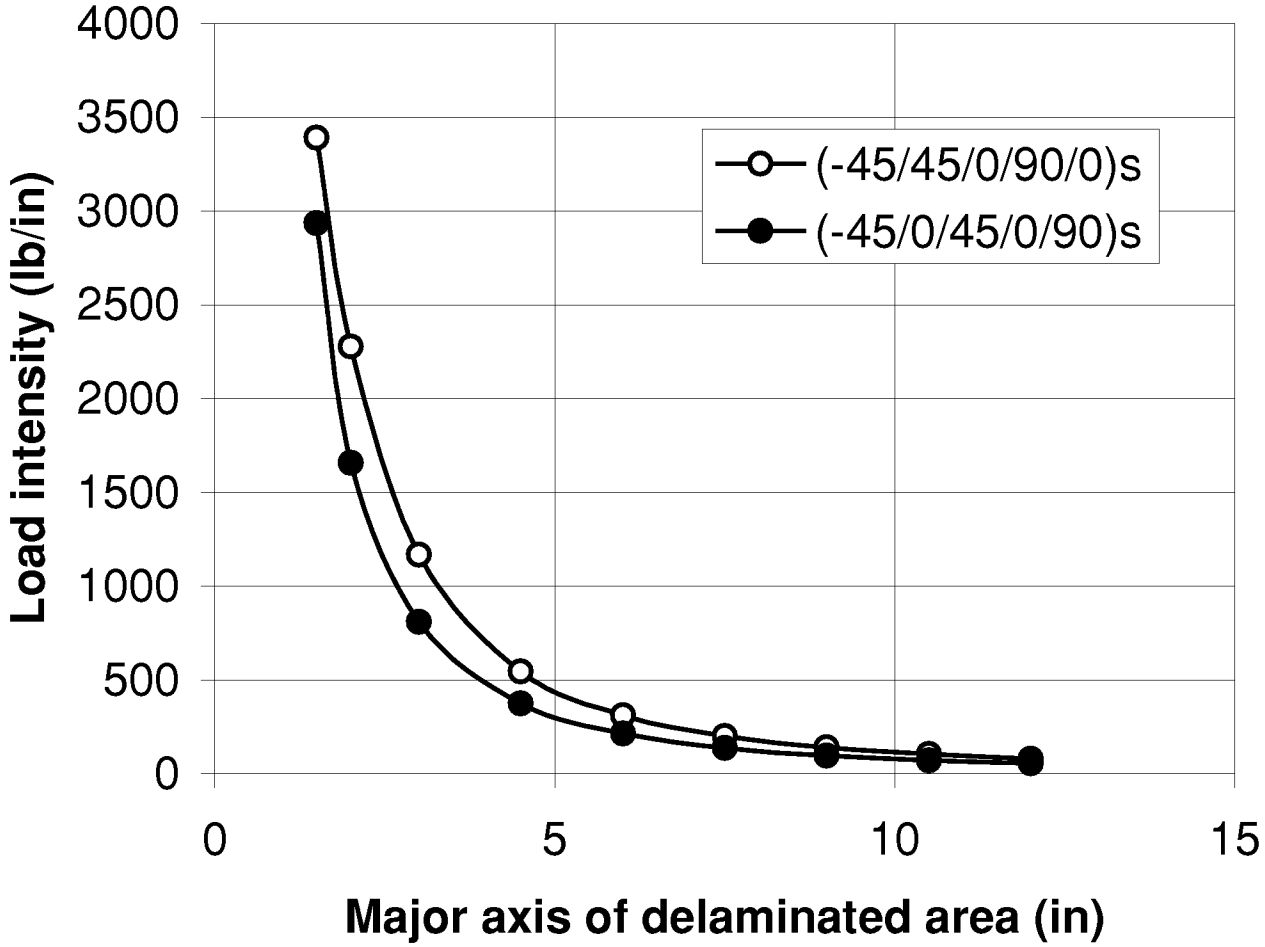

Figure 22. Case 2: Buckling Load of a Face Sheet with an Elliptical Delamination (Variation in Stacking Sequence)

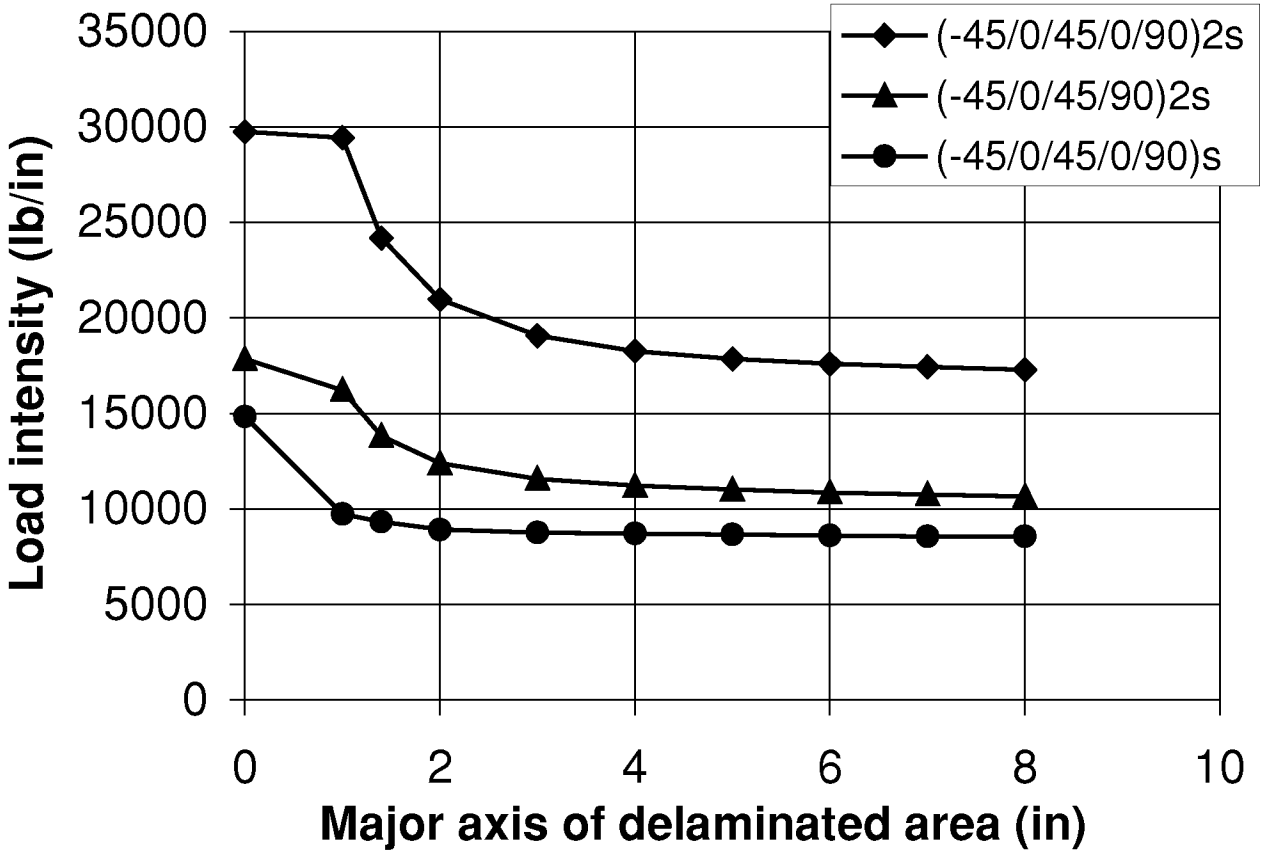

Figure 23. Case 2: Residual Strength of a Sandwich Panel with a Circular Delamination Loaded in Compression (Variation in Thickness)

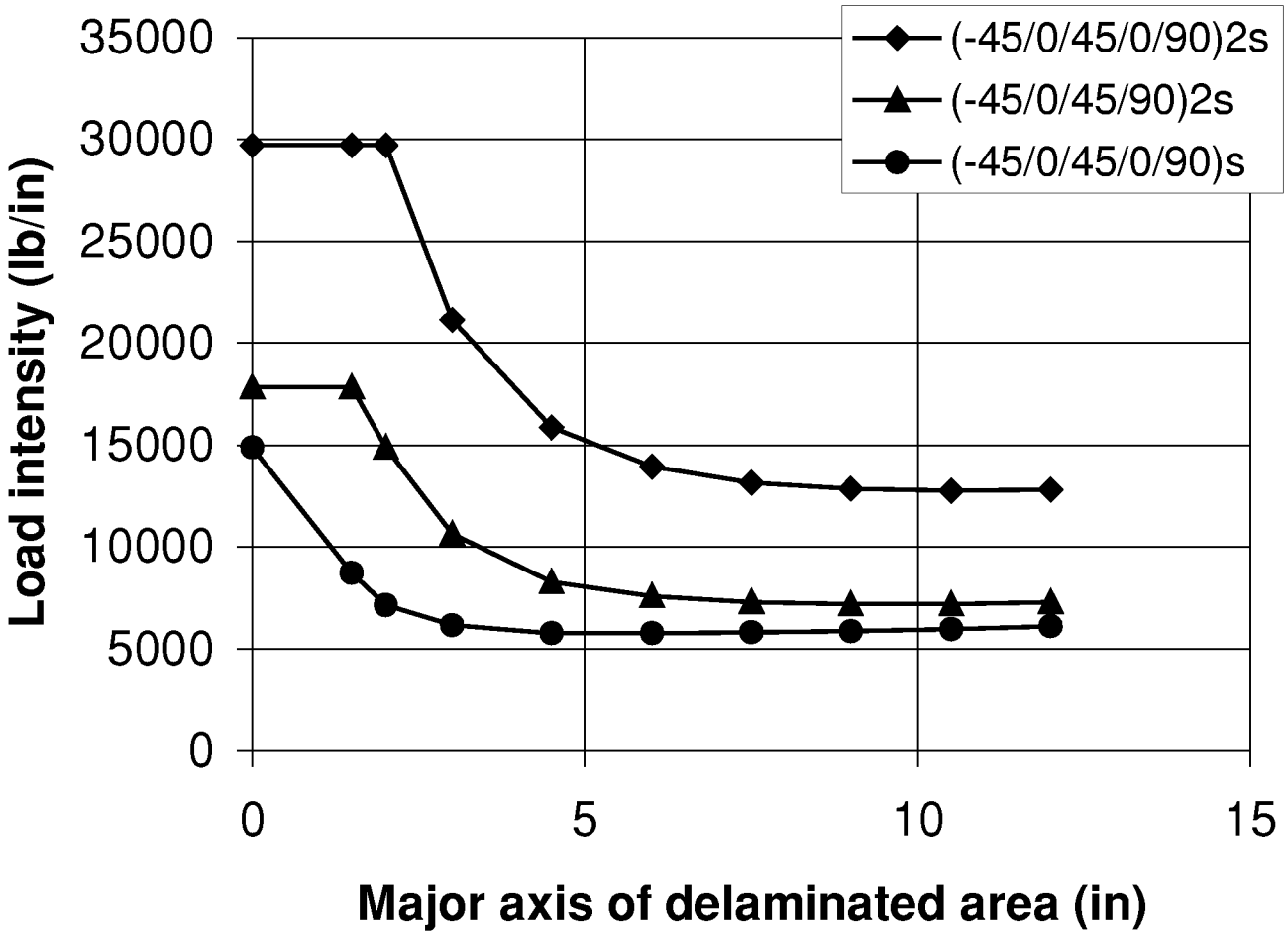

Figure 24. Case 2: Residual Strength of a Sandwich Panel with an Elliptical Delamination Loaded in Compression (Variation in Thickness)

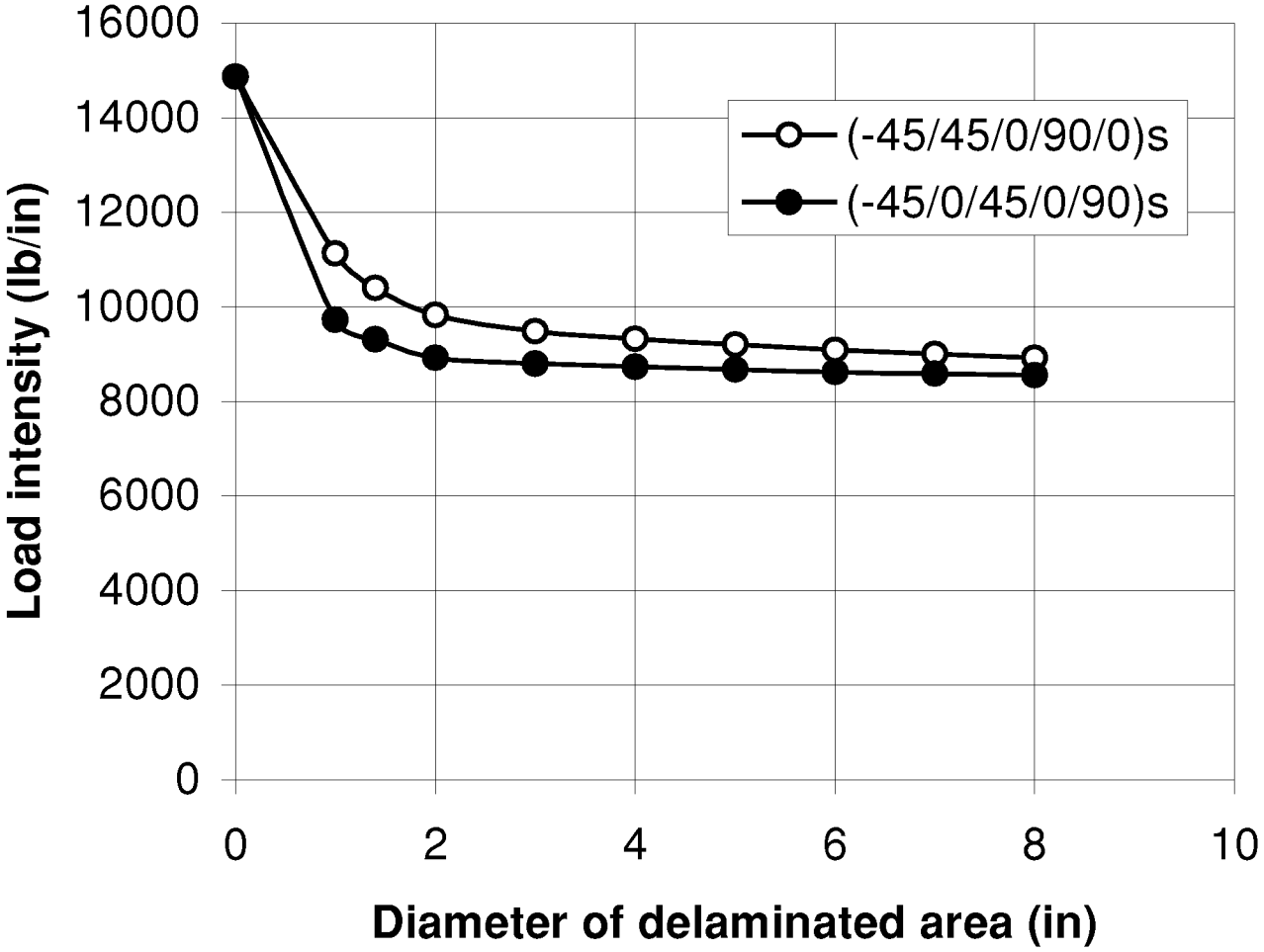

Figure 25. Case 2: Residual Strength of a Sandwich Panel with a Circular Delamination Loaded in Compression (Variation in Stacking Sequence)

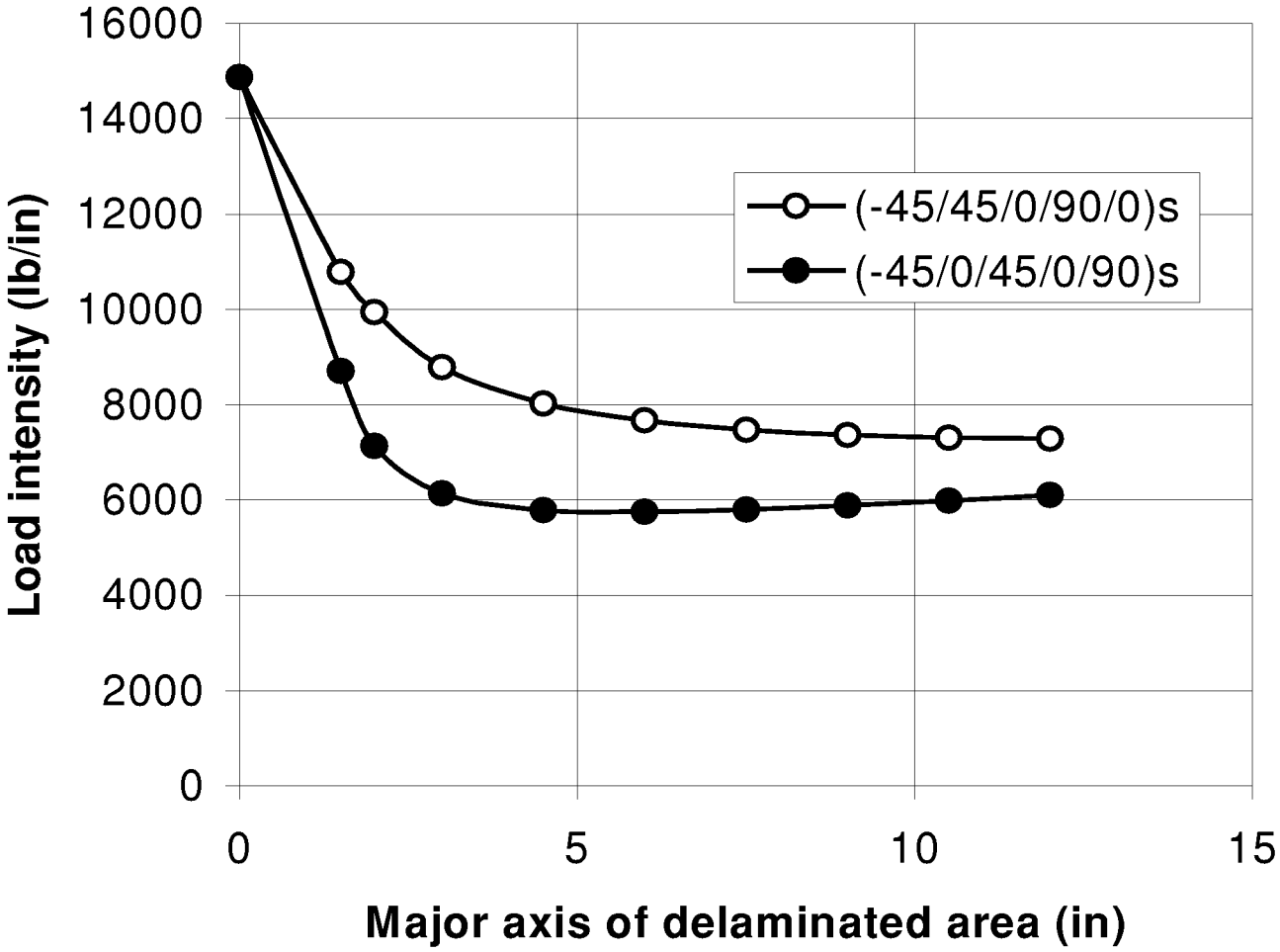

Figure 26. Case 2: Residual Strength of a Sandwich Panel with an Elliptical Delamination Loaded in Compression (Variation in Stacking Sequence)

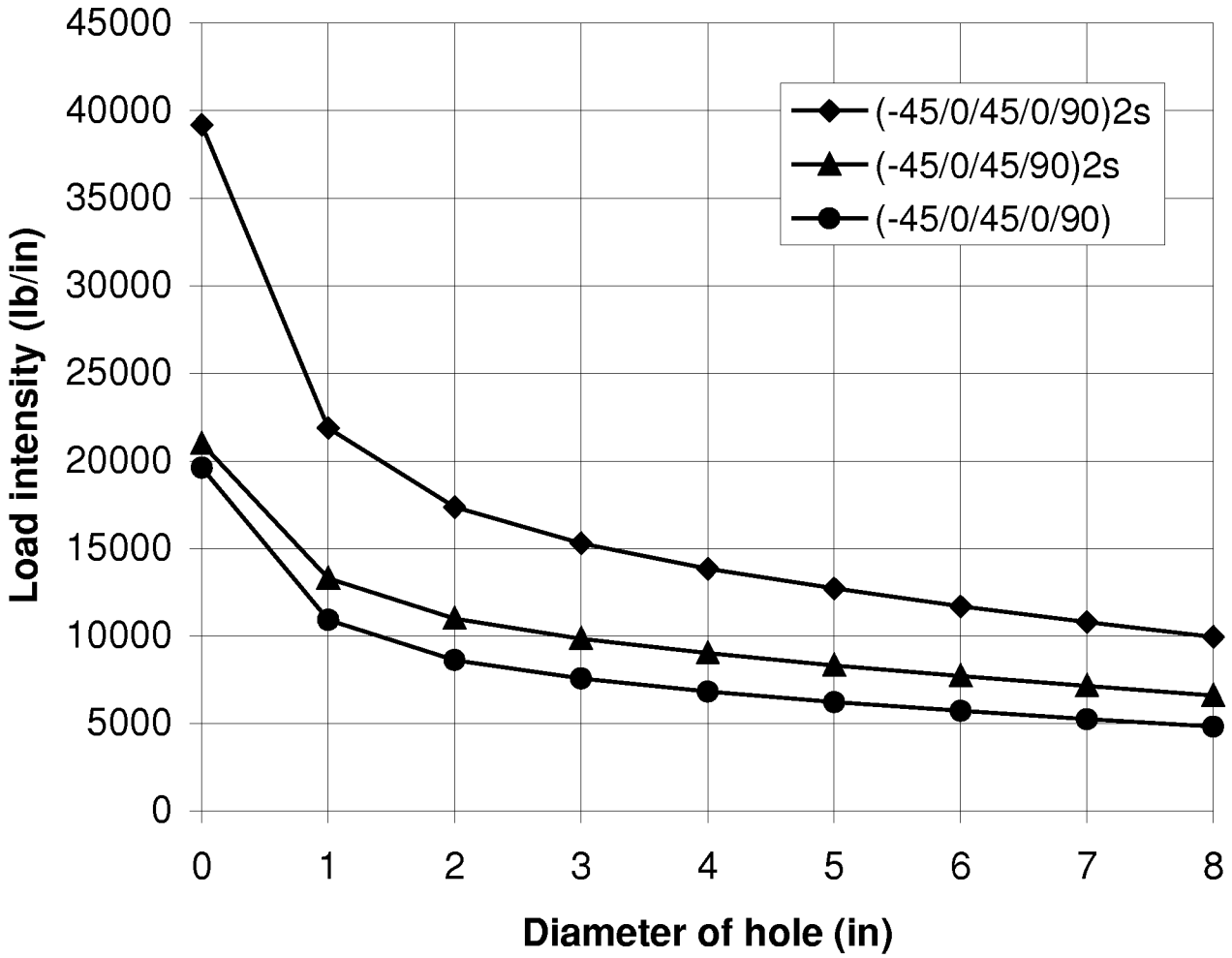

Figure 27. Case 3: Residual Strength of a Sandwich Panel with a Circular Hole on One Face Sheet Loaded in Tension (Variation in Thickness)

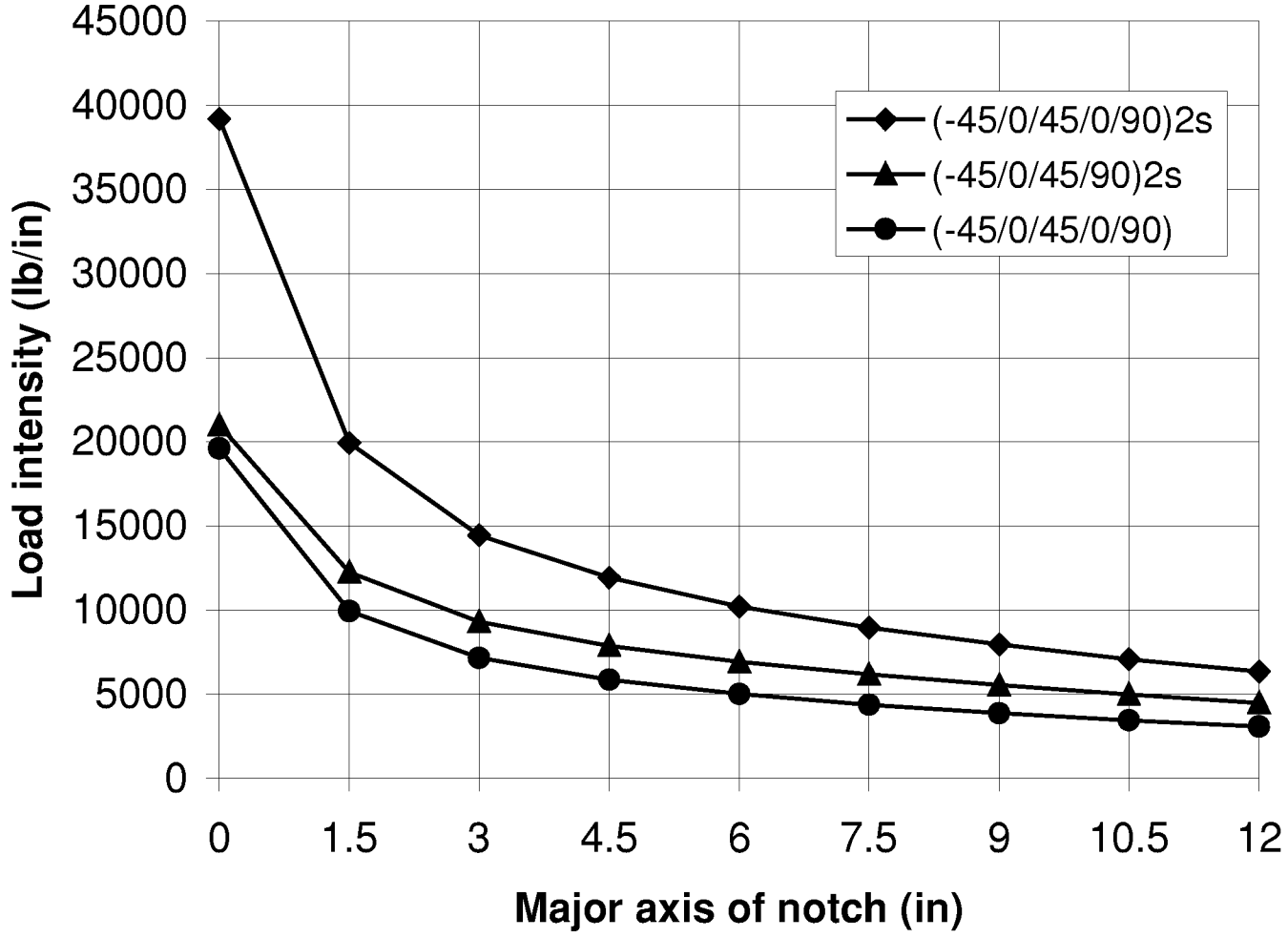

Figure 28. Case 3: Residual Strength of a Sandwich Panel with an Elliptical Notch on One Face Sheet Loaded in Tension (Variation in Thickness)

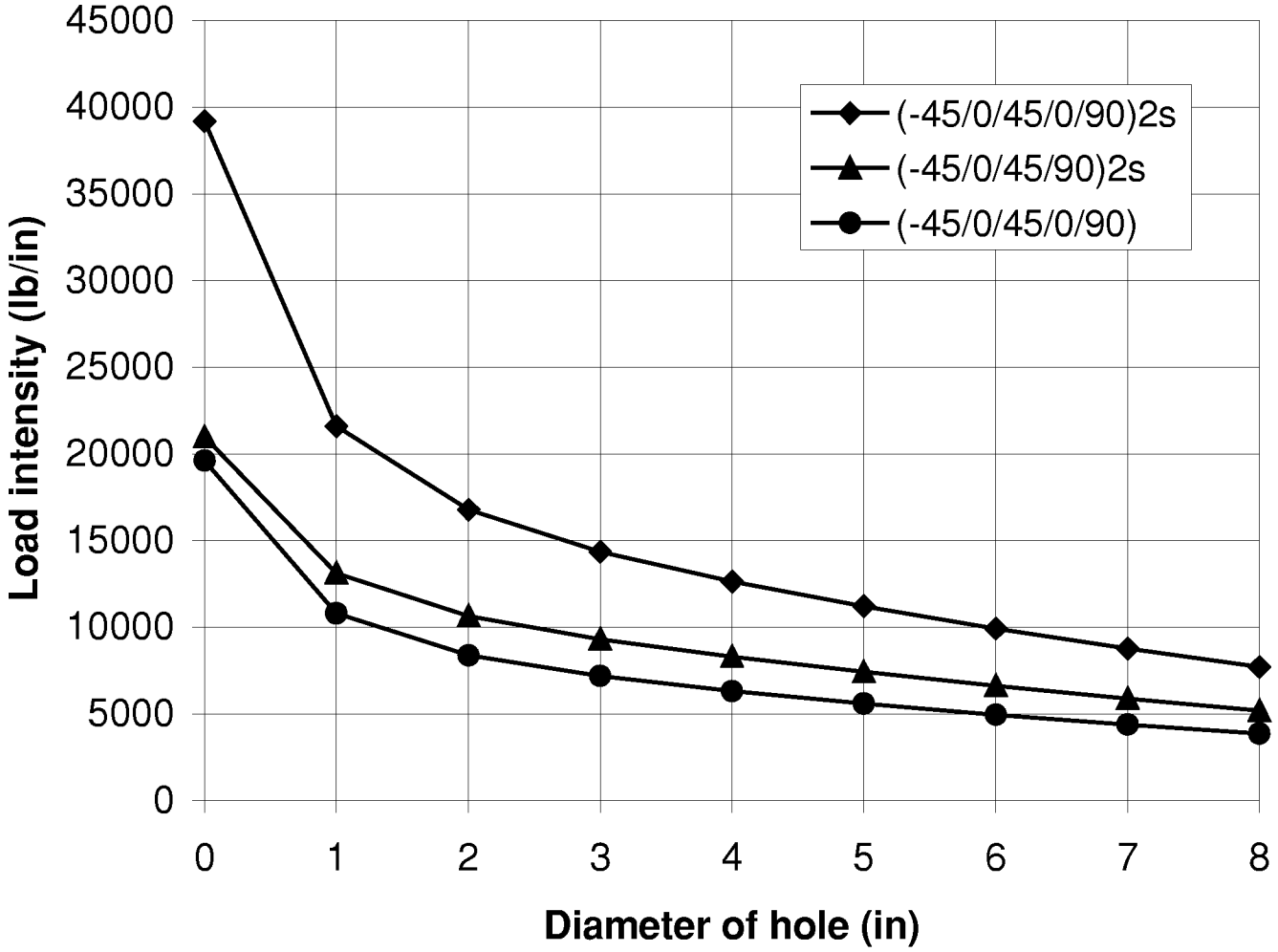

Figure 29. Case 3: Residual Strength of a Sandwich Panel with a Circular Through-the-Thickness Hole Loaded in Tension (Variation in Thickness)

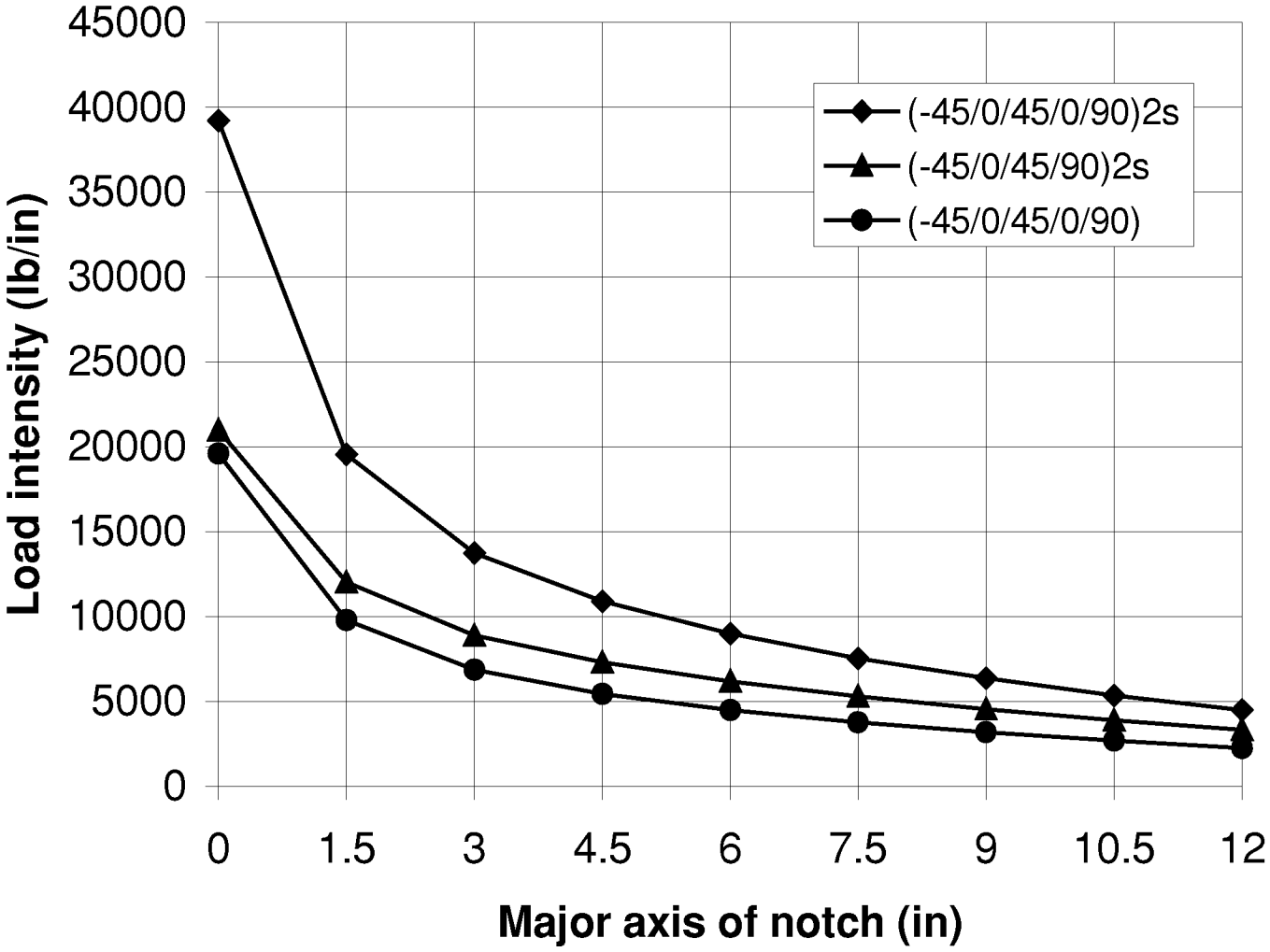

Figure 30. Case 3: Residual Strength of a Sandwich Panel with an Elliptical Through-the-Thickness Notch Loaded in Tension (Variation in Thickness)

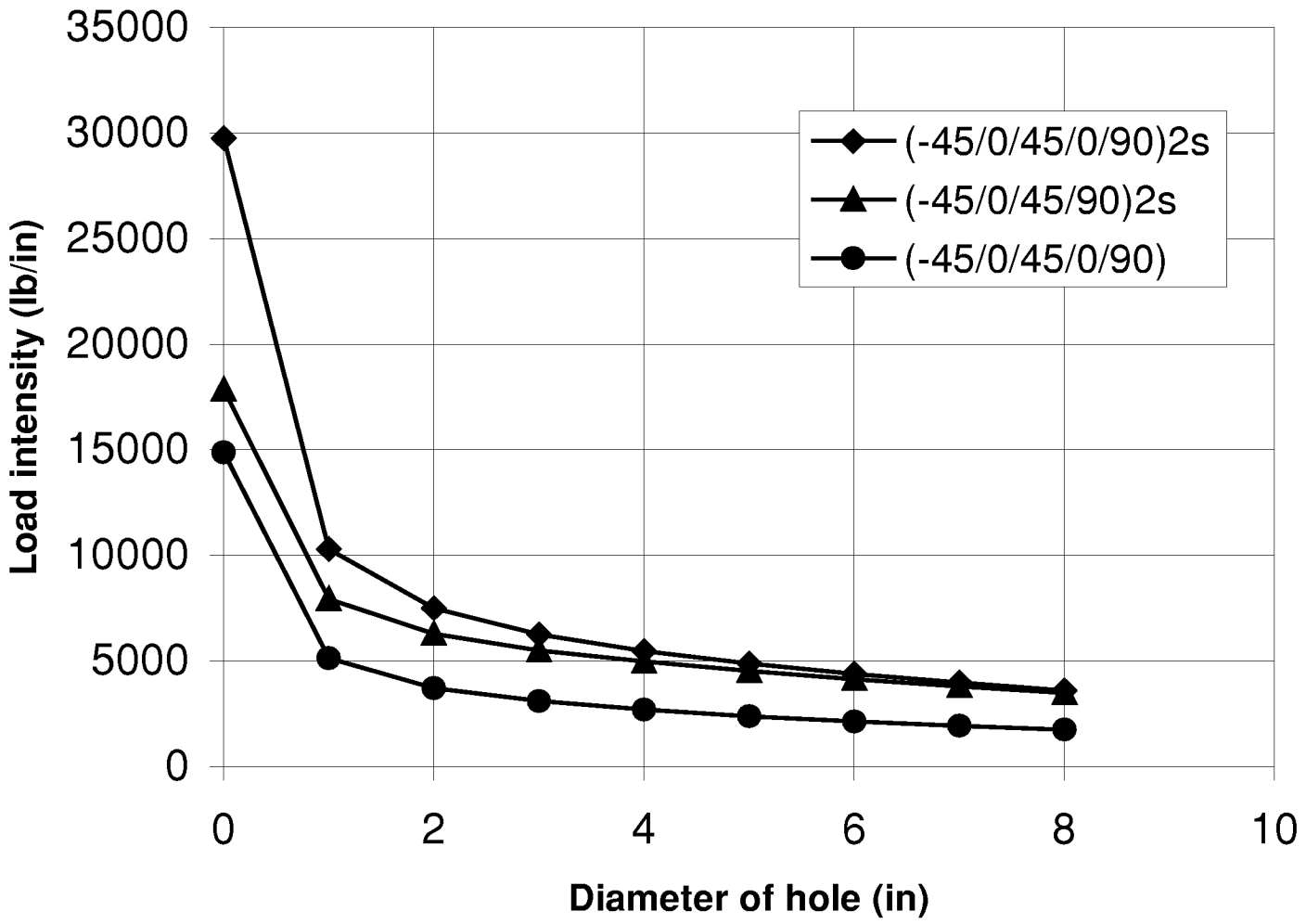

Figure 31. Case 3: Residual Strength of a Sandwich Panel with a Circular Hole on One Face Sheet Loaded in Compression (Variation in Thickness)

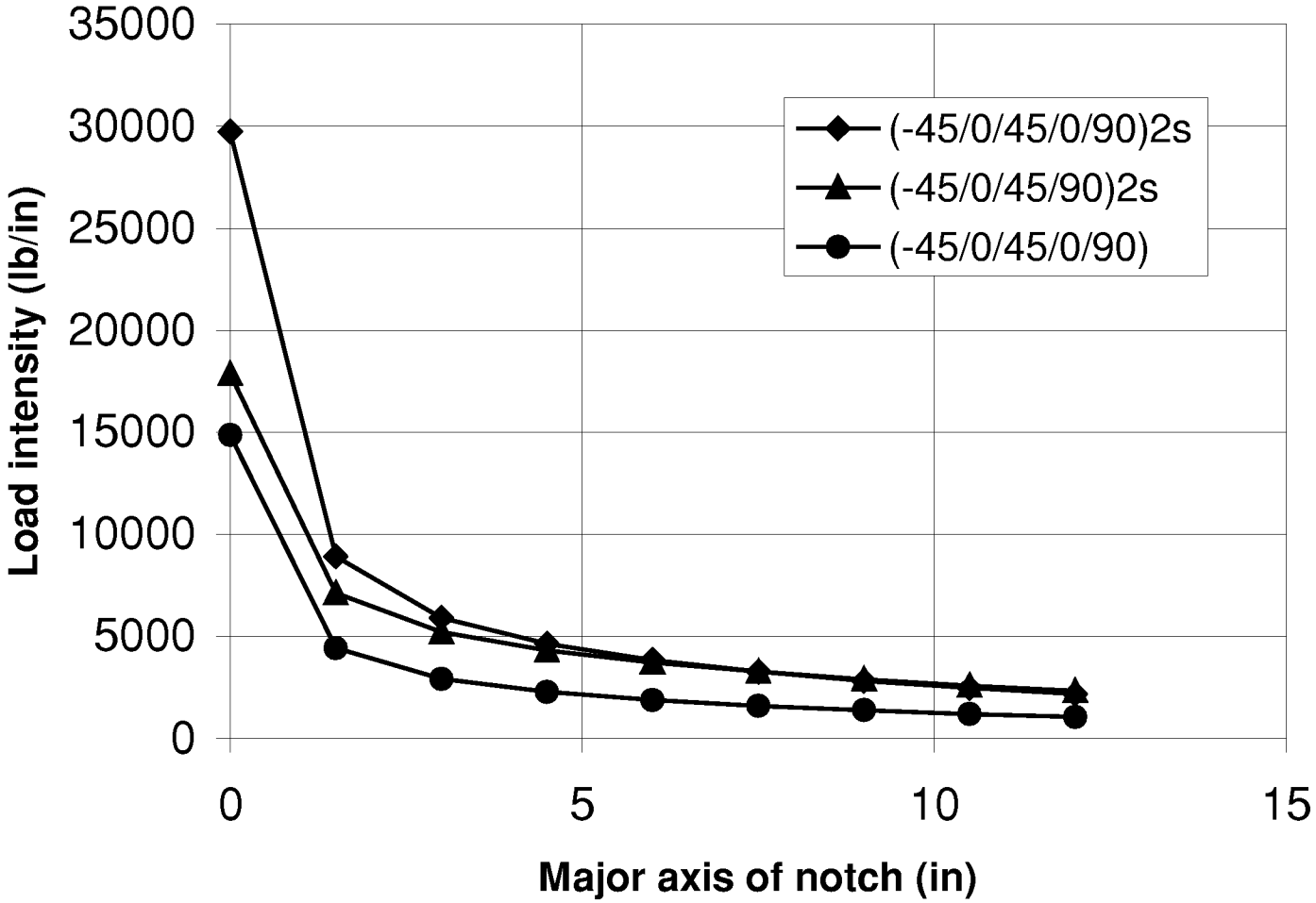

Figure 32. Case 3: Residual Strength of a Sandwich Panel with an Elliptical Notch on One Face Sheet Loaded in Compression (Variation in Thickness)

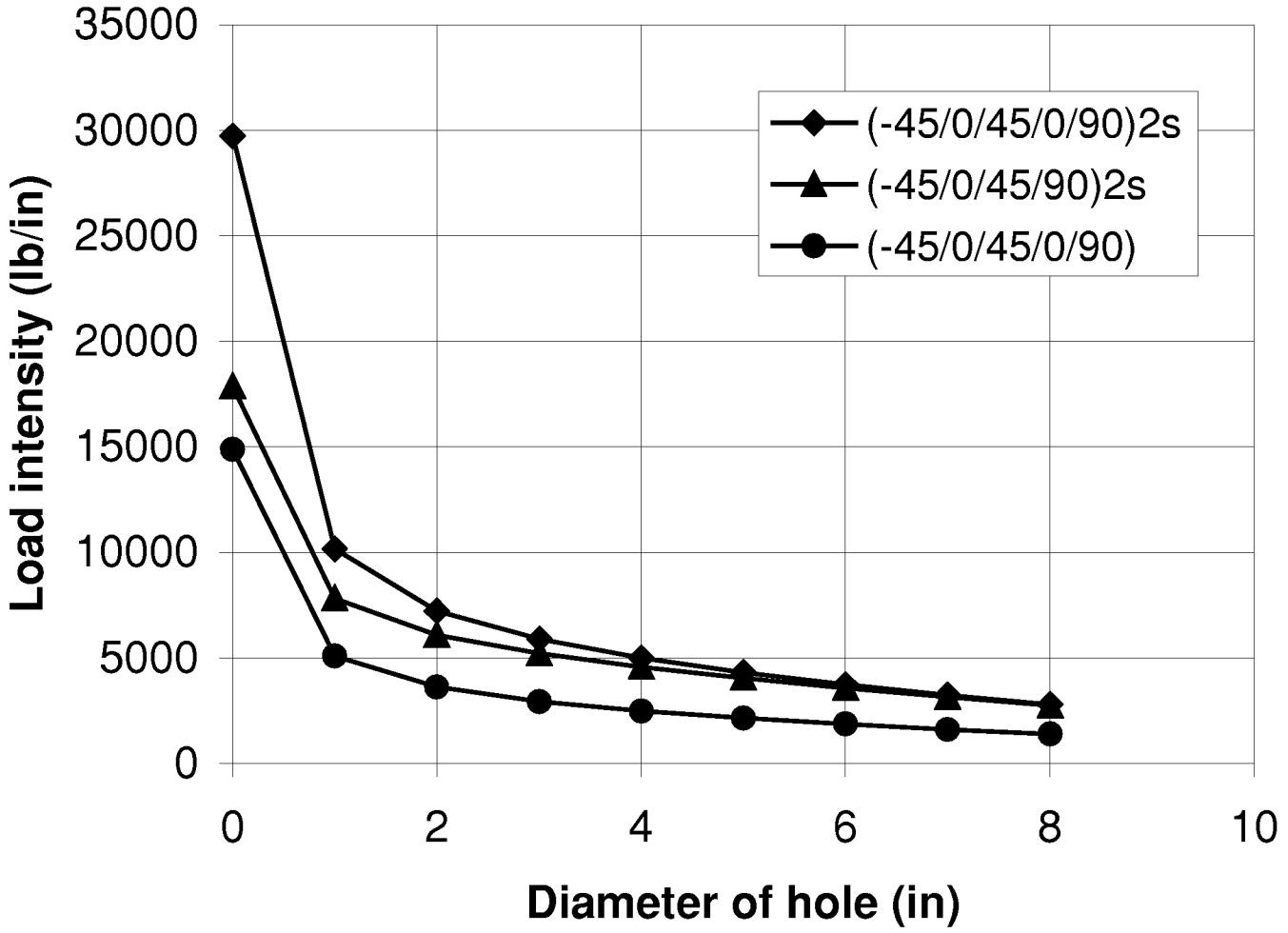

Figure 33. Case 3: Residual Strength of a Sandwich Panel with a Circular Through-the-Thickness Hole Loaded in Compression (Variation in Thickness)

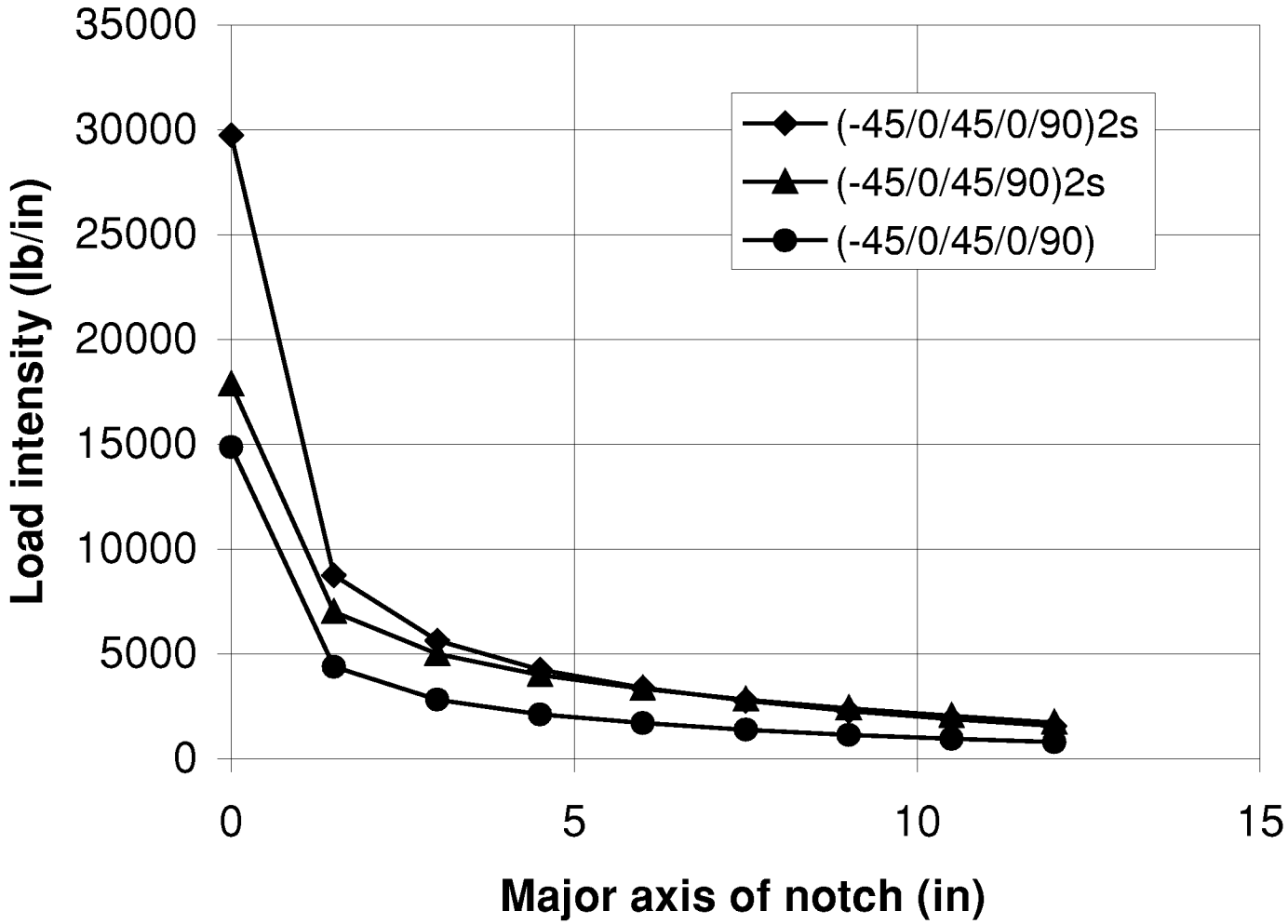

Figure 34. Case 3: Residual Strength of a Sandwich Panel with an Elliptical Through-the-Thickness Notch Loaded in Compression (Variation in Thickness)

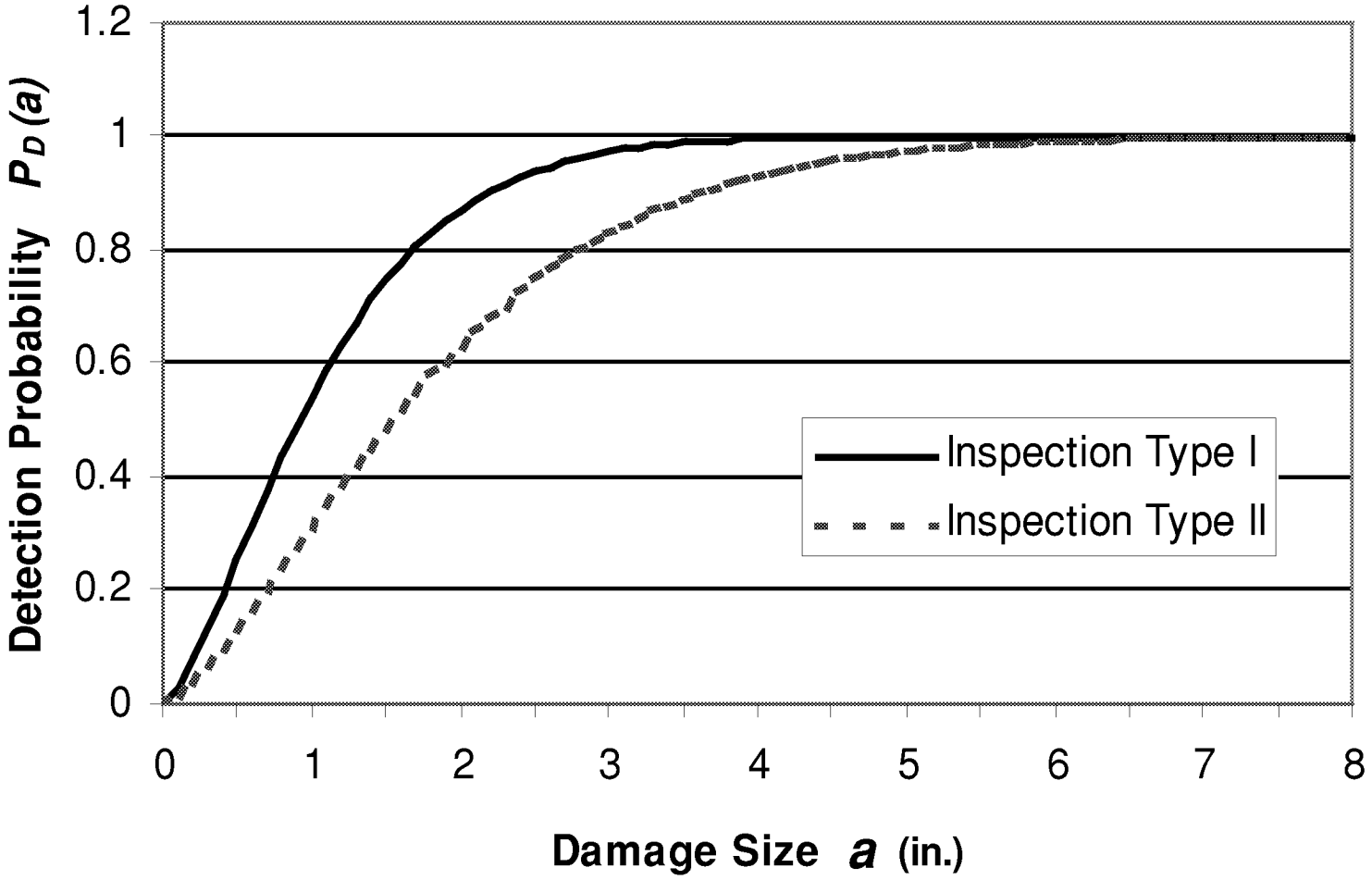

Figure 35. Probability of Damage Detection $P_D(a)$ with Various Inspection Types

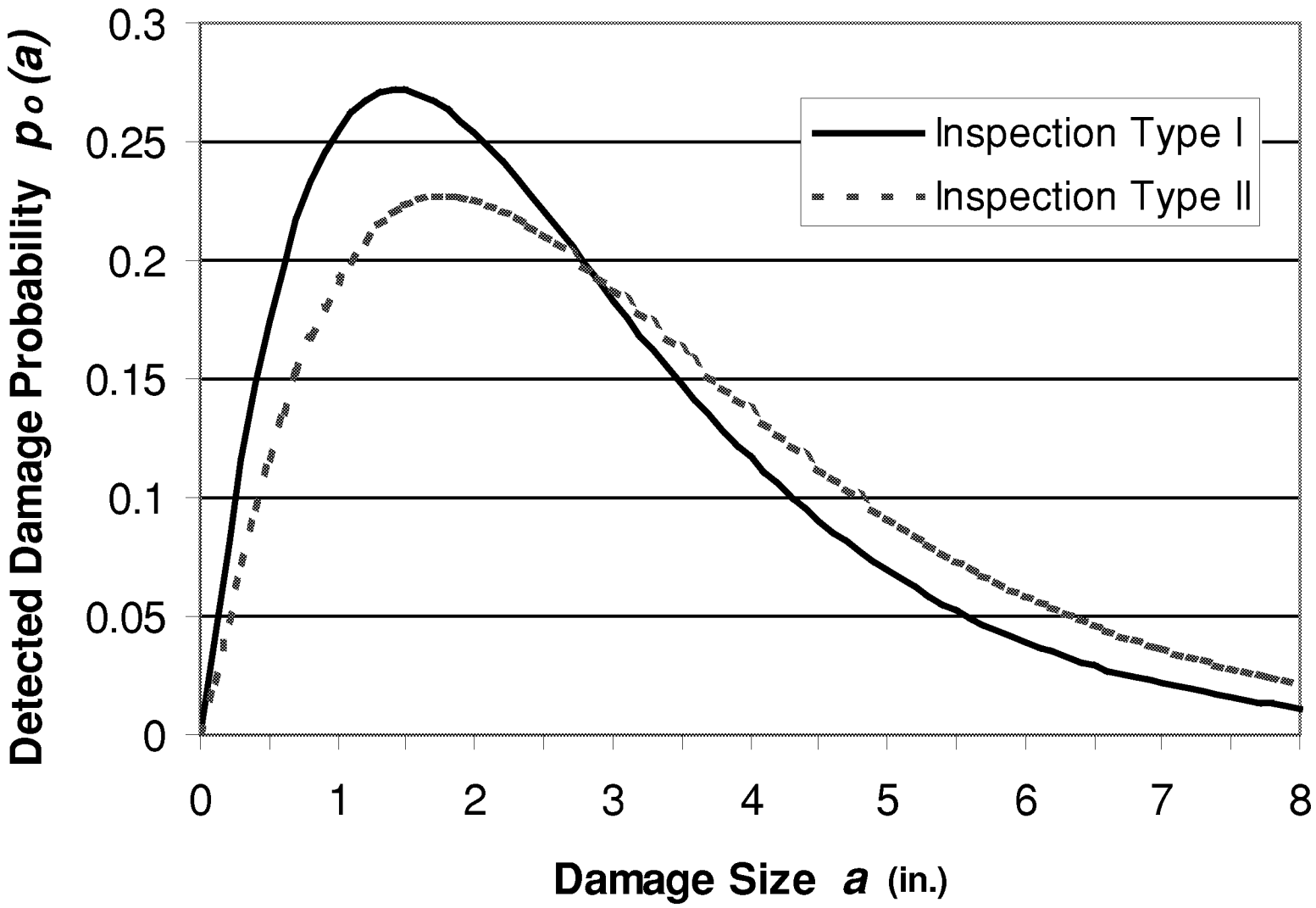

Figure 36. Probability Density Function for Detected Damage Size $p_o(a)$

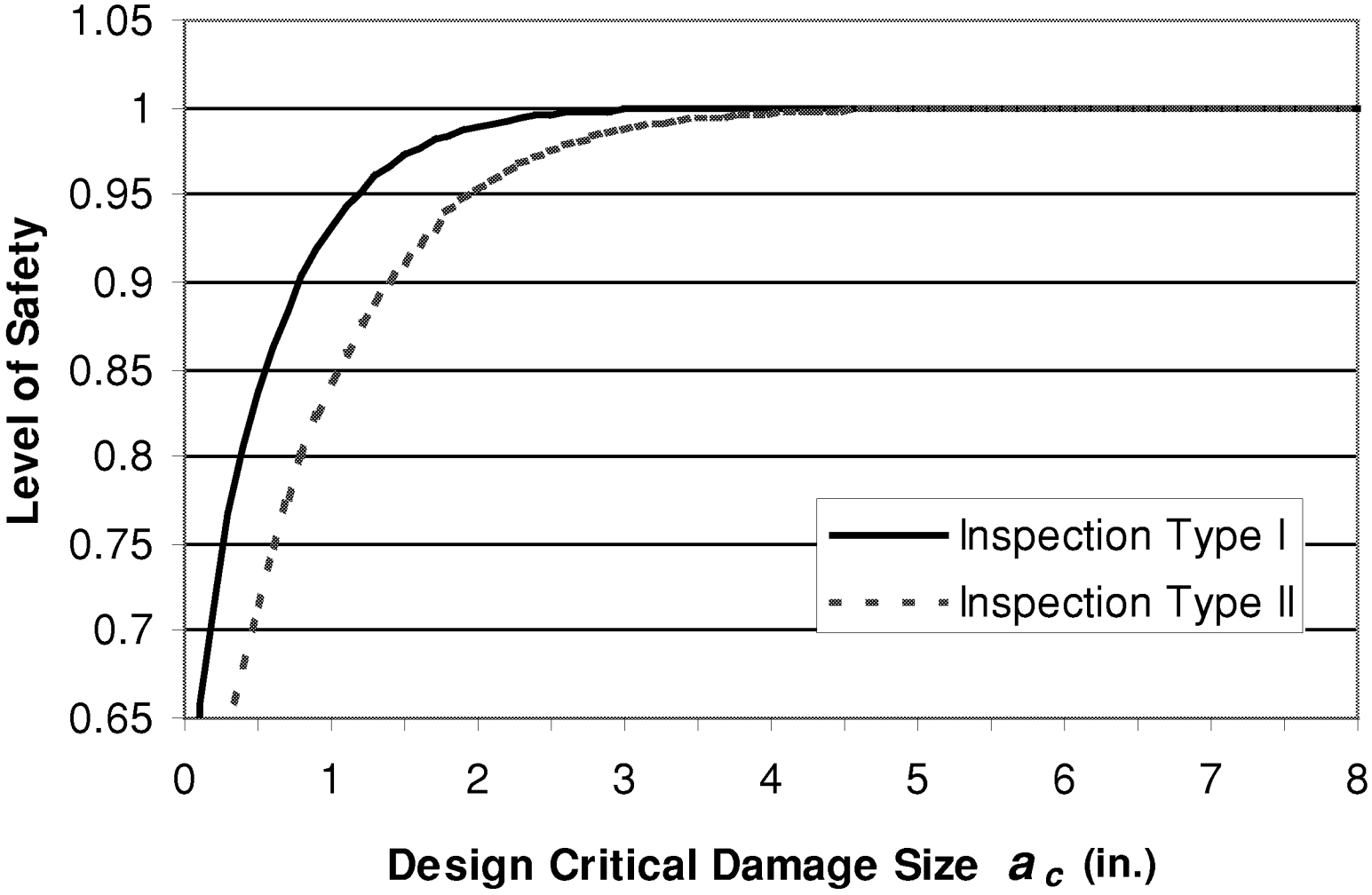

Figure 37. Level of Safety vs. Critical Damage Size with Various Inspection Types

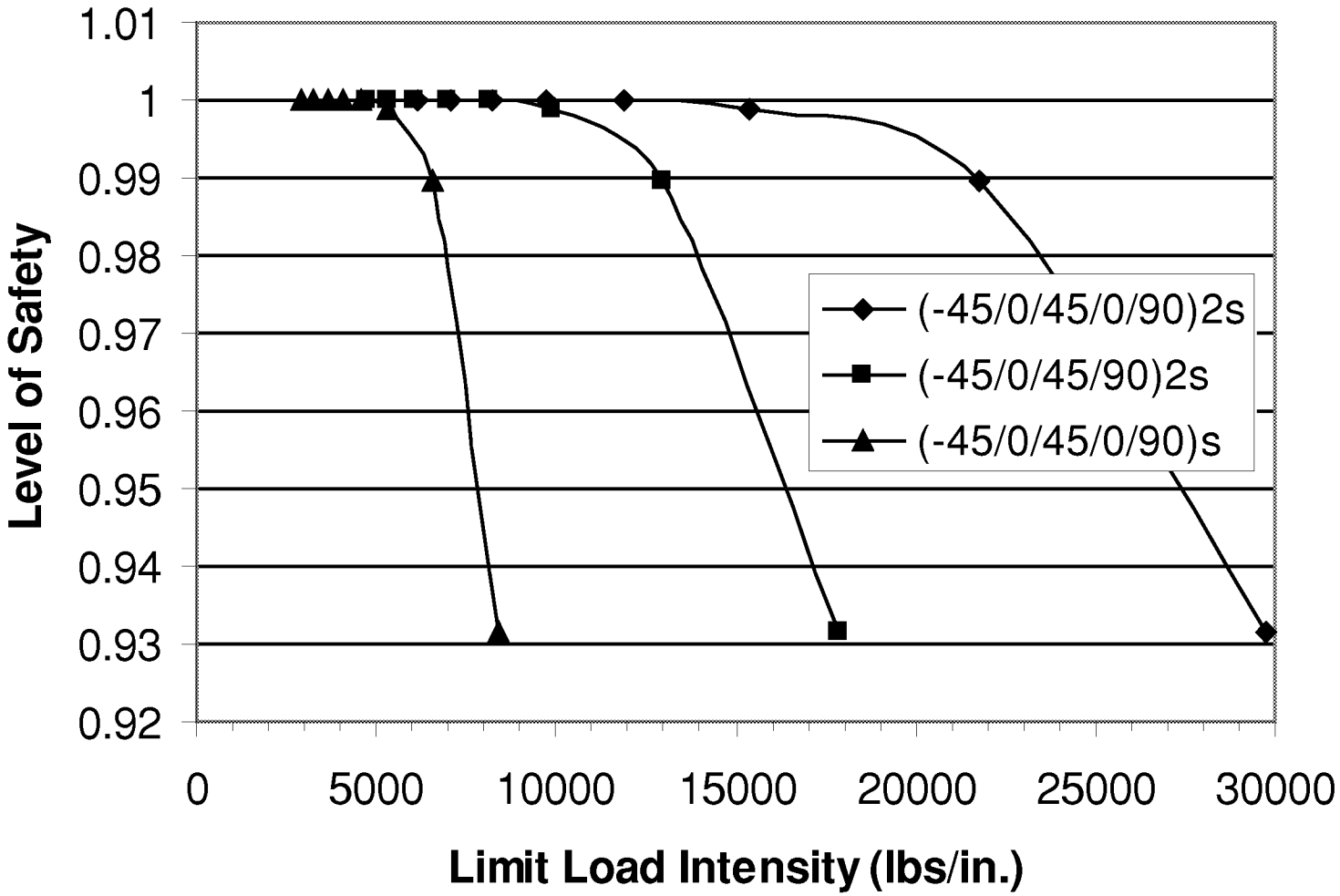

Figure 38. Design Load vs. Level of Safety for a Sandwich Panel with a Circular Disbond Loaded in Compression (Inspection Type I)

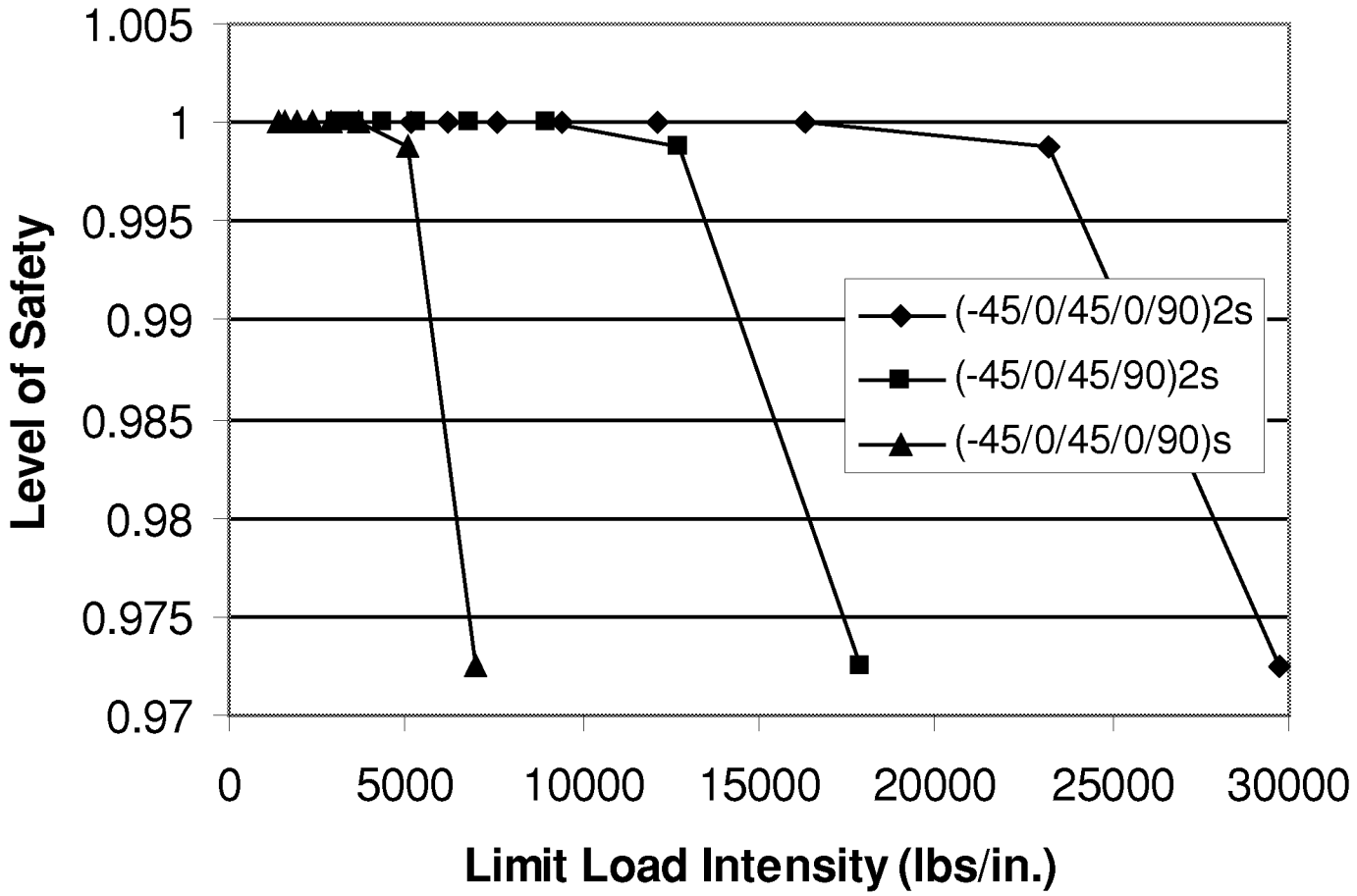

Figure 39. Design Load vs. Level of Safety for a Sandwich Panel with an Elliptical Disbond Loaded in Compression (Inspection Type I)

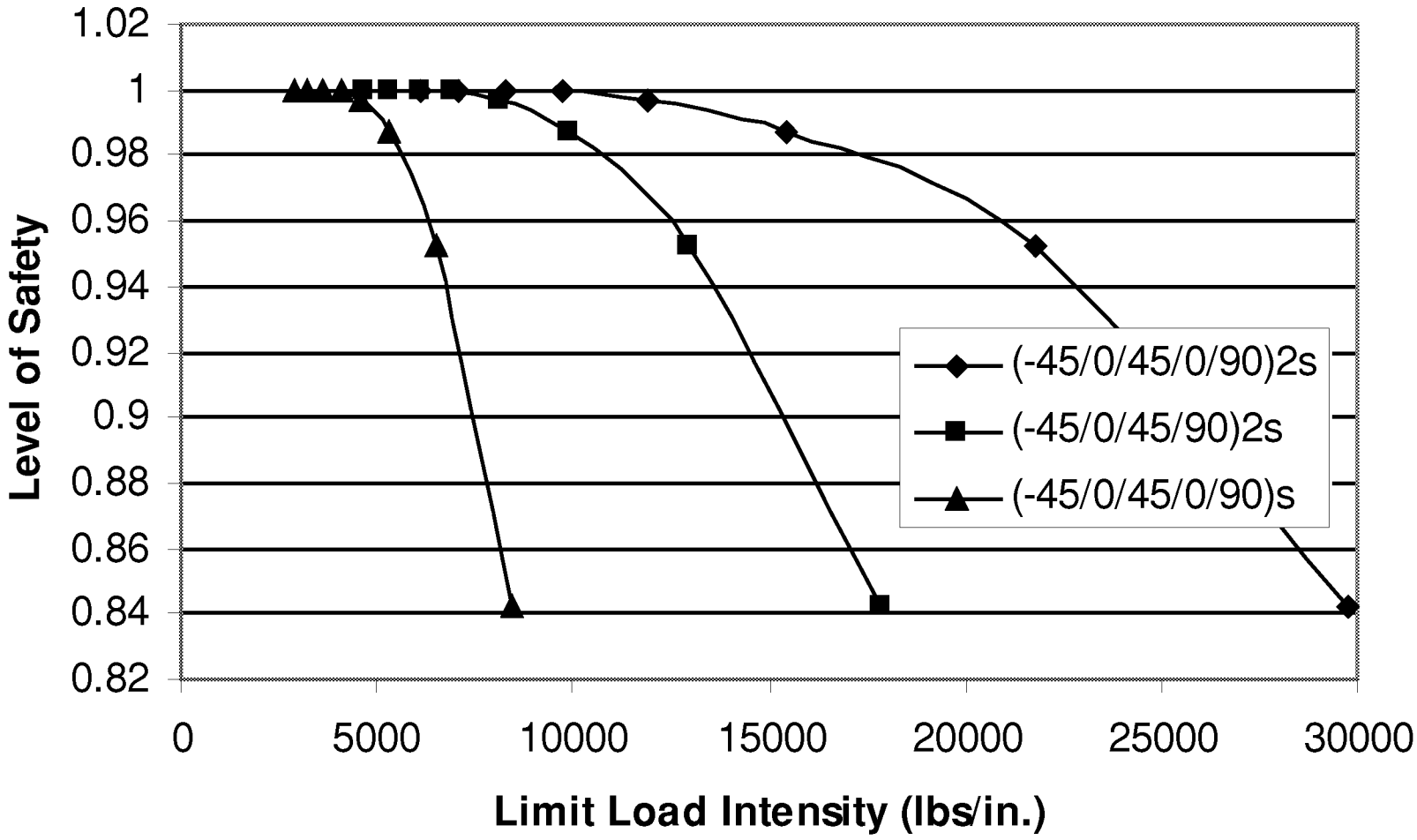

Figure 40. Design Load vs. Level of Safety for a Sandwich Panel with a Circular Disbond Loaded in Compression (Inspection Type II)

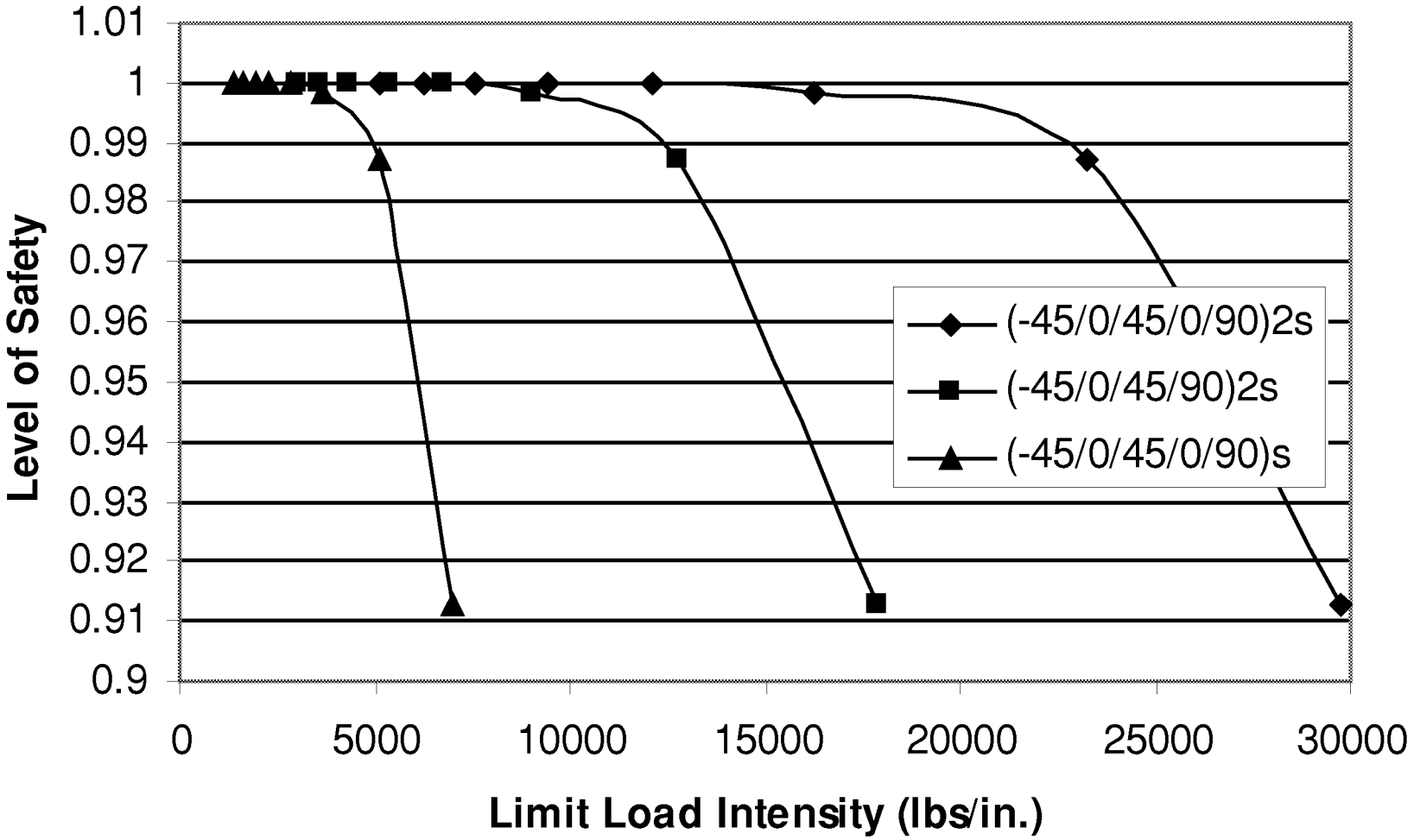

Figure 41. Design Load vs. Level of Safety for a Sandwich Panel with an Elliptical Disbond Loaded in Compression (Inspection Type II)

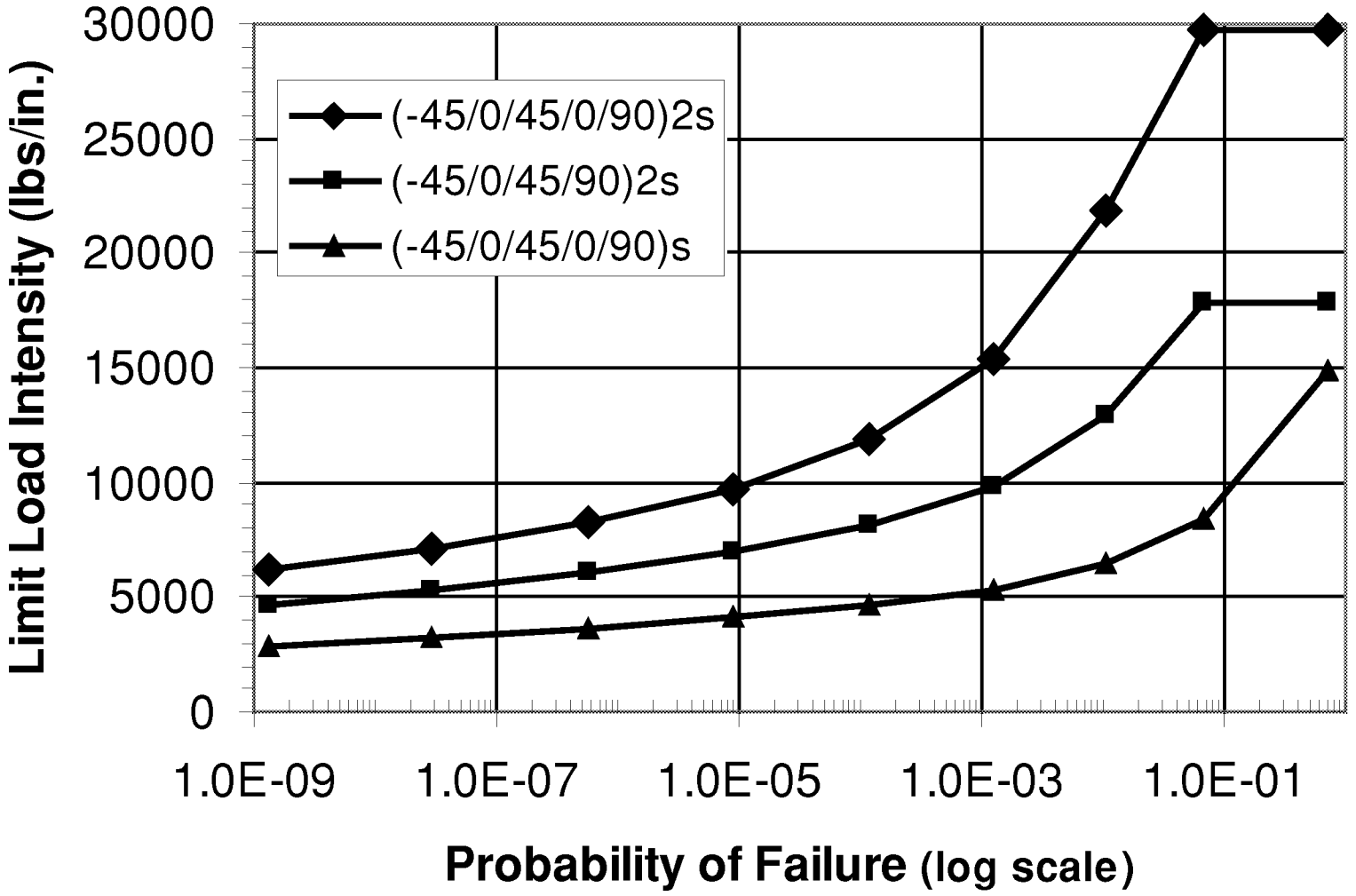

Figure 42. Design Load vs. Probability of Failure for a Sandwich Panel with a Circular Disbond Loaded in Compression (Inspection Type I)

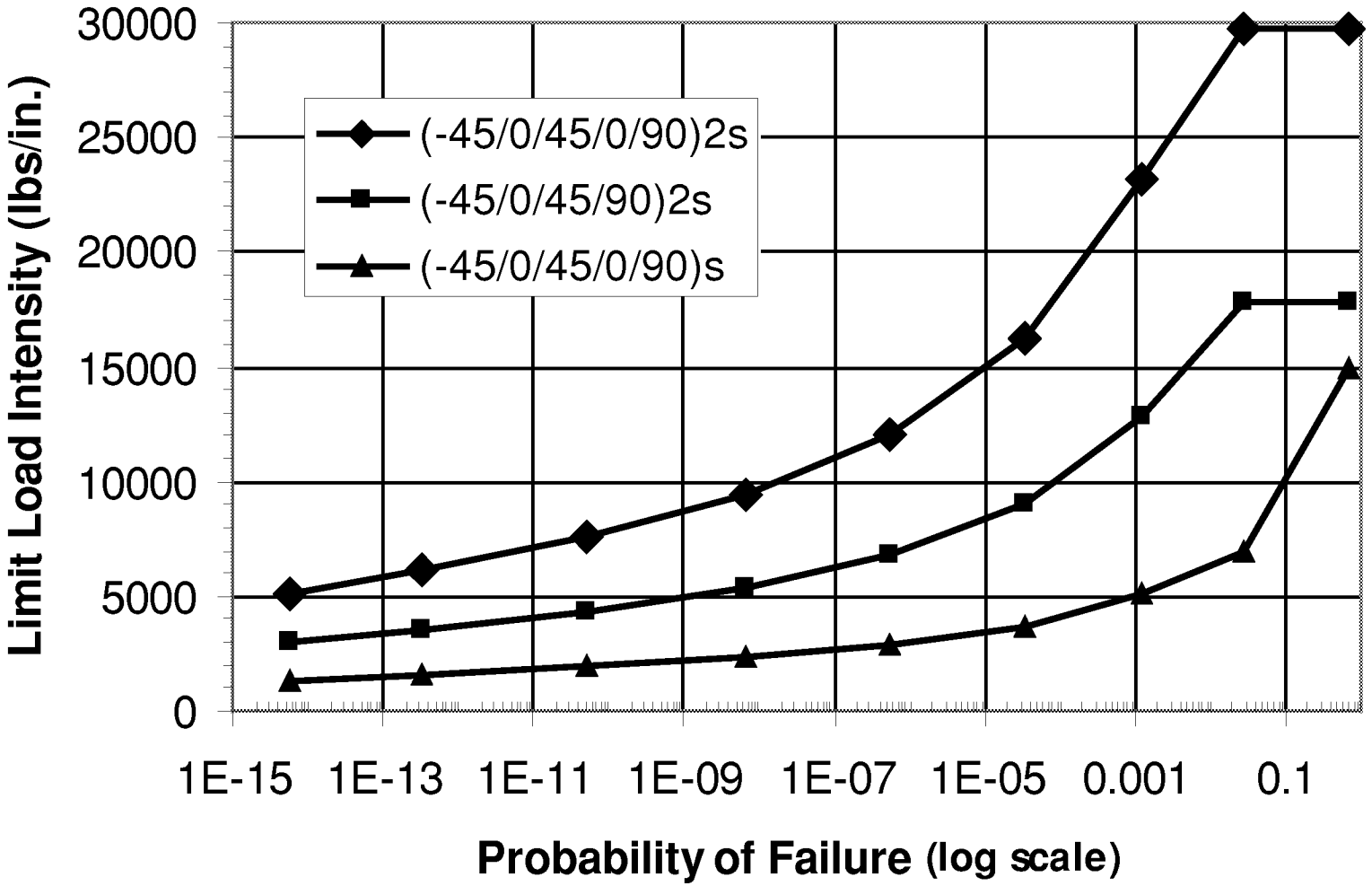

Figure 43. Design Load vs. Probability of Failure for a Sandwich Panel with an Elliptical Disbond Loaded in Compression (Inspection Type I)

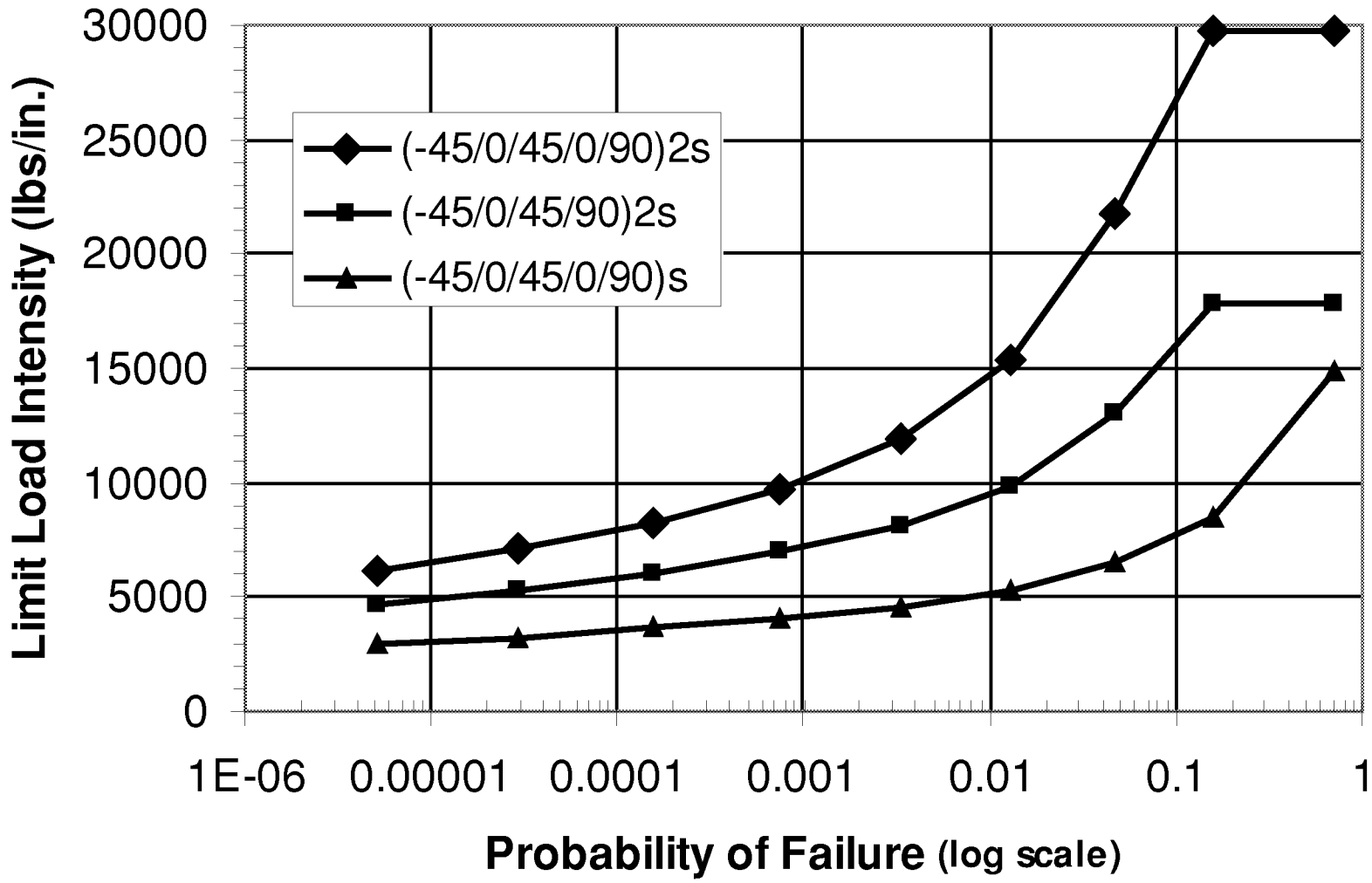

Figure 44. Design Load vs. Probability of Failure for a Sandwich Panel with a Circular Disbond Loaded in Compression (Inspection Type II)

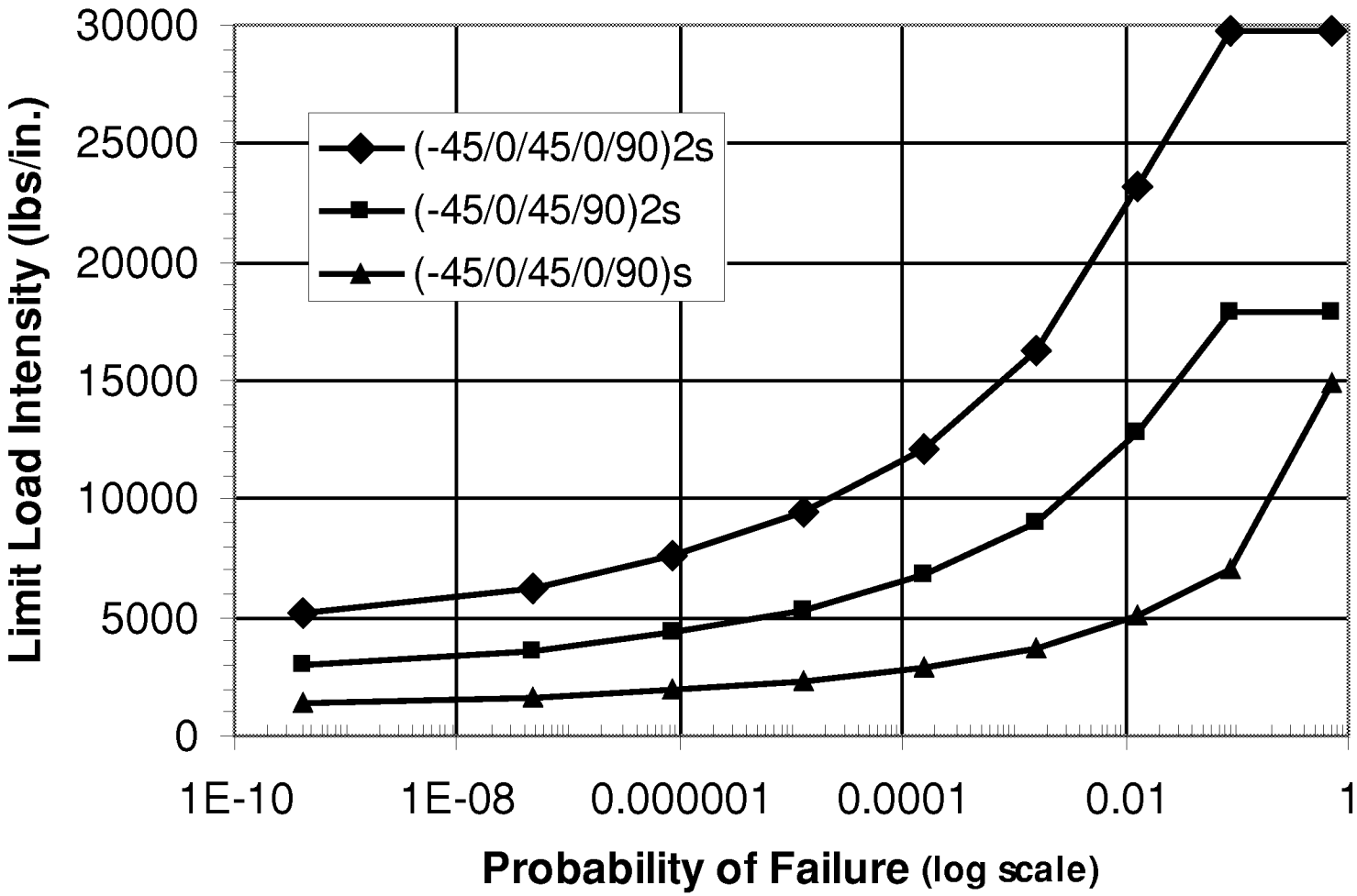

Figure 45. Design Load vs. Probability of Failure for a Sandwich Panel with an Elliptical Disbond Loaded in Compression (Inspection Type II)

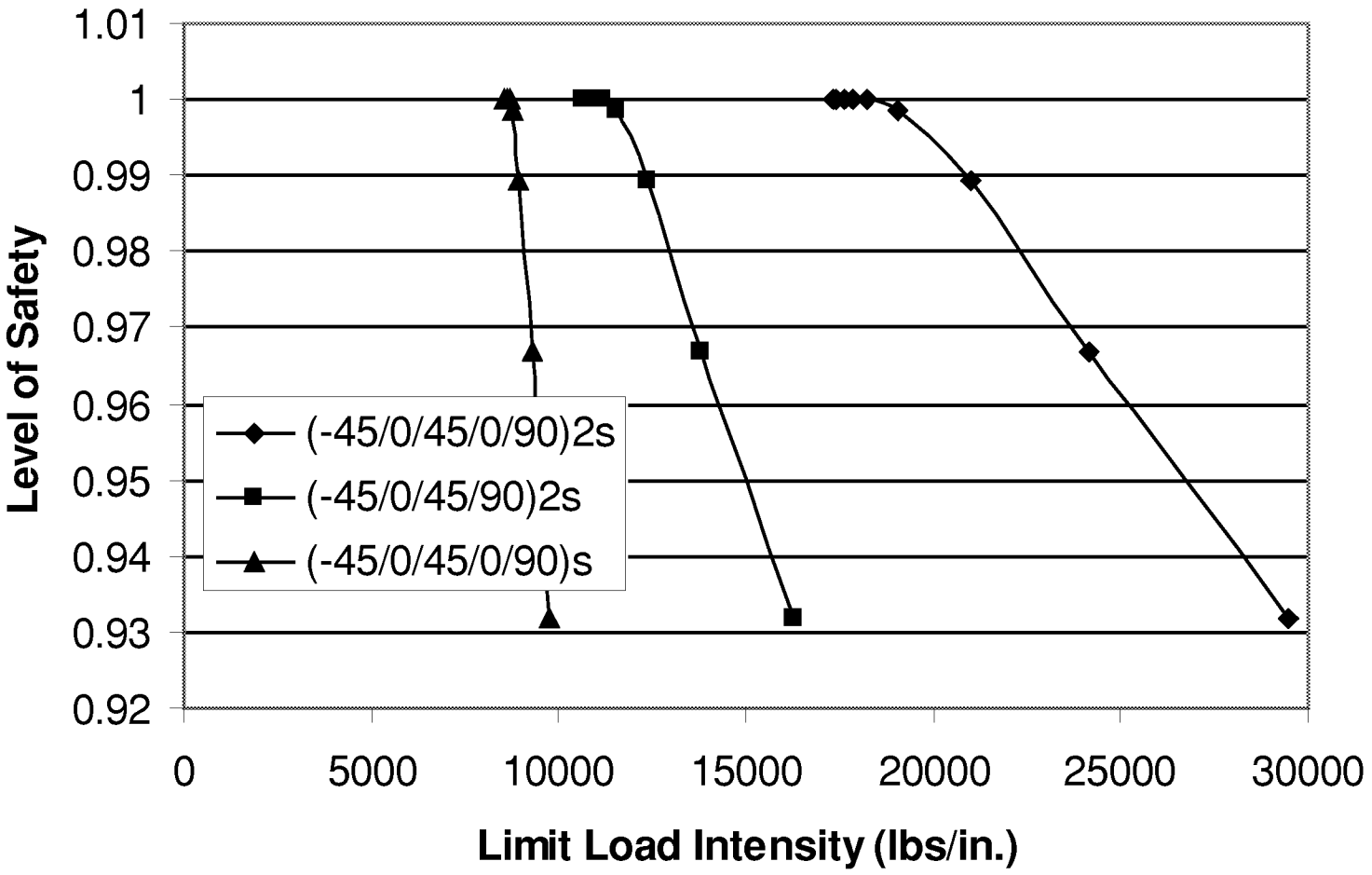

Figure 46. Design Load vs. Level of Safety for a Sandwich Panel with a Circular Delamination Loaded in Compression (Inspection Type I)

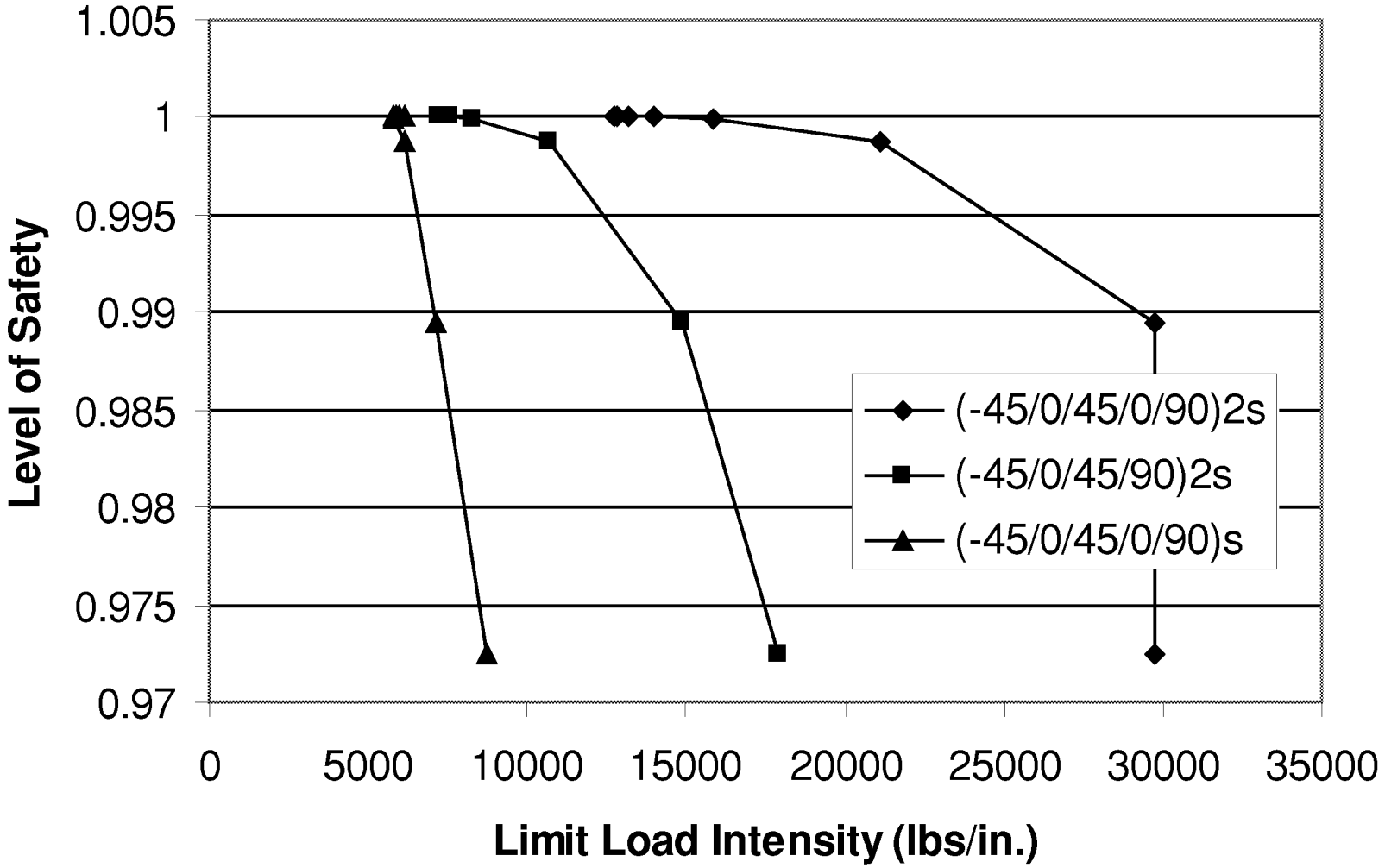

Figure 47. Design Load vs. Level of Safety for a Sandwich Panel with an Elliptical Delamination Loaded in Compression (Inspection Type I)

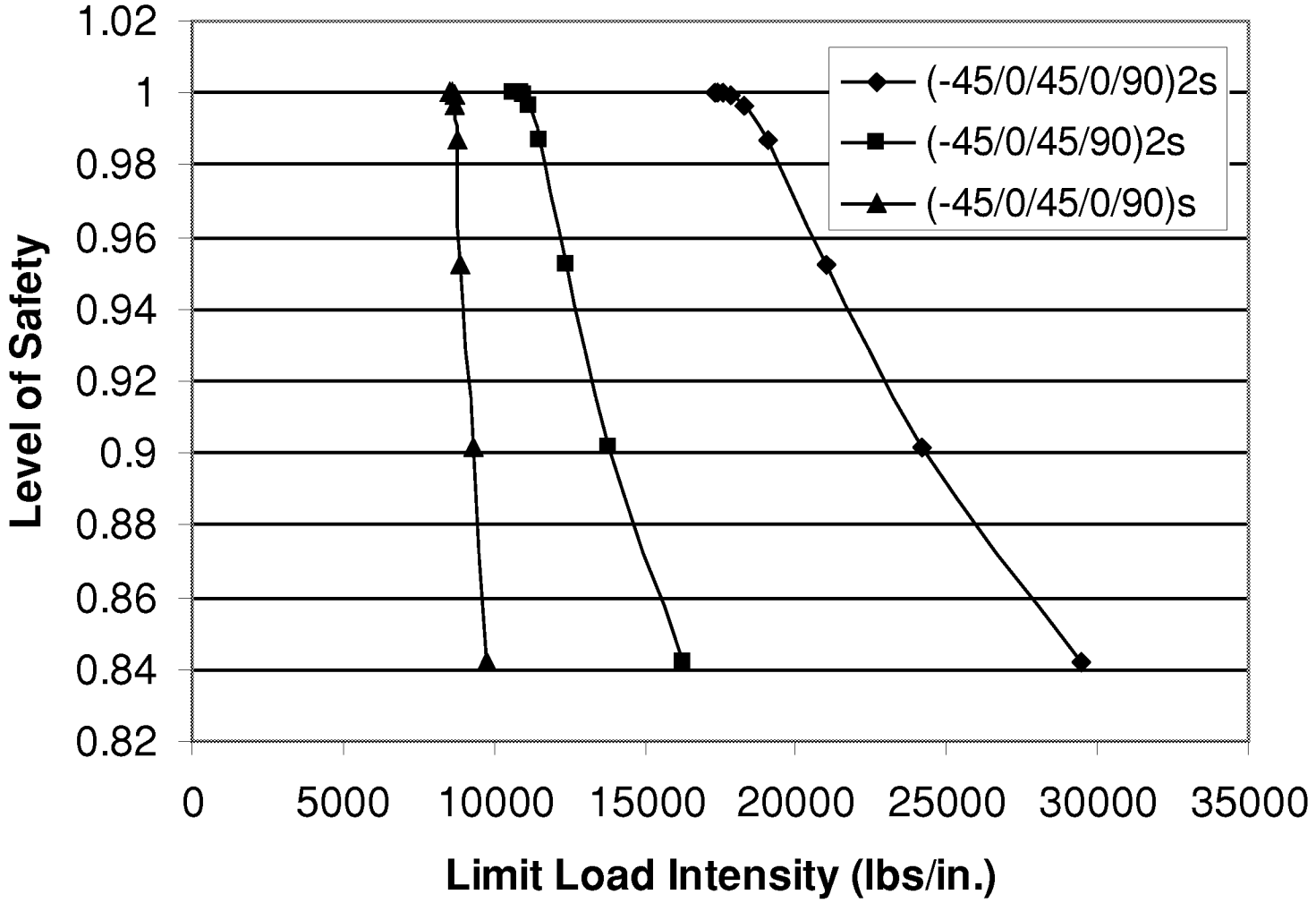

Figure 48. Design Load vs. Level of Safety for a Sandwich Panel with a Circular Delamination Loaded in Compression (Inspection Type II)

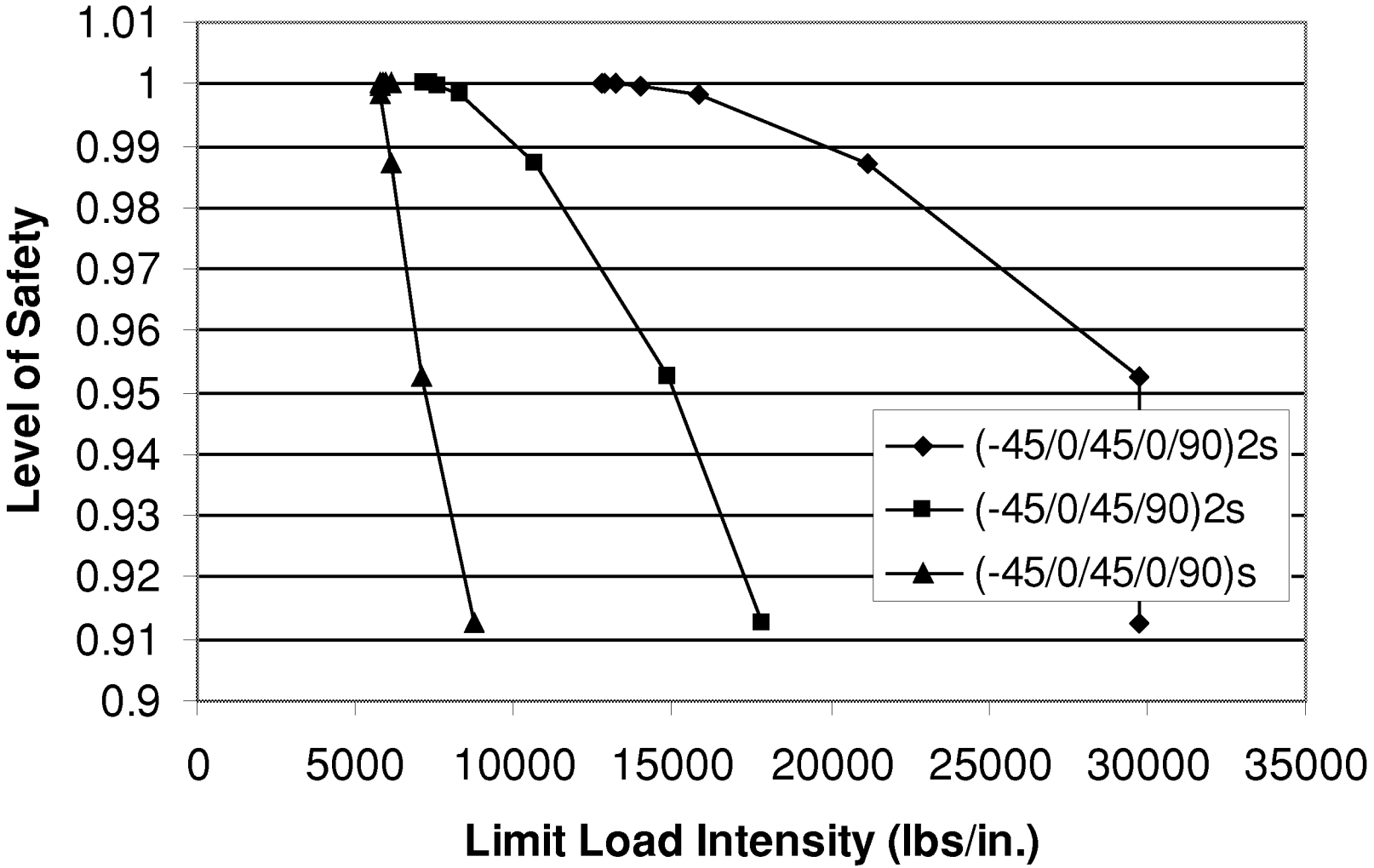

Figure 49. Design Load vs. Level of Safety for a Sandwich Panel with an Elliptical Delamination Loaded in Compression (Inspection Type II)

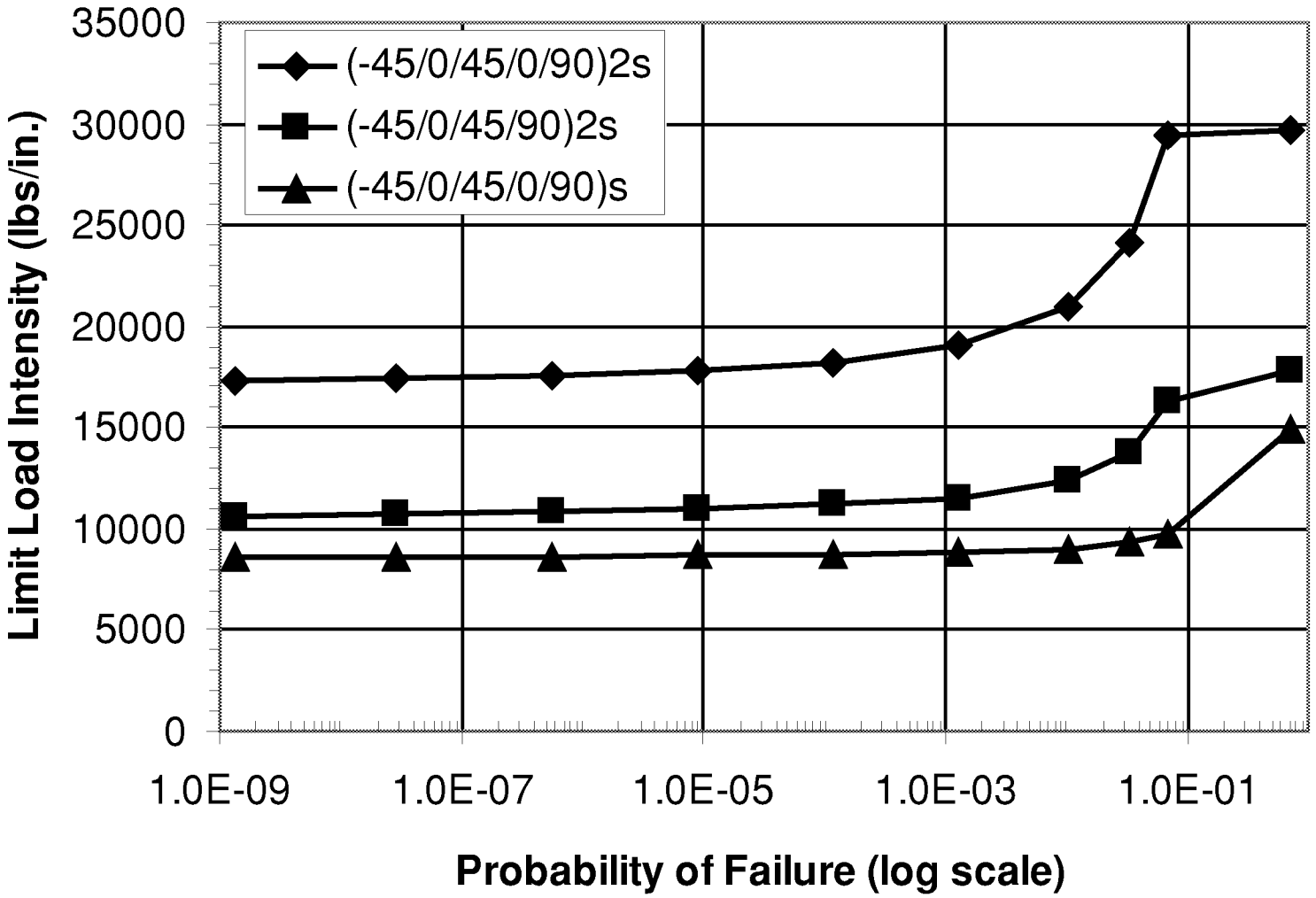

Figure 50. Design Load vs. Probability of Failure for a Sandwich Panel with a Circular Delamination Loaded in Compression (Inspection Type I)

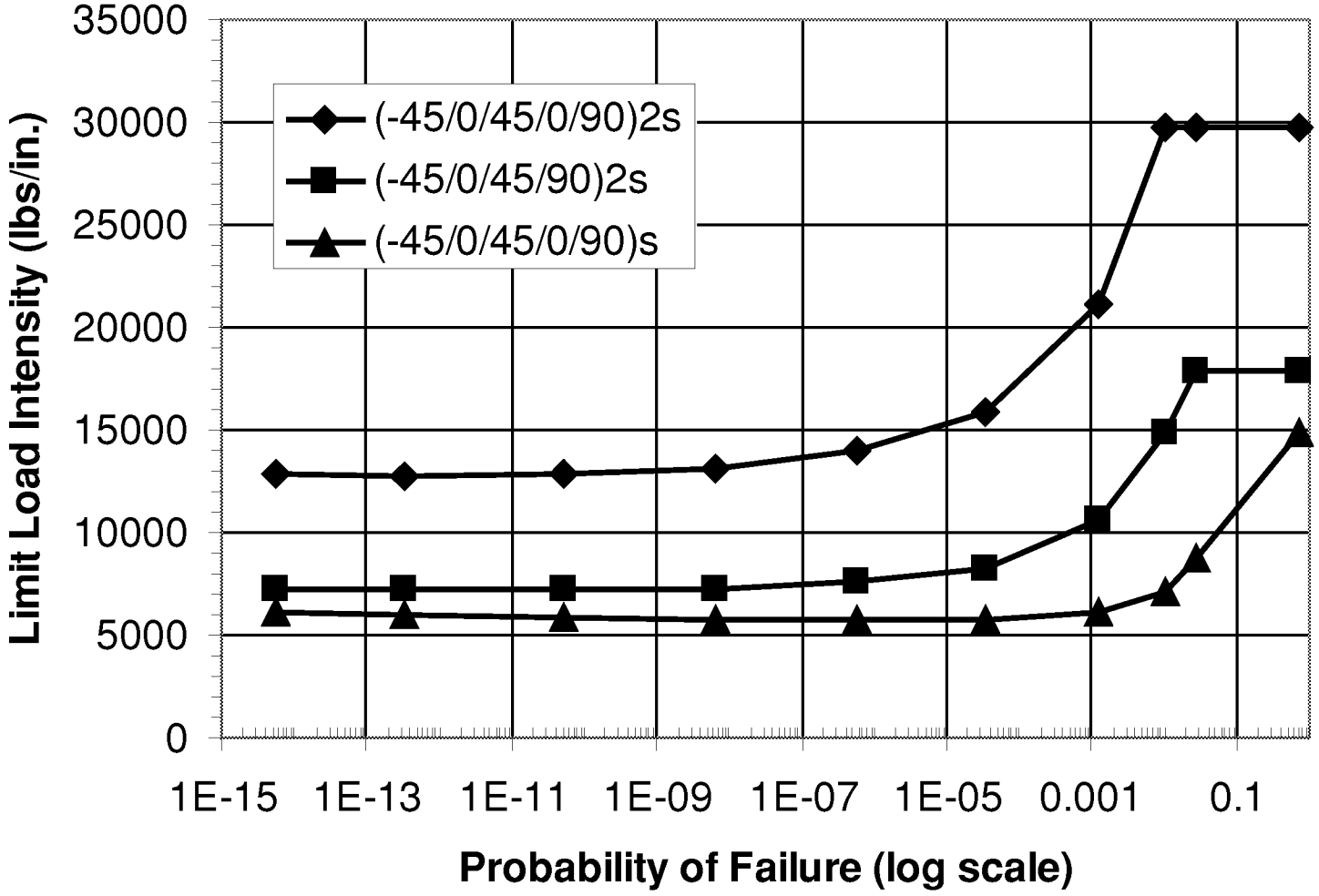

Figure 51. Design Load vs. Probability of Failure for a Sandwich Panel with an Elliptical Delamination Loaded in Compression (Inspection Type I)

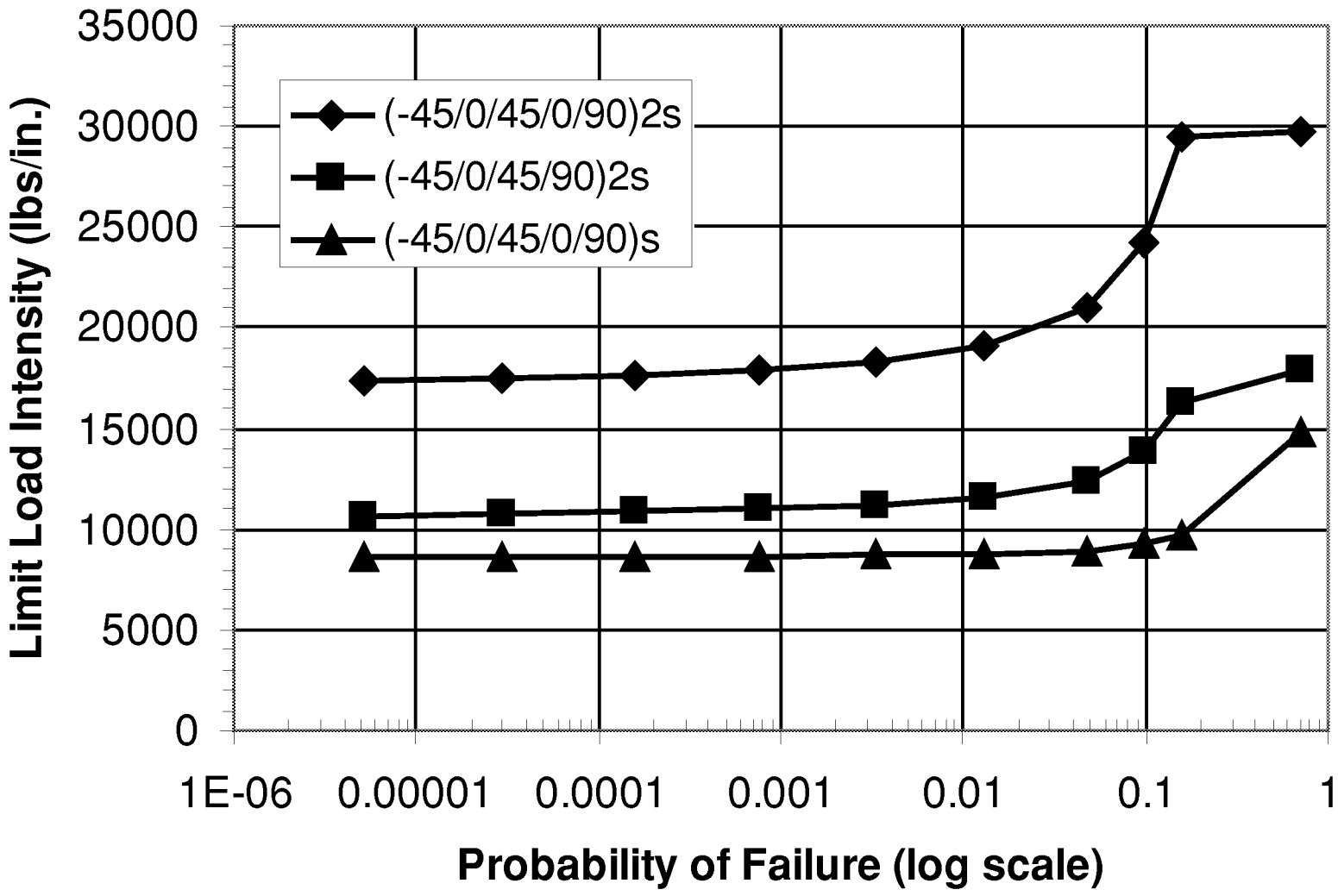

Figure 52. Design Load vs. Probability of Failure for a Sandwich Panel with a Circular Delamination Loaded in Compression (Inspection Type II)

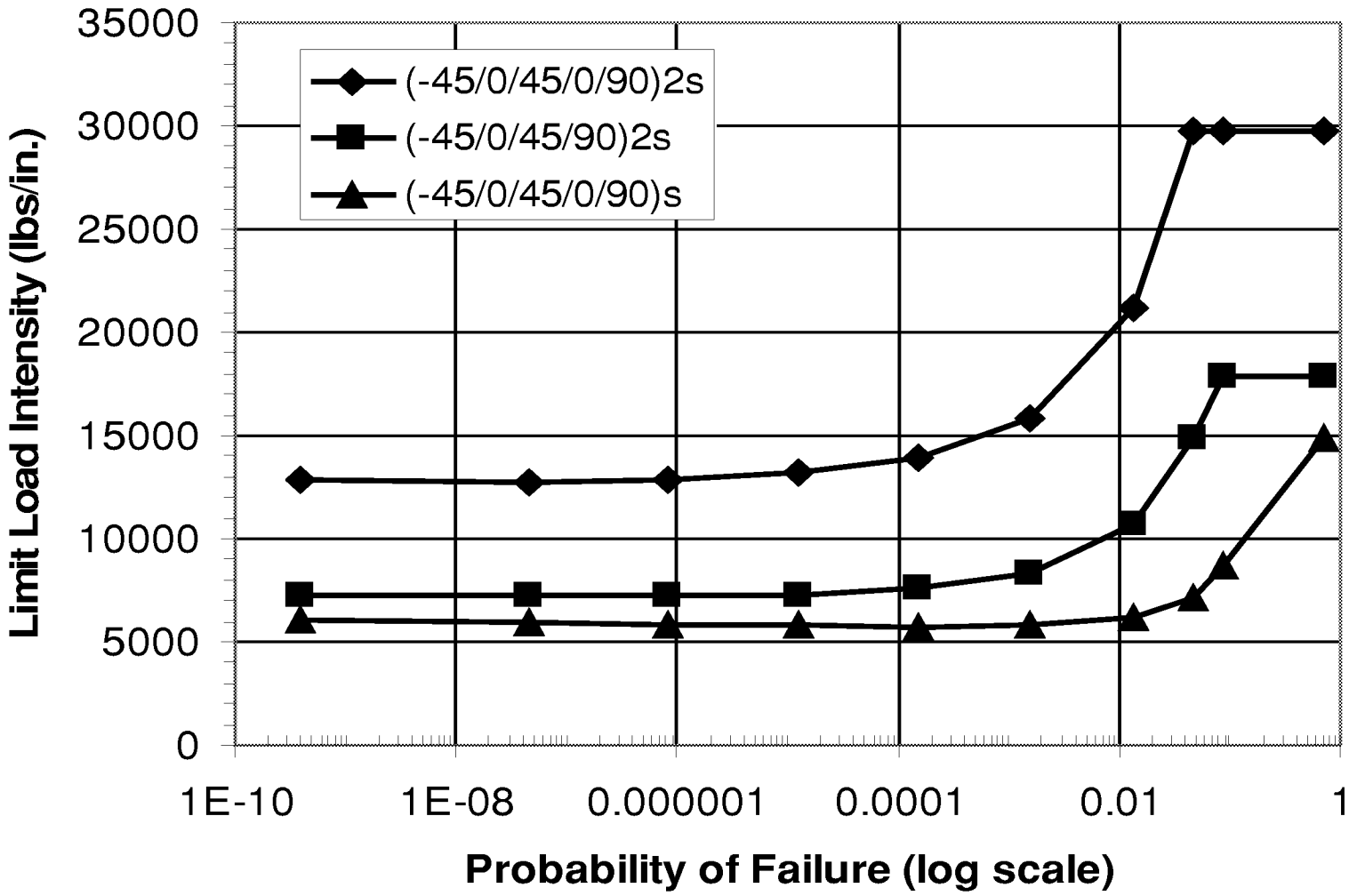

Figure 53. Design Load vs. Probability of Failure for a Sandwich Panel with an Elliptical Delamination Loaded in Compression (Inspection Type II)

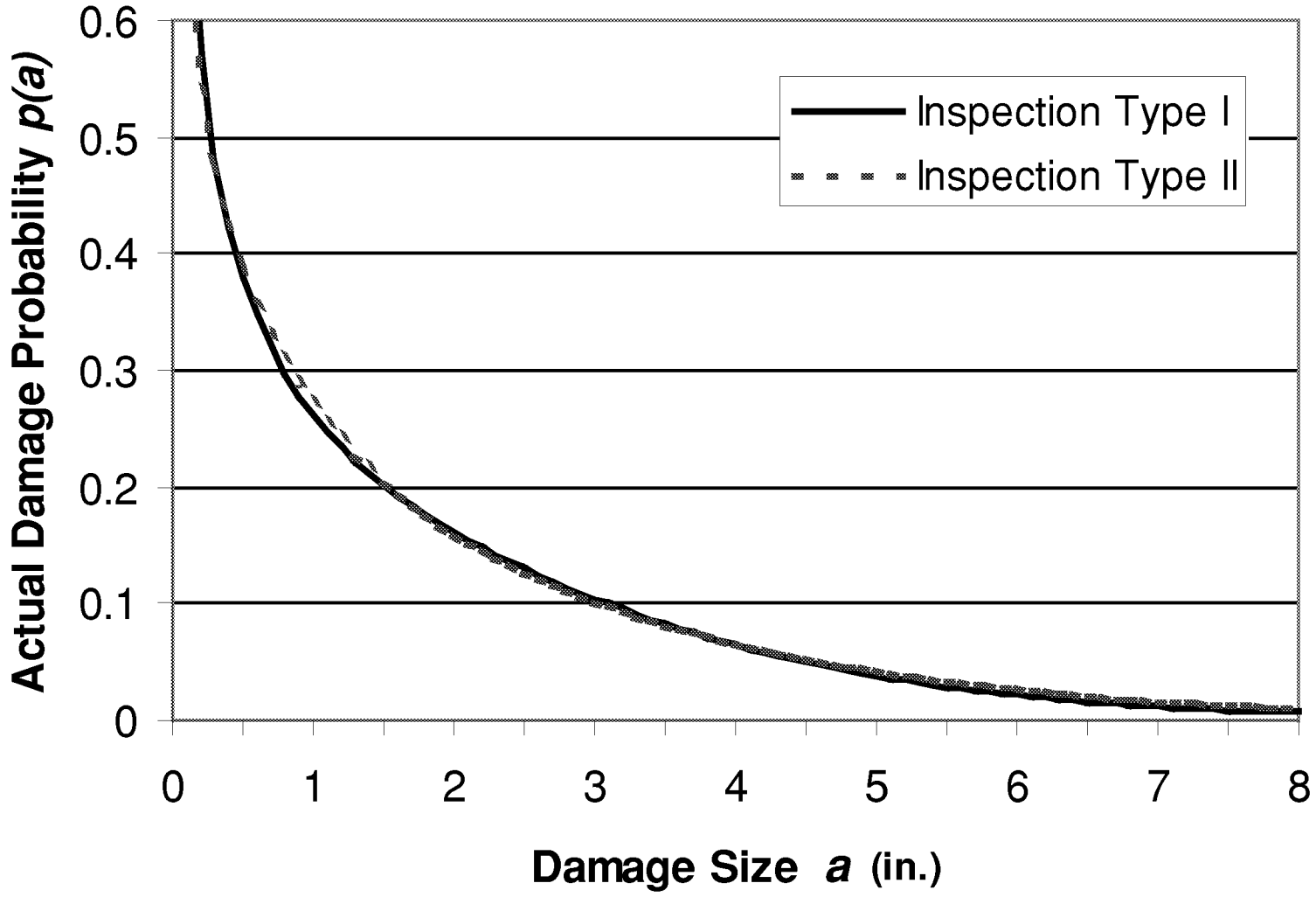

Figure 54. Probability Density of Actual Damage Size *p(a)* Derived from Two Different Inspection Methods

8 REFERENCES

1. Cruse, Thomas A., Reliability–based Mechanical Design, Marcel Dekker, Inc., New York, 1997.

2. Sundararajan, C., Probabilistic Structural Mechanics Handbook, Champman & Hall, 1995.

3. Ditlevsen, O. and Madsen, H.O., Structural Reliability Methods, John Wiley & Sons, Inc., 1996.

4. Soares, C. Guedes, Probabilistic Methods for Structural Design, Kluwer Academic Publishers, 1997.

5. Chamis, C.C., "Probabilistic Composite Design," Composite Materials: Testing and Design, Vol. 13, ASTM STP 1242, ed. by S. J. Hooper, pp. 23-42, 1997.

6. Whitehead, R.S., Kan, H.P., Cordero, R. and Saether, E.S., Certification Testing Methodology for Composite Structures, Northrop Corporation Aircraft Division, Hawthorne, CA, October 1986.

7. Kan, H. P., Cordero, R. and Whitehead, R.S., Advanced Certification Methodology for Composite Structures, Report No. DOT/FAA/AR-96/111, 1997.

8. Kan, H.P., Enhanced Reliability Prediction Methodology for Impact Damaged Composite Structures, Report No. DOT/FAA/AR-97/79, 1998.

9. Rouchon, J., "Certification of Large Airplane Composite Structures, Recent Progress and New Trends in Compliance Philosophy," Proceedings of 17th ICAS Congress, Stockholm, pp. 1439-1447, 1990.

10. Rouchon, Jean, "How to Address the Situation of the No-Growth Concept in Fatigue, with a Probabilistic Approach?: Application to Low-Velocity Accidental Impact Damage with Composites," ICAF' 97 Composite Workshop, Edinburgh, 17 June 1997.

11. Gary, P.M., and Riskalla, M.G., DOT/FAA/AR-95/17, Development of Probabilistic Design Methodology for Composite Structures, U.S. Department of Transportation, Federal Aviation Administration, Washington, DC, August 1997.

12. Rummel, Ward D, and Matzkanin, George A., Nondestructive Evaluation (NDE) Capabilities Data Book, Third Edition, Nondestructive Testing Information Analysis Center (NTIAC), Texas Research Institute Austin, Inc., Austin, TX, November 1997.

13. Spencer, Floyd W., DOT/FAA/AR-96/65, Visual Inspection Research Project Report on Benchmark Inspections, U.S. Department of Transportation, Federal Aviation Administration, Washington, DC, October 1996.

14. Spencer, Floyd W., DOT/FAA/AR-97/73, Detection Reliability for Small Cracks Beneath Rivet Heads Using Eddy-Current Nondestructive Inspection Techniques, U.S. Department of Transportation, Federal Aviation Administration, Washington, DC, December 1998.

15. Ang, Alfredo H.S., and Tang, Wilson H., Probability Concepts in Engineering Planning and Design, Vol.1: "Basic Principles", John Wiley & Sons, 1975.

16. Hibbitt, Karlsson & Sorensen, Inc., ABAQUS/Standard User's Manual, Version 5.7, 1997.

17. Timoshenko, S.P., Theory of Elastic Stability, 2nd Edition, McGraw-Hill, 1961.

18. Yin, W.L., and Jane, K.C., "Refined Buckling and Postbuckling Analysis of Two-Dimensional Delaminations, I: Analysis and Validation," International Journal of Solids and Structures, Vol.29, No.5, pp. 591-610, 1992.

19. Jane, K.C., and Yin, W.L., "Refined Buckling and Postbuckling Analysis of Two-Dimensional Delaminations, II: Results for Anisotropic Laminates and Conclusion," International Journal of Solids and Structures, Vol.29, No.5, pp. 611-639, 1992.

20. Whitcomb, J.D., "Three-Dimensional Analysis of a Postbuckled Embedded Delamination," Journal of Composite Materials, Vol.23, pp. 862-889, 1988.

21. Kassapoglou, C., "Buckling, Post-Buckling and Fracture of Elliptical Delaminations in Laminates Under Compression," Composite Structures, Vol.9, pp. 139-159, 1988.

22. Dost, E.F., Ilcewicz, L.B. and Gosse, J.H., "Sublaminate Stability Based Modeling of Impact-Damaged Composite Laminates," Proceedings. of the 3rd Technical Conference, American Society for Composites, p. 354-363, 1988.

23. Awerbuch, J., and Madhukar, M.S., "Notched Strength of Composite Laminates: Predictions and Experiments: A Review," Journal of Reinforced Plastics and Composites, Vol.4, pp.3-159, 1985.

24. Tan, Seng C., Stress Concentrations in Laminated Composites, Technomic Publishing Company, Inc., 1994.

25. Mar, J.W. and Lin, K.Y., "Fracture of Boron/Aluminum Composites with Discontinuities," Journal of Composite Materials, Vol.11, pp. 405-421, 1977.

26. Whitney, J.M. and Nuismer, R.J., "Stress Fracture Criteria for Laminated Composites Containing Stress Concentrations," Journal of Composite Materials, Vol. 8, pp. 253-265, 1974.

27. Waddoups, M.E., Eiswmann, J.R. and Kaminski, B.E., "Macroscopic Fracture Mechanics of Advanced Composite Materials," Journal of Composite Materials, Vol.5, pp. 446-454, 1971.

28. Chang, F.K. and Lessard, L.B., "Damage Tolerance of Laminated Composites Containing an Open Hole and Subjected to Compressive Loadings," Journal of Composite Materials, Vol.25, 1991.

REPORT DOCUMENTATION PAGE

Form Approved
OMB No. 0704-0188

1. AGENCY USE ONLY (*Leave blank*)	2. REPORT DATE	3. REPORT TYPE AND DATES COVERED
	February 2000	Contractor Report

4. TITLE AND SUBTITLE
Structural Design Methodology Based on Concepts of Uncertainty

5. FUNDING NUMBERS
522-31-71-02

6. AUTHOR(S)
K. Y. Lin, Jiaji Du, and David Rusk

7. PERFORMING ORGANIZATION NAME(S) AND ADDRESS(ES)
Department of Aeronautics and Astronautics
University of Washington
Box 352400
Seattle, WA 98195-2400

8. PERFORMING ORGANIZATION REPORT NUMBER

9. SPONSORING/MONITORING AGENCY NAME(S) AND ADDRESS(ES)
National Aeronautics and Space Administration
Langley Research Center
Hampton, VA 23681-2199

10. SPONSORING/MONITORING AGENCY REPORT NUMBER
NASA/CR-2000-209847

11. SUPPLEMENTARY NOTES
Langley Technical Monitor: W. Jefferson Stroud
Final Report

12a. DISTRIBUTION/AVAILABILITY STATEMENT
Unclassified-Unlimited
Subject Category 39 Distribution: Standard
Availability: NASA CASI (301) 621-0390

12b. DISTRIBUTION CODE

13. ABSTRACT (*Maximum 200 words*)

In this report, an approach to damage-tolerant aircraft structural design is proposed based on the concept of an equivalent "Level of Safety" that incorporates past service experience in the design of new structures. The discrete "Level of Safety" for a single inspection event is defined as the compliment of the probability that a single flaw size larger than the critical flaw size for residual strength of the structure exists, and that the flaw will not be detected. The cumulative "Level of Safety" for the entire structure is the product of the discrete "Level of Safety" values for each flaw of each damage type present at each location in the structure.

Based on the definition of "Level of Safety", a design procedure was identified and demonstrated on a composite sandwich panel for various damage types, with results showing the sensitivity of the structural sizing parameters to the relative safety of the design. The "Level of Safety" approach has broad potential application to damage-tolerant aircraft structural design with uncertainty.

14. SUBJECT TERMS
damage tolerance, probability, Bayesian statistics, inspection, uncertainty
reliability, damage detection, composite sandwich, aircraft structures

15. NUMBER OF PAGES
130

16. PRICE CODE
A07

17. SECURITY CLASSIFICATION OF REPORT	18. SECURITY CLASSIFICATION OF THIS PAGE	19. SECURITY CLASSIFICATION OF ABSTRACT	20. LIMITATION OF ABSTRACT
Unclassified	Unclassified	Unclassified	UL